European Journal of Environmental Sciences

CONTENTS

TREATMENT OF PIG FARM EFFLUENTS BY AERATION, STRUVITE PRECIPITATION AND FILTRATION

ONDŘEJ LHOTSKÝ[1,2,*], EVA SÝKOROVÁ[3], TEREZA HUDCOVÁ[1], ALENA FILIPOVÁ[4], and TOMÁŠ CAJTHAML[2,4]

[1] Dekonta, Stehelčeves, Czech Republic
[2] Institute for Environmental Studies, Charles University in Prague, Czech Republic
[3] Department Technology of Water, ICT Prague, Czech Republic
[4] Institute of Microbiology, Academy of Sciences of the Czech Republic
* Corresponding author: lhotsky@dekonta.cz

ABSTRACT

These experiments were performed to verify the potential ways of treating pig farm effluents using aeration, struvite precipitation and filtration. $MgCl_2$ brine was added as a source of magnesium for struvite precipitation. Following aeration, precipitated struvite was separated from the effluent by filtration through a compressed straw filter. The filter plus struvite can be composted to yield struvite-enriched compost. A series of 5 batch pilot-scale experiments (effluent volumes from 200–400 l) was carried out and laboratory tests on the same effluent were performed to validate the pilot-scale results. Following 24 hours of aeration the pH increased to from 8.5 to 9, providing good conditions for struvite precipitation. Filtration proved to be efficient for separating precipitated struvite and total suspended solids. The efficiency of orthophosphate phosphorus removal in the pilot system varied from 63 to 96%, ammonia nitrogen removal varied from 22 to 79%, but magnesium removal efficiency was low due to the high natural Mg concentration, suggesting that the addition of Mg might not be necessary. Chemical oxidation demand declined significantly as a result of very high bacterial activity and the treated effluent no longer had an unpleasant smell.

Keywords: struvite, aeration, piggery effluent, filtration, nutrient recovery

Introduction

Precipitation of magnesium-ammonium phosphate ($MgNH_4PO_4 \cdot 6H_2O$; MAP; struvite) from wastewater is a recently developed method for sequestering and recycling nutrients (EPA 2013). Struvite is a biogenic mineral that can be directly applied as a slow release fertilizer. Struvite precipitation occurs in water with high concentrations of magnesium (Mg), orthophosphate phosphorus (P_{ortho}) and ammonia nitrogen (N_{amon}) under alkaline conditions. According to the literature, the apparent pH value of struvite minimum solubility varies from 9 to 11 (Snoeyink and Jenkins 1980; Stumm and Morgan 1996). The basic chemical reaction of struvite precipitation according to Doyle and Parsons (2002) can be described by the following equation (1).

$$Mg^{2+} + NH_4^+ + PO_4^{3-} + 6H_2O \leftrightarrow MgNH_4PO_4 \cdot 6H_2O \quad (1)$$

Struvite precipitation for wastewater treatment and phosphorus removal was studied intensively in the past. Information on a wide spectrum of factors influencing the process can be found in the literature e.g. (Snoeyink and Jenkins 1980; Stumm and Morgan 1996; Ohlinger et al. 1998). Munch and Barr (2001) state that the most important factors for struvite precipitation are the $Mg:N_{amon}:P_{ortho}$ molar ratio and the pH of the solution. A number of pilot-scale wastewater treatment systems utilizing struvite precipitation to remove phos-

phorus were tested recently, e.g. removal from municipal wastewater (Ohlinger et al. 2000), industrial wastewater (Matynia et al. 2013), source-separated urine (Wilsenach et al. 2007), wastewater from agriculture (Liu et al. 2011), etc. Currently, a number of technologies for struvite precipitation from municipal and industrial wastewater are commercially available and several different methods based on struvite precipitation were designed and tested for small wastewater producers in agriculture. However, their use in practice is limited due to low cost effectiveness and lack of relevant legislation. Application to the land is still considered to be the most cost effective and common method for disposing of the majority of agricultural effluents, especially piggery effluents (Münch et al. 2001). But application of piggery effluents to the land results in eutrophication and other environmental problems. Although anaerobic digestion provides an effective solution for the treatment of the majority of agricultural effluents (Holm-Nielsen et al. 2009) it might not be feasible for small producers. A number of studies have recently focused on struvite precipitation from piggery effluents. Utilization of aerated reactors and the addition of a source of magnesium to the effluent proved to be efficient (Suzuki et al. 2005; Shepherd et al. 2009a). However some problems associated with the technology remain unresolved.

Separation of the precipitated struvite from piggery effluents is reported to be a major problem by Shepherd et al. (2009b). The high concentration of total suspend-

ed solids and bacterial biomass in some piggery effluents prevents separation based on a difference in density (e.g. sedimentation or hydrocyclone). The high heterogeneity of the effluent over time causes significant problems for automating treatment systems. For this reason, we performed a series of 5 batch pilot-scale experiments, which were duplicated with the same wastewater in the laboratory. Piggery effluent collected from a concrete storage tank placed under pig stables in central Bohemia was used. The numbers and age of the pigs varied during the study. The pilot-scale reactor used for the experiments was constructed according to the experience gathered during laboratory experiments performed prior to the pilot testing. Aeration of the effluent (CO_2 stripping) was used for effluent alkalization and $MgCl_2$ brine (used for dust-control on roads) as a source of magnesium. Filtration through compressed straw was used to separate the suspended solids and struvite from the effluent. This material can be composted. The high temperatures reached during the thermophilic phase of composting provide effective sanitation.

Materials and Methods

Pilot Scale Treatment System (Layout in Fig. 1)

This system consisted of tank *A* (1 m³ plastic IBC container) for fresh effluent, which was pumped into the tank from the underground bunker. Effluent was pumped from tank *A* into the aerated reactor *B* (1 m³ metal IBC container with 3 aeration segments (FORTEX AME-350) connected to aeration pump Secoh EL-S-200) placed on a 2.4 m high frame so that the treated effluent could be drained gravitationally into the filtration vessel *C* (1 m³ plastic IBC container filled with compressed straw). The treated effluent was collected in tank *D* after filtration.
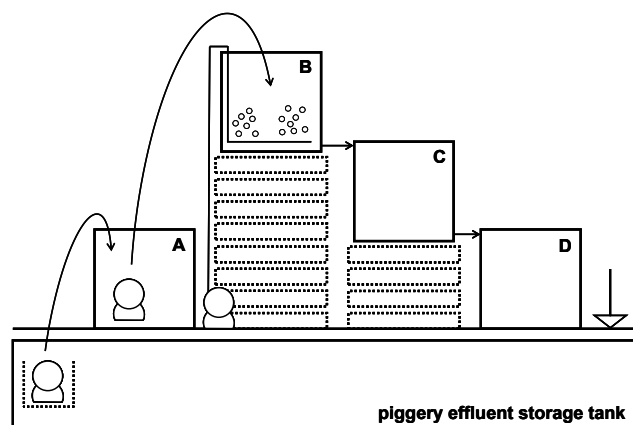

Fig. 1 Pilot system layout.

Pilot Testing

The tests were performed during the summer of 2013. The effluent was pumped from the concrete storage tank

into tank *A* by a sludge pump equipped with a protective filter basket wrapped in plastic filter fabric with a mesh size of 1 mm. From tank *A*, samples of piggery effluent were taken for laboratory tests and for determination of the inlet concentrations of the chemical parameters (*In*). Immediately after filling tank *A*, test determination of the P_{ortho} concentration (hereinafter P_{ortho} equals $c(H_nPO_4^{n-3})$; n = 0; 1; 2; 3) was performed on site using colorimetric kits (Aquaterm, s.r.o.). Dosage of $MgCl_2$ brine (33% w/w) was calculated according to the test determination of the P_{ortho} concentration (see Table 1, the same molar ratio of $Mg:N_{amon}:P_{ortho}$ was tested in the laboratory the same day). Brine was added to aerated reactor *B* after filling it with the effluent. The volumes of effluent varied in the tests. Reactor *B* was aerated (310 l/min.) for 24 hours. Throughout aeration, the effluent physicochemical parameters (pH, oxidation-reduction potential (ORP), electrolytic conductivity and dissolved O_2 concentration) were monitored using a Hanna HI9628 multi-meter. Samples of the treated effluent were taken from reactor *B* (*R out NF*) after switching off the aeration. The effluent was then drained into filtration vessel *C* and samples of the output treated effluent (*R out F*) were taken. Identical tests on a small scale were repeated in the laboratory, but the filtration step was excluded.

Laboratory Tests

Tests were performed on a coagulation bench in 1 l vessels. The vessels filled with 800 ml of the effluent were aerated continuously (2.4 l/min.) for 24 hours. Samples were taken for analysis after switching off the aeration (*L out*). There were three replicates of all the laboratory tests.

Testing for Microbial Activity during Aeration

This test was performed to determine why there was a decrease in the O_2 concentration during aeration of the effluent and assess microbial activity during aeration. The test was carried out in the laboratory on a coagulation bench using 2.5 l vessels containing 2 l of the effluent in 3 replicates during the winter of 2014. The effluent was aerated continuously (2.4 l/min.) and no Mg source added. 60 ml samples of each effluent replicate were collected during aeration. 10 ml were immediately frozen and analyzed later for chemical oxygen demand (COD) and biochemical oxygen demand after 5 days (BOD_5). 50 ml were centrifuged and the separated solid was then frozen and analyzed later for phospholipid fatty acids – PLFA. The separated solid samples for PLFA were extracted and analyzed using the method described by Snajdr et al. (2011). Samples were taken after 1, 2, 6, 9, 14, 16, 18, 20 and 24 hours of aeration. Input and output effluent samples were analyzed routinely. The test results are marked as **M** in the figures and tables.

Effluent Analysis

Before the analysis of the chemical parameters monitored, except for COD, BOD_5 and total suspended sol-

Table 1 The input information for the pilot tests.

Test No.		1	2	3	4	5
Effluent volume	(l)	200	275	400	400	400
P_{ortho} tentative	(mg/l)	500	120	150	300	150
Volume of $MgCl_2$ brine	(ml/l effluent)	1.0	0.73	0.625	0.625[b]	x
Calculated ratio Mg:P[a]		1.38 (0.78)	4.41 (2.89)	4.32 (3.08)	1.95 (1.55)	2.38

[a] The ratios were calculated using data obtained from laboratory determinations of the input samples with the source of the Mg being from added $MgCl_2$ brine. Numbers in brackets are original Mg:P ratios before the addition of the brine.
[b] In case of test 4 in the laboratory two different experiments were performed, one with 0.625 ml of brine added per l of effluent and one without the addition of brine.
x Not analyzed.

ids (TSS), effluent samples were centrifuged to separate the macroscopic TSS and increase the repeatability of the laboratory analysis. *In* and *R out* samples were centrifuged at 4000 rpm at 20 °C for 6 min. *L out* samples were centrifuged at 5000 rpm at 20 °C for 12 min. The *L out* samples were centrifuged to separate all the struvite crystals. Orthophosphates (P_{ortho}) were determined using the ammonium molybdate spectrometric method (ISO 2004). The ammonium molybdate solution is characterized by a low pH, which facilitates complete dissolution of residual microscopic struvite crystals. Ammonia nitrogen ($N_{amon} = c(NH_{3+n}^{+n})$; n= 0, 1) was determined using Nessler's reagent spectrophotometry (Greenberg et al. 1992); the concentrations of magnesium (Mg) and calcium (Ca) were determined using emission spectrometry with inductively coupled plasma (ISO 2009). The concentration of chlorides (Cl^-) and COD values were determined using titration methods (ISO 1989; ISO 2002) and TSS was determined gravimetrically (Kenkel 2013). The ISO method was used to determine BOD_5 (ISO 2003).

Analysis of Separated Solids

Separated solids obtained by centrifugation (5000 rpm, 20 °C, 12 min) were dried at laboratory temperature. Separated solids of the samples taken directly from the reactor (*R* out NF) and the separated solids obtained from the laboratory tests were analyzed. The qualitative composition of the crystalline phase of the separated solids was assessed using X-ray powder diffraction (XRD). Measurements were made at 25 °C with a Co anode with a step size of 0.02 [°2Theta]. The obtained diffraction patterns were compared with the results in the literature. The same method has been used by a number of authors e.g. (Ohlinger et al. 1998; Le Corre et al. 2005).

The amount of struvite in the separated solids was estimated by dissolution tests. 100 mg of the separated solids were stirred in 250 ml of mixed (900 rpm) HCl solution (pH 4.5) for 2 hours. All the struvite dissolved under these conditions, which was earlier experimentally verified with chemically pure struvite. The ionic composition of the final solution was then determined.

The concentration of struvite components in the test solution was compared to the theoretical concentration assuming all the separated solids were pure struvite and the fraction of struvite in the separated solids estimated.

Results and Discussion

Quality of Input Effluent

Information on the tests is summarized in Table 1. The concentrations of the parameters monitored in the input effluent and its pH and electrolytic conductivity determined in the laboratory are listed in Table 2. High heterogeneity of the concentrations of the struvite components in the effluents tested can be clearly seen. The P_{ortho} concentration varied from 211 to 723 mg/l. The N_{amon} concentration varied from 1,698 to 2,325 mg/l. N_{amon} molar concentrations were significantly higher than the concentrations of the other struvite components; therefore, only the $Mg:P_{ortho}$ molar ratio is shown in Table 1. Mg concentrations were high and varied from 143 to 262 mg/l, Ca varied from 77 to 178 mg/l and COD from 2,688 to 11,711 mg/l; high COD correlated with high TSS. Shepherd et al. (2009a) report similar P_{ortho} concentrations in two piggery effluents. Liu et al. (2011) record the P_{ortho} concentrations in the piggery effluent they used in their tests varied from 76 to 1,862 mg/l and N_{amon} varied from 1,562 to 5,336 mg/l. Huang et al. (2011) used effluent with average concentrations of P_{ortho} of 555 mg/l, N_{amon} of 1,266 mg/l, Ca of 135 mg/l and Mg of 6.7 mg/l. The electrolytic conductivity varied from 12,220 to 15,750 mS/m and the pH was between 7.5 and 7.9. A surprisingly a high Cl^- concentration (709 mg/l) was recorded in the effluent treated in test 1 together with the highest P_{ortho} concentration, although the concentrations of the other struvite components and COD and TSS were lower than in the other tests. We assume that the effluent was somehow altered compared to the other samples. This may be due to the heavy rain in the region before the tests, which might have washed out some fertilizers and other chemicals stored close the effluent storage tank.

Table 2 Determination of the input parameters of the effluent – *In samples.*

|	P_{ortho}	N_{amon}	Mg	Cl^-	COD	Ca	TSS	Elec. Conduct.	pH
test No.	(mg/l)							(mS/m)	–
1	723	1698	143	709	2688	124	1524	12220	7.46
2	211	2204	154	x	6481	151	3125	15140	7.71
3	221	2325	172	92	6196	178	x	15520	7.87
4	670	2298	262	43	10304	77	4420	13500	7.66
5	367	2193	221	x	11711	80	4983	15 750	7.78
M	21	2201	183	x	4160	94	1200	x	8.02

Tentative P_{ortho} determination enabled relatively accurate, although in all cases underestimated, values of the P_{ortho} concentration. The heterogeneity of the Mg concentrations leads to difficulties in estimating the ideal amounts of $MgCl_2$ brine.

Physicochemical Parameters

The dissolved oxygen concentration and pH measured throughout the tests (in the laboratory and pilot reactor) are shown in Fig. 2. The data were not recorded in test 5 due to failure of the multi-meter. In the pilot reactor, the pH increased gradually throughout the test, reaching values higher than 8.5. In the laboratory, the pH increased rapidly after the start of aeration

and then remained more or less constant, probably due to the higher aeration rates. The pH value of approximately 8.5 is similar to the results published by Korchef et al. (2011) and are high enough for effective struvite precipitation.

The O_2 concentration shows similar trends in the reactor and laboratory; it gradually increased in the first hours of aeration and usually reached full saturation at the prevailing temperatures after a few hours. However, subsequently the O_2 concentration decreased sharply and oxygen was often completely depleted. After about 14 hours of aeration, the O_2 concentration began to increase again and usually reached full saturation at the end of the tests. This phenomenon can be explained
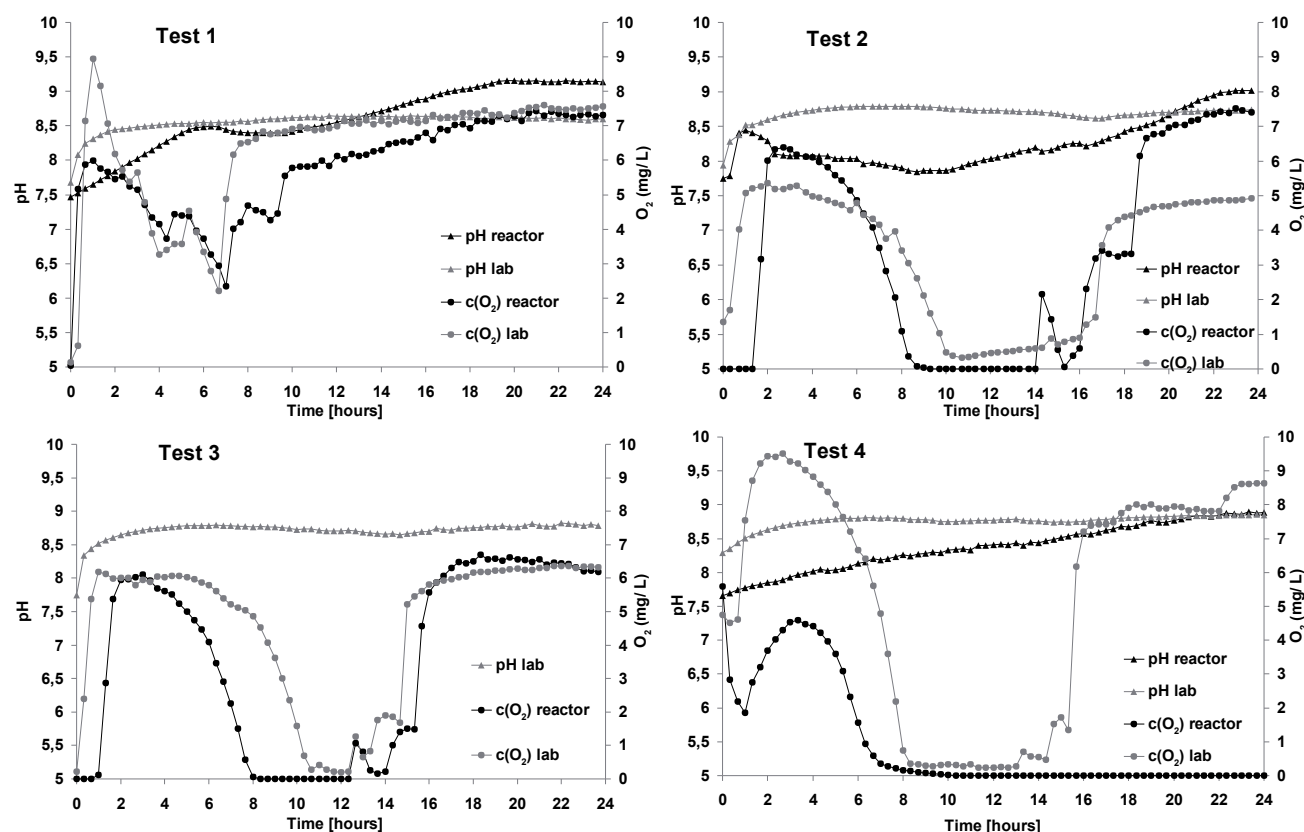
Fig. 2 Dissolved oxygen concentration and pH measured throughout the test in the laboratory (average values shown) and reactor (in case of test 3 pH data in the reactor were not recorded due to failure of the multi-meter).

by the activity of the microorganisms and is discussed below.

Further data (temperature, electrolytic conductivity and ORP) measured throughout the tests in the pilot reactor are shown in Fig. 3.

The temperature varied throughout the tests as the reactor was placed outdoors and the aeration provides efficient heat exchange. Maximum temperature reached about 30 °C and the minimum temperature was approximately 15 °C.

The electrolytic conductivity increased after addition of the $MgCl_2$ brine at the beginning of the tests. It dropped significantly after approximately one hour of aeration, then increased slightly and then gradually and continually decreased. The differences in the input and output effluent electrolytic conductivities varied from

2,500 to 4,000 mS/m. The decrease in the conductivity is caused mainly by the precipitation of various minerals including struvite.

ORP increased swiftly after the beginning of aeration. In tests 3 and 5, ORP reached values of approx. −15 mV and remained constant for the rest of the test. In tests 1 and 4, it continued to gradually increase throughout aeration and reached values of approx. −34 mV (test 4) or −100 mV (test 1). A decrease in ORP was recorded in test 2 following a rapid increase. Later ORP increased again, but the values at the end of test 2 were still approx. −300 mV.

Chemical Parameters

The chemical parameters of the output effluents from the different tests and the calculated decrease in the parameters compared to the input effluent are summarized in Table 3. The efficiencies of removal of the struvite components in the tests are shown in Fig. 4. Higher rates of aeration in the laboratory compared to the pilot reactor, together with more effective TSS (and struvite) separation via intensive centrifugation, could be one of the reasons for slightly better removal efficiencies recorded in the laboratory. The compressed straw filter was efficient in capturing the TSS including struvite, which is clearly confirmed by the TSS concentrations before and after filtration, as well as the differences in the P_{orto} removal efficiencies. This efficiency for the reactor-treated effluent after filtration varied from 63% (test 2) to 96% (test 1) and surprisingly was higher when the Mg:P ratio was lower. The N_{amon} removal efficiency varied from 22% (test 5) to 79% (test 4). It seems that stripping of NH_3 by aeration and possibly also the nitrification processes played a substantial role in N_{amon} sequestering. The concentrations of N_{amon} dropped significantly more than would occur if N_{amon} was only precipitated in the form of struvite. NH_3 is in equilibrium with the air according to Henry's Law and facilitates air stripping of N_{amon}. NH_3 is the predominant N_{amon} form in aqueous solution with a high pH and temperature (Negulescu 1985). The output Mg concentrations were higher than the input ones in tests 2 and 3. Even in test 5 without the addition of a source of Mg, the removal efficiency did not exceed 27%, which indicates that part of the P_{ortho} was sequestered in a different way than by struvite precipitation. It can be assumed that part of the P_{ortho} was sequestered through precipitation of other minerals and part through incorporation into the biomass. The Ca concentrations of the output filtered effluents are summarized in Table 4. The removal efficiencies of Ca varied from 25% (test 5) to 79% (test 3). Part of the Ca was precipitated in the form of magnesium calcium carbonate (CCM; (6% Mg, 94% $CaCO_3$) or hydrated calcium carbonate ($CaCO_3 \cdot nH2O$). It can be assumed that one of the forms in which Ca and P_{ortho} precipitate was hydroxylapatite ($Ca_{10}(PO_4)_6(OH)_2$) as Ca^{2+} ions interact effectively with P_{ortho} to form calcium phosphates in wastewater systems, commonly as poorly crystallized hydroxylapatite
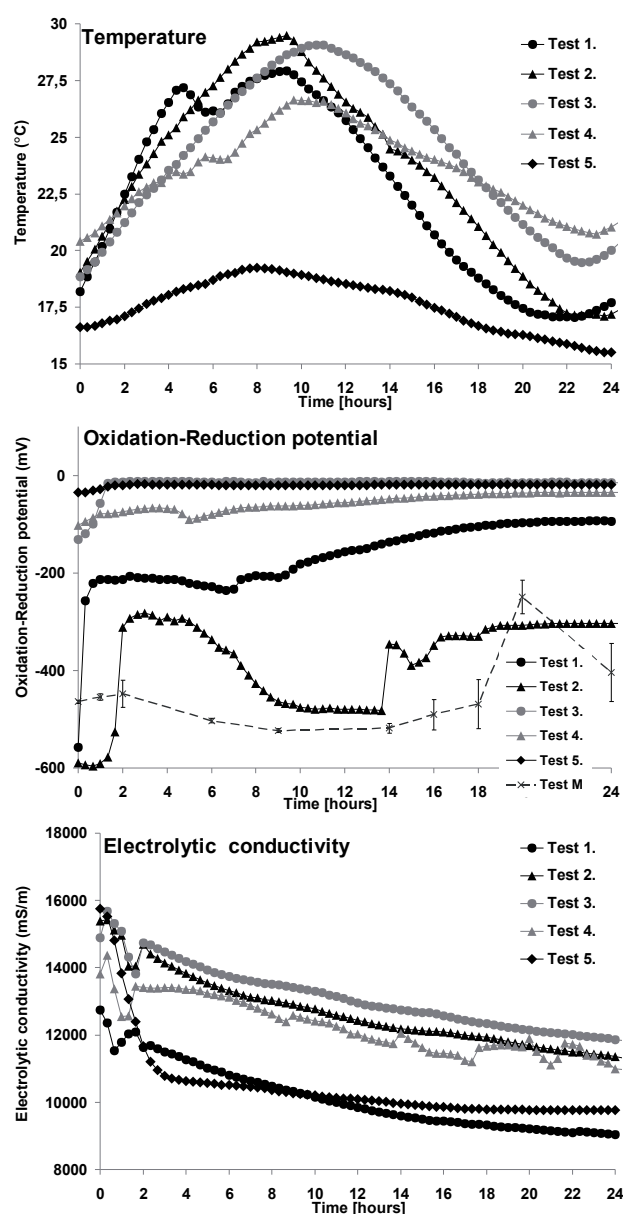
Fig. 3 Temperature, electrolytic conductivity and oxidation-reduction potential measured throughout the test in the pilot reactor and oxidation-reduction potential of the samples measured during test M.

Table 3 Chemical parameters monitored in the output effluents from the different tests and calculated removal (or increase marked by minus) of the chemicals compared to those in the input effluent.

| Test No.		Portho	Namon	Mg	Cl⁻	COD	TSS
					(mg/l)		
1	R out NF	252	631	163	1250	1870	1172
	Removal	471	1067	−20	−541	818	352
	R out F	32	931	114	1280	1720	779
	Removal	691	767	29	−571	968	745
	L out[a]	4.7 ± 0.2	887 ± 69	103 ± 4	x	1458 ± 5	x
	Removal	719	861	40	x	1230	x
2	R out NF	154	1170	284	981	x	2540
	Removal	57	1034	−130	x	x	585
	R out F	78	1160	216	1070	3260	1150
	Removal	133	1044	−62	x	3221	1975
	L out[a]	6.5 ± 0.5	1009 ± 64	210 ± 2.6	x	2551 ± 19	x
	Removal	205	1241	−56	x	3930	x
3	R out NF	98	1120	295	1160	4324	x
	Removal	123	1205	−123	−1068	1872	x
	R out F	79	1120	222	1110	3876	x
	Removal	142	1205	−50	−1018	2320	x
	L out[a]	6 ± 0.2	869 ± 85	212 ± 5.7	x	2402 ± 63	x
	Removal	214	1414	−40	x	3794	x
4	R out NF	173	359	225	445	4967	4 210
	Removal	497	1939	37	−402	5337	210
	R out F	106	479	192	454	3654	3020
	Removal	564	1819	70	−411	6650	1400
	L out[a]	9 ± 1.1	1115 ± 155	193 ± 11	x	3013 ± 246	x
	Removal	660	1185	69	x	7292	x
	L out no Mg[a]	10 ± 0	941 ± 125	149 ± 11.5	x	2762 ± 65	x
	Removal	660	1359	113	x	7542	x
5	R out NF	286	1980	164	x	9598	4 231
	Removal	81	214	12	x	2113	752
	R out F	64	1721	161	x	4921	2345
	Removal	303	472	12	x	6790	2638
	L out[a]	7.1 ± 0.1	1342 ± 125	156 ± 6	x	3656 ± 469	x
	Removal	360	854	20	x	8055	x
M	M out[a]	1.2 ± 1.6	1080 ± 159	197± 11	x	3103 ± 138	x
	Removal	19.8	1121	− 14	x	1057	x

[a] In the laboratory experiments standard deviations of the three parallel tests performed are shown after a ± sign.

Table 4 Ca concentration in the output effluent from the filtered pilot reactor (R out F) recorded in the different tests and the amount removed compared to that in the input effluent.

Test No.:		1	2	3	4	5
Ca concentration	(mg/l)	52	43	38	38	60
Ca removal	(mg/l)	72	108	140	39	20

Table 5 Calculated COD and TSS removal (reactor output compared to input).

Test No.:		1	2	3	4	5
COD removal	(%)	36	50	37	65	58
TSS removal	(%)	49	63	x	32	53
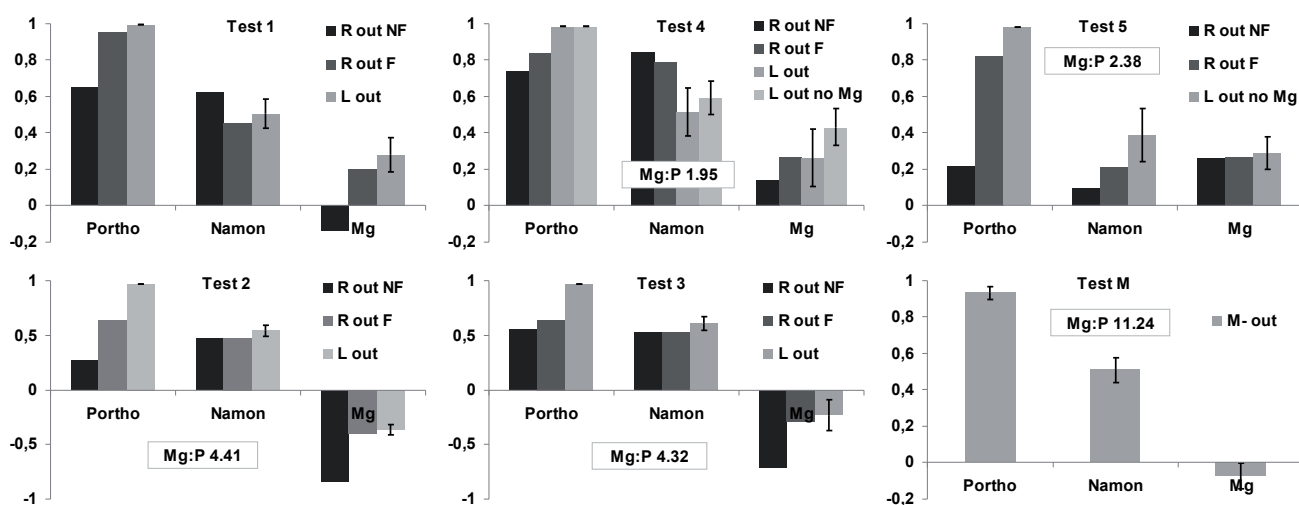
Fig. 4 Removal efficiency of the struvite components in the tests (when negative, an increase in the parameter was recorded) in the pilot reactor before and after filtration and in the laboratory (in the case of test 4 in the laboratory an additional test (*L out no Mg*) without brine was performed; Mg:P ratio in this case was 1.53).

(Le Corre et al. 2005). The removal efficiencies of COD and TSS varied from about 30 to 65% for both parameters (see Table 5). The average removal efficiencies throughout the 8 months operation of the demonstration reactor reported by Suzuki et al. (2005) are 50% for P_{ortho}, 37.5% or Mg, 20% for Ca and 77% for TSS.

Analysis of the Separated Solids

The results of XRD and estimation of the amount of struvite in the separated solids are summarized in Table 6. It is obvious that struvite was present in all the separated solids obtained in the tests, although its concentration varied substantially. In pilot test 1, the input effluent had a high P_{ortho} concentration and low concentrations of

COD and TSS. In this test, struvite forms about 95% of the crystalline phase and its content in the separated solids was estimated at 68%. In the other pilot tests, struvite forms from 65% (test 5) to 45% (test 3) of the crystalline phase of the separated solids. Magnesium calcium carbonate was the second most abundant mineral in the crystalline phase and it forms from 35 to 45% of the crystalline phase in tests 2 to 4. In test 1, it forms only 5% of the crystals and it was not detected at all in test 5. Hydrated calcium carbonate was present in crystalline form, although it is probable that part of it also precipitated in an amorphous form. Graphite was present in quite a high concentration in test 5. Quartz crystals were also detected, probably due to their flushing into the effluent in the

Table 6 XRD results – identified minerals and semi-quantitative estimates of their share of the crystalline phase and estimates of the percentage of the struvite in the precipitate based on the dissolution tests.

Mineral		Struvite	CCM[a]	Hydrated calcium carbonate[b]	Quartz	Graphite	Calculated average percentage weight of struvite in the precipitate
Test No.		\multicolumn{5}{c}{(w % of crystalline phase)}			(w % of precipitate ± standard deviation) ±standard deviation)
1	*R out NF*	95	5	–	–	–	68 ± 15
	L out[d]	94	6	–	–	–	–
2	*R out NF*	60	35	4	1	–	19 ± 20
	L out[d]	44	49	6	1	–	–
3	*R out NF*[d]	45	45	7	–	3	22 ± 4
4	*R out NF*	56	38	5	–	1	24 ± 6
	L out	59	36	4	–	1	–
	L out no Mg	58	37	4	1	–	–
5	*R out NF*	65	–	8	5	22	19 ± 3
	L out	67	–	9	6	18	–

[a] CCM – magnesium calcium carbonate – (6% Mg, 94% Ca)(CO$_3$)
[b] Hydrated calcium carbonate – CaCO$_3$ · nH$_2$O
[c] Three different estimates were obtained using dissolution tests based on three different chemical parameters (P_{ortho}, N_{amon}, Mg), standard deviations of the results are shown after ± sign
[d] Samples containing this phase, which was not identified.

form of small sand particles. The estimated fraction of struvite in the total separated solids was approximately the same for tests 2 to 5 and varied around 20%.

Microbial Activity during Aeration

The test was performed with effluent collected during the winter of 2014. The effluent quality was significantly different from that collected during the summer of 2013, as there were fewer pigs stabled and the effluent was not as frequently spread on the fields. The main difference was in the concentration of P_{ortho}, which was significantly lower than in the effluents collected during summer. The concentrations of the parameters monitored in the input effluent are listed in Table 2 (marked as M).

The pH and the O_2 concentration is shown together with the COD, BOD_5 and PLFA results in Fig. 5. The pH gradually increased during aeration from 8.02 at the beginning to 9.10 at the end. The O_2 concentration followed a similar dependence as in the tests performed earlier, both in the laboratory and the pilot reactor, although O_2 depletion occurred somewhat later, around the 18th hour. The ORP values of the samples taken throughout the tests are shown in Fig. 3. It was highly negative around −450 mV at the beginning and increased only to approx. −400 mV at the end of the test.

The COD and BOD_5 curves are similar. There was a slight decrease in both curves after one hour of aeration. Later both parameters decreased very slowly. Af-

ter the 14th to 16th hour of aeration, the slopes of the curves changed and both parameters decreased more rapidly.

The PLFA results clearly show that the input effluent is rich in total microbial biomass, consisting mainly of bacteria. After the beginning of aeration, the concentration of specific PLFA representing total microbial biomass and bacterial biomass decreased and remained low until the 14th hour of aeration. From that moment on, the concentration of total microbial biomass and bacteria began to increase and continued to increase until the end of the test, although the slope of the curve was not as sharp after the 20th hour of aeration. A very similar curve was recorded for G− bacteria, although in this case the concentrations after the 2nd hour of aeration were very low. The concentration increased after the 9th hour, but a sharp break in the curve appeared after the 14th hour. It is interesting that the concentrations of G+ bacteria remained more or less stagnant throughout whole test. Anaerobic bacteria were present in the input effluent but the aeration caused a decrease in their concentration. After the 14th hour of aeration and a decrease in the O_2 concentration of the effluent, anaerobic bacteria started to grow once again, reaching a maximum after the 16th hour of aeration. The concentration of anaerobic bacteria decreased from that moment on.

It can be concluded that the increase in O_2 concentration at the beginning of aeration negatively affected
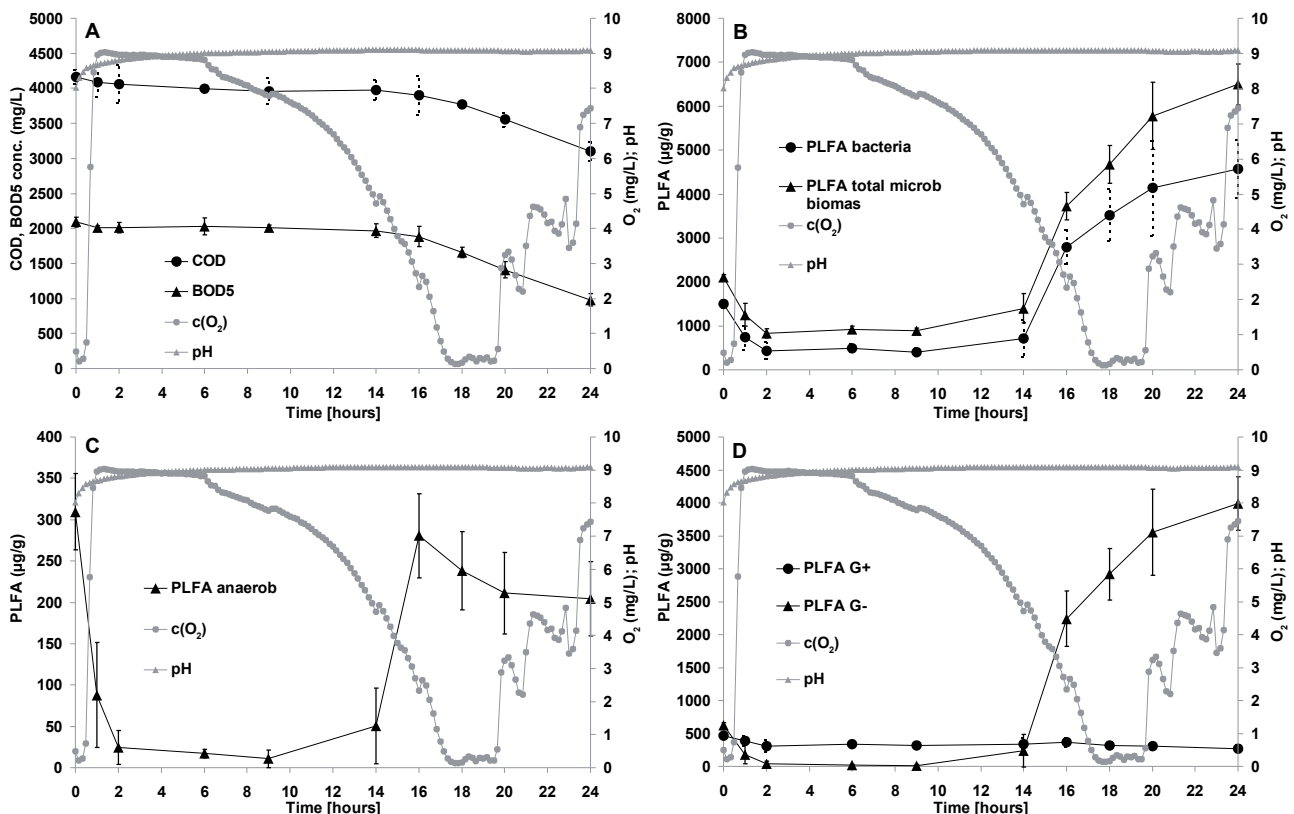
Fig. 5 Graphs of COD and BOD5 concentration in aerated effluent (A) and concentration of PLFA specific for bacteria and total microbial biomass (B); anaerobic bacteria (C); G+ and G− bacteria (D) in the solids separated by centrifugation, compared to the O_2 concentration and pH of the effluent.

the microbial biomass adapted to low O_2 concentrations, causing a lag phase after the 2nd hour of aeration. After adaptation of the microbial community to higher oxygen concentrations, the microbial biomass began to grow exponentially. After a certain time microorganisms began to use greater quantities of O_2 than was dissolved in the effluent due to aeration. From that moment on, the O_2 concentration in the effluent decreased, reaching complete oxygen depletion after about 18 hours. All the dissolved O_2 was immediately used by the aerobic microorganisms, giving the anaerobic bacteria an opportunity to grow in the effluent. It seems that after several hours the microbes decomposed the majority of the readily degradable organic compounds and started to utilize more complex compounds in the effluent, resulting in a lower O_2 consumption. Then the O_2 concentration once again increased gradually and the growth in the microbial biomass slowed down slightly. This theory is supported by the significant decrease in COD and BOD_5 values during the low O_2 concentration phase. We think that an analogous phenomenon was responsible for the decrease in the O_2 concentration during tests 1 to 5.

A similar phenomenon is typical for thermophilic aerobic biological wastewater treatment (Lapara and Alleman 1999). Gehm (1956) report that these processes are characterized by high biodegradation rates, low dissolved oxygen concentrations in the aeration basin resulting from these high biodegradation rates and potential complications associated with poor bacterial settling. Beaudet et al. (1990) studied liquid pig manure treatment at 55 °C and report a COD reduction of approx. 80% after 70 hours of aeration and total elimination of N_{amon} by stripping. They report that thermophilic treatment facilitates the rapid stabilization of the effluent and elimination of the unpleasant smell. Although the temperatures reached in our tests did not exceed 30 °C, we assume that the processes in the effluent were similar. Abeynayaka and Visvanathan (2011) report that the half-velocity constant (Ks; substrate concentration (COD) at one-half of the maximum growth rate [mass/unit volume]) in aerated wastewater increases with temperature but the Ks value recorded in their experiments at 30 °C was 30 times higher than the value recorded for domestic wastewater by Metcalf and Eddy (2003). Nevertheless, there were substantial changes in the output effluent as it did not have an unpleasant smell and its colour had changed from black/dark brown to light brown.

Conclusions

The experiments demonstrated that struvite can be precipitated from piggery effluent by aeration and $MgCl_2$ brine does not need to be added in the majority of cases. The precipitated struvite and other suspended solids were effectively separated from the treated effluent by filtration through compressed straw. The efficiency of

orthophosphate removal in the pilot system varied from 63 to 96%. Ammonia nitrogen removal was surprisingly high and varied from 22 to 79%, mainly due to ammonia stripping into the air facilitated by the high temperature and the increased pH of the effluent. The original input effluent Mg:P molar ratio varied from 1.55 to 3.08 (except for the effluent in test 1). Surprisingly, a higher molar ratio corresponded to a lower efficiency of the orthophosphate removal. The COD concentration declined significantly (40–65%), probably due to a high biodegradation rate, as did the TSS concentration (32–63%), the colour of the treated effluent changed from black/dark brown to light brown and no longer had an unpleasant smell. Long residence times in the pilot reactor (24 hours) led to a significant increase in the pH and sufficient supply of oxygen for degradation of organic compounds by aerobic bacteria.

Additional testing demonstrated that several hours of aeration caused a significant increase in G– bacteria and total microbial biomass, although the O_2 concentration decreased and the concentration of G+ bacteria remained constant.

Acknowledgements

REFERENCES

Abeynayaka A, Visvanathan C (2011) Mesophilic and thermophilic aerobic batch biodegradation, utilization of carbon and nitrogen sources in high-strength wastewater. Bioresour Technol 102: 2358–66.

Beaudet R, Gagnon C, Bisaillon JG, Ishaque M (1990) Microbiological aspects of aerobic thermophilic treatment of swine waste. Appl Environ Microbiol 56: 971–6.

Doyle JD, Parsons SA (2002) Struvite formation, control and recovery. Water Res 36: 3925–40.

EPA (2013) Emerging technologies for wastewater treatment and in-plant wet weather management. Office of wastewater management, U.S. Environmental Protection Agency, Washington D.C.

Gehm HW (1956) Activated sludge at high temperatures and pH values. In: McCabe J, Eckenfelder WW (eds) Biological treatment of sewage and industrial wastes. Reinhold Publishing, New York, USA.

Greenberg AE, Clesceri LS, Eaton AD (eds) (1992) Standard methods for the examination of water and wastewater. American Public Health Association, Washington D.C., USA.

Holm-Nielsen JB, Al Seadi T, Oleskowicz-Popiel P (2009) The future of anaerobic digestion and biogas utilization. Bioresour Technol 100: 5478–84.

Huang H, Xu C, Zhang W (2011) Removal of nutrients from piggery wastewater using struvite precipitation and pyrogenation technology. Bioresour Technol 102: 2523–2528.

ISO (1989) ISO 9297: 1989 Water quality – Determination of chloride – Silver nitrate titration with chromate indicator (Mohr's method). International Organization for Standardization.

ISO (2002) ISO 2002: 15705 Water quality – Determination of the chemical oxygen demand index (ST-COD) – Small-scale sealed-tube method. International Organization for Standardization.

ISO (2003) ISO 2003: 5815–1; 2 Water quality – Determination of biochemical oxygen demand after n days (BODn) – Part 1: Dilution and seeding method with allylthiourea addition, Part 2: Method for undiluted samples. International Organization for Standardization.

ISO (2004) ISO 2004: 6878 Water quality – Determination of phosphorus – Ammonium molybdate spectrometric method. International Organization for Standardization.

ISO (2009) ISO 2009: 11885 Water quality – Determination of selected elements by inductively coupled plasma optical emission spectrometry (ICP–OES). International Organization for Standardization.

Kenkel J (2013) Analytical Chemistry for Technicians. Lewis Publishers, Boca Raton.

Korchef A, Saidou H, Ben Amor M (2011) Phosphate recovery through struvite precipitation by CO_2 removal: effect of magnesium, phosphate and ammonium concentrations. J Hazard Mater 186: 602–613.

Lapara TM, Alleman JE (1999) Thermophilic aerobic biological wastewater treatment. Water Res 33: 895–909.

Le Corre KS, Valsami-Jones E, Hobbs P, Parsons SA (2005) Impact of calcium on struvite crystal size, shape and purity. J Cryst Growth 283: 514–522.

Liu Y, Kwag J, Kim J, Ra C (2011) Recovery of nitrogen and phosphorus by struvite crystallization from swine wastewater. Desalination 277: 364–369.

Matynia A, Wierzbowska B, Hutnik N, Mazienczuk A, Kozik A, Piotrowski K (2013) Separation of Struvite from Mineral Fertilizer Industry Wastewater. Procedia Environ Sci 18: 766–775.

Metcalf E, Eddy H (2003) Wastewater Engineering Treatment and Reuse. McGraw-Hill, New York.

Münch EV, Barr K (2001) Controlled struvite crystallisation for removing phosphorus from anaerobic digester sidestreams. Water Res 35: 151–159.

Münch EV, Benesovsky-Scott A, Josey J, Barr K (2001) Making business from struvite crystallisation for wastewater treatment: turning waste into gold. 2nd international conference on recovery of phosphates from sewage and animal wastes. Noordwijkerhout, Holland.

Negulescu M (1985) Municipal Waste Water Treatment. Elsevier, Amsterdam.

Ohlinger KN, Young TM, Schroeder ED (1998) Predicting Struvite Formation in Digestion. Water Res 32: 3607–3614.

Ohlinger KN, Young TM, Schroeder ED (2000) Postdigestion Struvite Precipitation Using a Fluidized Bed Reactor. J Environ Eng 126: 361–368.

Shepherd TA, Burns RT, Moody LB, Raman DR, Stalder KJ (2009a) Development of a Bench-Scale Air Sparged Continuous Flow Reactor for Struvite Precipitation from Two Different Liquid Swine Manure Storage Systems. Appl Eng Agric 25: 425–430.

Shepherd TA, Burns RT, Raman DR, Moody LB, Stalder KJ (2009b) Performance of a Pilot–Scale Air Sparged Continuous Flow Reactor and Hydrocyclone for Struvite Precipitation and Removal from Liquid Swine Manure. Appl Eng Agric 25: 257–267.

Snajdr J, Cajthaml T, Valaskova V, Merhautova V, Petrankova M, Spetz P, Leppanen K, Baldrian P (2011) Transformation of Quercus petraea litter: successive changes in litter chemistry are reflected in differential enzyme activity and changes in the microbial community composition. FEMS Microbiol Ecol 75: 291–303.

Snoeyink VL, Jenkins D (1980) Water chemistry. Wiley, New York.

Stumm W, Morgan JJ (1996) Aquatic chemistry: chemical equilibria and rates in natural waters. Wiley, New York.

Suzuki K, Tanaka Y, Kuroda K, Hanajima D, Fukumoto Y (2005) Recovery of phosphorous from swine wastewater through crystallization. Bioresour Technol 96: 1544–1550.

Wilsenach JA, Schuurbiers CA, van Loosdrecht MC (2007) Phosphate and potassium recovery from source separated urine through struvite precipitation. Water Res 41: 458–466.

EFFECT OF CYANOBACTERIAL PEPTIDES AND PROTEINS ON COAGULATION OF KAOLINITE

KATEŘINA NOVOTNÁ[1,2], MAGDALENA BAREŠOVÁ[1,3], LENKA ČERMÁKOVÁ[1,3], JANA NAČERADSKÁ[1,3], and MARTIN PIVOKONSKÝ[1,3,*]

[1] Institute of Hydrodynamics, Academy of Sciences of the Czech Republic, Pod Paťankou 30/5, 166 12 Prague 6, Czech Republic
[2] Department of Water Technology and Environmental Engineering, University of Chemistry and Technology, Prague, Technická 5, 166 28 Prague 6, Czech Republic
[3] Institute for Environmental Studies, Faculty of Science, Charles University, Benátská 2, 128 01 Prague 2, Czech Republic
* Corresponding author: pivo@ih.cas.cz

ABSTRACT

Coagulation of peptides and proteins produced by the cyanobacterium *Microcystis aeruginosa* and their influence on the coagulation of hydrophobic kaolinite particles were investigated. For this purpose, the dose of ferric sulphate used as the coagulant was optimized and jar tests with kaolinite, peptides/proteins and both kaolinite and peptides/proteins were carried out under different pH conditions. At pH 4–5.5, the peptides/proteins were efficiently coagulated and peptides/proteins were also found to contribute to the coagulation of kaolinite particles at this pH. Charge neutralization and adsorption were found to be the dominant coagulation mechanisms. The coagulation efficiency and the character of the prevailing coagulation mechanism were strongly dependent on the charge characteristics of the peptides/proteins, kaolinite and hydrolysis products of iron, thus on the pH value. At a pH of about 6, the coagulation process deteriorated due to the formation of soluble Fe-peptide/protein complexes.

Keywords: cellular organic matter (COM), coagulation, complex formation, *Microcystis aeruginosa*, water treatment

Introduction

Eutrophication of surface waters leads to seasonal occurrence of algal blooms and excess growth of cyanobacteria. Algal organic matter (AOM) interferes with the water treatment process, which includes a reduction in the coagulation efficiency resulting in increased coagulant demand (Bernhardt et al. 1985; Takaara et al. 2007; Ma et al. 2012), membrane fouling (Campinas and Rosa 2010), higher production of hazardous disinfection by-products (Huang et al. 2009; Fang et al. 2010) and disagreeable odour and taste compounds (Li et al. 2012). Cyanobacteria, usually a prevailing component of algal blooms, also produce many toxins (Harada 2004). The current knowledge of the influence of AOM on water quality and the water treatment processes are reviewed in detail by Pivokonsky et al. (2016). AOM includes extracellular organic matter (EOM) derived from the metabolic activity of algae and cellular organic matter (COM) released when cells are damaged. COM is released into water at higher rates when pre-oxidation methods are used to enhance the coagulation of algal cells (Ma et al. 2012; Xie et al. 2013) and especially during the decay of algal blooms, which usually lead to a sudden decrease in coagulation efficiency (Pivokonsky et al. 2009a). This could be temporarily overcome by increasing coagulant dose. However, this generates subsidiary problems, e.g. an increase in operating cost and yield of sludge.

COM includes a wide spectrum of substances such as oligosaccharides, polysaccharides, proteins, peptides, amino acids and some other organic acids (Lüsse et al. 1985; Maksimova et al. 2004). In general, the composition of COM can be characterized as non-protein and protein organic matter (Pivokonsky et al. 2006). Some studies have demonstrated that, for instance, proteins produced by the cyanobacterium *Microcystis aeruginosa* during its stationary growth phase make up about 60–65% of its COM (Pivokonsky et al. 2006; Henderson et al. 2008). As a result of the release of COM during algal growth, there are increasing amounts of proteins in the cultivation media of several species. The peptide/protein portion reached up to 47% of the total organics for *Microcystis aeruginosa*, 42% for the diatom *Fragilaria crotonensis* and 28% for the green alga *Chlamydomonas geitleri* (Pivokonsky et al. 2014).

COM peptides and proteins may have either a positive or negative effect on coagulation. They can improve coagulation by acting as polymer aids under specific conditions (Bernhardt et al. 1985; Ma et al. 2012). On the other hand, COM peptides and proteins may adversely affect the coagulation process and increase the consumption of coagulant by forming soluble complexes with metal ions (Fe and Al) used as coagulants (Pivokonsky et al. 2006, 2012; Takaara et al. 2007). In addition, COM influences the coagulation of other impurities present in inpurified water, e.g. inorganic colloids or humic substances (HS). The COM peptides/proteins produced by *M. aeruginosa* can enhance coagulation of humic substances if the process is operated within a certain pH range. The positive effect occurs due to electrostatic, hydrophobic and

dipole-dipole interactions between proteins and HS (Pivokonsky et al. 2015). Some studies have also revealed the effect of AOM components on coagulation of quartz (Bernhardt et al. 1985) or kaolin particles (Takaara et al. 2007, 2010). However, the effect of reaction conditions (pH, coagulant dose etc.) and the character of COM (molecular weight, surface charge of molecules, functional group content etc.) on coagulation of particulate impurities has not been adequately explained. Therefore, this study is aimed at the elucidation of the effect of COM peptides/proteins (isolated from cyanobacterium *Microcystis aeruginosa*) on the coagulation of a hydrophobic kaolinite suspension and description of the mechanisms of the interactions between peptides/proteins, kaolinite particles and hydrolysis products of the coagulant.

Materials and Methods

Kaolinite Samples

The kaolinite clay (particles < 4 μm) was obtained from the deposit at Sedlec (Sedlecky kaolin a.s., Czech Republic). Aqueous suspension of kaolinite particles was homogenized using an ultrasonic homogenizer (UP400S, Hielscher Ultrasonics, Germany) at 100% amplitude of ultra-sonication (400 W) in pulse mode for 30 min, and subsequently used in coagulation experiments.

Kaolinite Surface Charge Determination

The surface charge of kaolinite was determined using potenciometric titrations performed at three electrolyte concentrations. Specifically, 40 g of kaolinite clay (< 4 μm) was mixed with 1.0, 0.1 and 0.01 M solutions of NaCl so that the final volume was 400 ml. The samples were homogenized using an ultrasonic homogenizer (UP400S, Hielscher Ultrasonics, Germany) at 100% amplitude of ultra-sonication (400 W) in pulse mode for 30 min. Then, 0.1 M NaOH was added to obtain an initial pH of 12 and the samples were titrated with 0.1 M HCl to pH 2.5 in a nitrogen atmosphere using an Orion 960 Autotitrator (Thermo Scientific, USA). Blank titrations were also performed. Relative surface charge was determined from the difference between the surface titration curves and the blank curves. Relative surface charge was then plotted against pH. The pH at which the curves of three electrolyte concentrations crossed was the pH at which kaolinite particles exhibit zero net charge at the surface (pH of point of zero charge, i.e. pH_{pzc}). This method is described in detail in the literature (van Raij and Peech 1972; Coles and Yong 2002).

COM peptide/protein preparation

Cyanobacterium *Microcystis aeruginosa* used in this study was harvested at the Svihov water reservoir (Czech Republic). Sampling was done using a plankton net with a mesh size of 0.01 mm. The sampled cells were separat-

ed from coarse impurities by washing in ultra-pure water and passing the sample through a sieve with mesh size of 0.1 mm. Subsequently, the cells were separated from water by filtration through 0.22 μm membrane filter (Millipore, USA). Quantitative microscopic analysis of the separated cells showed that samples consisted of approximately 99% *M. aeruginosa*. Thereafter, the cells were stirred with ultra-pure water and disrupted in an ice bath using an ultrasonic homogenizer (UP400S, Hielscher Ultrasonics, Germany) at 60% amplitude of ultra-sonication (240 W) in pulse mode for 5 min. The residual solids were removed by centrifugation and subsequently by a 0.22 μm membrane filter (Millipore, USA). Peptides/proteins were isolated from the COM using $(NH_4)_2SO_4$ to precipitate protein (Dawson et al. 1986). The peptide/protein precipitate was then separated from the non-protein organic matter by filtration through a 0.22 μm membrane filter (Millipore, USA), dissolved in 200 ml of ultra-pure water and purified using an ultrafiltration membrane PLAC 1000 Da (Millipore, USA) and a Solvent Resistant Stirred Cell (Millipore, USA).

COM peptide/protein characterization

Dissolved organic carbon (DOC) concentration was monitored in samples filtered through 0.22 μm membrane filter (Millipore, USA) using a Shimadzu TOC-V_{CPH} analyzer (Shimadzu Corporation, Japan) that measured the organic carbon content by the TC-IC method as the difference between TC (total carbon) and IC (inorganic carbon). The average DOC value for each sample was determined from three measurements and the error was less than 2%.

Apparent molecular weights (MW) of COM peptides/proteins were determined by high performance size exclusion chromatography (HPSEC) using the method described in the literature (Hnatukova et al. 2011; Pivokonsky et al. 2012). Reproducibility of the MW fractionation of COM protein samples was very good, with MW deviations of less than 3% between repeated measurements.

Isoelectric points (pI) of COM peptides/proteins were determined by isoelectric focusing (IEF) using a Multiphor II electrophoresis system (Pharmacia, Sweden) according to the method described in the literature (Hnatukova et al. 2011).

Peptides/proteins, which are able to form soluble complexes with iron, were isolated by affinity chromatography. The samples of peptides/proteins were passed through an affinity column (1 ml HiTrap[TM], Amersham Bioscience Corp., Japan) in which Fe^{3+} ions were immobilized as ligands. Binding buffer was prepared with 0.02 M sodium phosphate and 0.5 M NaCl (pH 6). Elution buffer was of the same composition as the binding buffer, but its pH was set to 9. The elution strategy was developed in order not to damage peptides/proteins and prepare a sample suitable for UV detection. The flow rate of buffer was 1 ml min^{-1} and the volume of the fractions

collected was 15 ml. Then, the eluted fractions were desalted and concentrated using an ultrafiltration membrane PLAC 1000 Da (Millipore, USA) and a Solvent Resistant Stirred Cell (Millipore, USA). MWs of isolated peptides/proteins were determined using HPSEC. All analyses were done in triplicate.

Coagulation Tests

The influence of COM peptides/proteins on the coagulation process was investigated using standard jar tests (Bratby 2006). Jar testing was done with a variable speed eight paddle stirrer LMK 8–03 (IH AS CR, Czech Republic) in 2 l jars. Ferric sulphate (Sigma-Aldrich, USA) was used as a coagulant because the study of Pivokonsky et al. (2009b) has shown that its efficiency in COM peptide/protein coagulation is higher than that of aluminium coagulants. Its optimum dose for efficient peptide/protein removal was determined by using tests without pH control and with coagulant doses ranging from 0.025 to 0.250 mmol l^{-1} of Fe (1.4–14.0 mg l^{-1}). For experiments in which the pH was controlled and coagulant dose optimized, 0.1 M HCl and 0.1 M NaOH were added to achieve the target pH varying between 3 and 9. The jar test procedure consisted of 1 minute of high intensity agitation ($G = 300$ s^{-1}), 15 minutes of low intensity agitation ($G = 80$ s^{-1}) and 60 minutes of settling. The results of coagulation tests were evaluated by water analysis after sedimentation of the suspension. Residual Fe, dissolved organic carbon (DOC), turbidity, pH, alkalinity and molecular weight of residual peptides/proteins were monitored. In order to evaluate the influence of COM peptides/proteins on coagulation of kaolinite suspension, three types of jar tests were operated within the pH range 3–9 using the optimum coagulant dose of 7 mg l^{-1}, i.e. 0.125 mmol l^{-1} of Fe. Moreover, the comparison of jar testing results enabled the description of probable coagulation mechanisms. To facilitate the comparison between different types of jar tests, the optimum dose for peptide/protein removal was also used in other types of jar tests. The jar tests were as follows:

1) coagulation of suspended kaolinite particles,
2) coagulation of COM peptides/proteins,
3) coagulation of suspended kaolinite particles together with COM peptides/proteins.

The corresponding samples of synthetic raw water were used:

1) Ultra-pure water with an alkalinity of 1.5 mmol l^{-1} (75 mg l^{-1} CaCO$_3$) with NaHCO$_3$ + 25 mg l^{-1} of kaolinite particles < 4 μm.
2) Ultra-pure water with an alkalinity of 1.5 mmol l^{-1} (75 mg l^{-1} CaCO$_3$) with NaHCO$_3$ + COM peptides/proteins of DOC concentration 8 mg l^{-1}.
3) Ultra-pure water with an alkalinity of 1.5 mmol l^{-1} (75 mg l^{-1} CaCO$_3$) with NaHCO$_3$ + 25 mg l^{-1} of kaolinite particles < 4 μm + COM peptides/proteins of DOC concentration 8 mg l^{-1}.

DOC concentration of 8 mg l^{-1} is the common COM peptide/protein content in natural surface water (Pivokonska et al. 2008).

Results and Discussion

COM Peptide/Protein Characterization

The COM peptides/proteins were characterized in terms of MW distribution. Fig. 1 shows peptides/proteins isolated from COM produced by the cyanobacterium *M. aeruginosa* of apparent MWs of 1, 2.8, 4, 4.5, 5, 5.7, 6, 6.8, 8, 8.5, 12, 30, 40, 52, 106, 266, 470 and 1077 kDa. The values of peptide/protein isoelectric points (pI) determined by isoelectric focusing (IEF) were 4.79, 5.12, 5.25, 5.45, 5.62, 5.80, 6.10, 6.33, 6.47, 6.63, 7.05, 7.39, 7.82, 7.93 and 8.05. The character of COM peptides/proteins of *M. aeruginosa* has been discussed in our previous studies (Pivokonsky et al. 2006, 2012, 2014; Hnatukova et al. 2011).
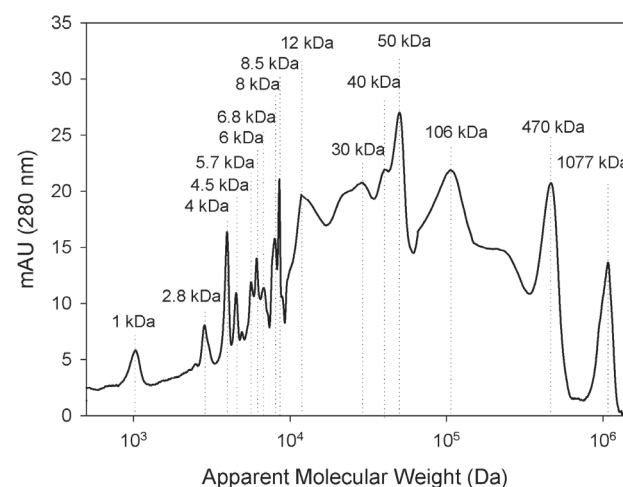

Fig. 1 HPSEC profile of COM peptides/proteins.

Coagulation of Kaolinite Suspension

Fundamental mechanisms of kaolinite coagulation are charge neutralization and adsorption (Bache and Gregory 2007). Their efficiency is closely related to the surface charge value (of both kaolinite particles and hydrolysis products of coagulation agent), which is pH dependent. As for ferric hydroxocomplexes, at pH < 2, Fe^{3+} ions occur in a water environment as Fe-hexaaquacomplex [Fe(H$_2$O)$_6$]$^{3+}$. At pH ~ 2, double nuclear Fe-hydroxocomplex [Fe$_2$(OH)$_2$]$^{4+}$ ions are formed due to the release of protons from the ion. As the pH rises (pH > 2), hydrolysis proceeds and the positively charged polynuclear Fe-hydroxopolymers (i.e. [Fe$_2$(OH)$_3$(H$_2$O)$_7$]$^{3+}$, [Fe$_2$(OH)$_4$(H$_2$O)$_5$]$^{5+}$ and [Fe$_4$(OH)$_6$(H$_2$O)$_{12}$]$^{6+}$) and Fe-oxide-hydroxides α-FeO(OH) or γ-FeO(OH) are formed. At pH > 8, iron largely occurs as anionic hydroxocomplexes, e.g. [Fe(OH)$_4$]$^-$ (Stumm and Morgan 1996). The surface charge of a kaolinite suspension, specifically

its point of zero charge (pH_{pzc}), depends on the chemical composition of kaolinite. In this study, pH_{pzc} was determined by potentiometric titrations at three different electrolyte concentrations (0.01, 0.1 and 1.0 M NaCl) and was set to approximately pH = 3. It implies that negatively charged sites on the kaolinite surface prevail at pH > 3 and that the total kaolinite charge is negative.

The coagulation tests performed with aqueous suspension containing 25 mg l^{-1} of kaolinite particles and with an iron dose of 7 mg l^{-1} (i.e. 0.125 mmol l^{-1} Fe) showed that the lowest residual concentrations of both kaolinite (expressed as residual turbidity) and iron were reached in the pH range 6.5 to 8 (Fig. 2). Very similar results for kaolinite coagulation are reported by Kim and Kang (1998) who recorded the highest kaolinite removal by ferric nitrate (initial kaolinite concentration 25 mg l^{-1}) at a pH between 6.7 and 8.2. Within this pH range, positively charged iron hydroxocomplexes and iron oxides-hydroxides are adsorbed on negatively charged kaolinite particles, which results in a gradual neutralization of the kaolinite surface charge and efficient coagulation. Adsorption of iron constituents is explained by electrostatic interactions, exchanging reactions and hydrogen bonding (Bache and Gregory 2007).

Coagulation of COM Peptides and Proteins

The results of coagulation tests with peptides/proteins (DOC 8 mg l^{-1}) and ferric sulphate (7 mg l^{-1} = 0.125 mmol l^{-1} of Fe) are shown in Fig. 3. The lowest residual peptide/protein concentration (expressed as residual DOC concentration) was achieved within the pH range 4 to 6. The capability of COM peptides/proteins to be coagulated stems depended on the character and content of functional groups and also their molecular weight, which will be discussed later. Some of the functional groups, such as –OH, –COOH, –SH, –NH$_2$, –CONH$_2$ etc. may bear a charge under certain pH conditions, which allows coagulation by charge neutralization and/ or adsorption (Bernhardt et al. 1985). If the isoelectric

points of peptides/proteins are taken into consideration, it is obvious that at the pH of the highest coagulation efficiency (4–6), peptides/proteins bear both negatively and positively charged functional groups on their surface. They are therefore able to interact electrostatically with positively charged hydrolysis products of iron. At pH around 6, a noticeable increase in residual DOC and iron concentration was recorded, which means that a portion of the peptides/proteins and iron remained in solution owing to the formation of soluble Fe-peptide/protein surface complexes. Our previous study (Pivokonsky et al. 2012) showed that the mechanisms of Fe-peptide/protein complex formation are largely of electrostatic character and that the ability of peptides/proteins to form complexes with Fe (i.e. their binding capacity) is dependent on pH. It reaches its maximum at pH 6–7. Naturally, if Fe ions are bound to peptides/proteins, they cannot take part in the coagulation process (Bernhardt et al. 1985; Pivokonsky et al. 2006; Takaara et al. 2007). Moreover, iron bound to peptides/proteins blocks negatively charged sites on the peptide/protein surface, which prevents peptides/proteins from being coagulated by adsorption and charge neutralization mechanisms (Pivokonsky et al. 2012). As seen in Fig. 3, residual DOC and Fe concentrations sharply increased at pHs > 7. At this pH value, the negative charge of both hydrolysis products of iron and peptides/proteins prevails and thus, repulsive electrostatic interactions lead to inefficient coagulation.

In order to characterize peptides/proteins able to form soluble complexes with iron, affinity chromatography followed by HPSEC was performed. Fig. 4 shows that complex forming peptides/proteins have MWs of 1, 2.8, 6, 8, 8.5, 10 and 52 kDa. It is well known that cyanobacterial COM may contain several groups of metal binding compounds. The low-MW region probably includes iron-binding peptides of MW of 500–1500 Da called siderophores, which are secreted by cyanobacteria under conditions of iron stress and enable the transport of ferric ions into cells (Albrecht-Gary and Crumbliss 1998). In addition, low-MW compounds might be cyanobacteri-
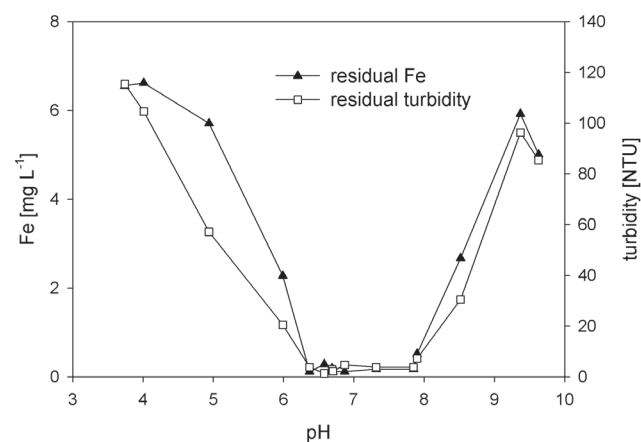
Fig. 2 Jar tests with kaolinite - dependence of residual Fe and turbidity on pH value (D_{Fe} = 7 mg l^{-1}).
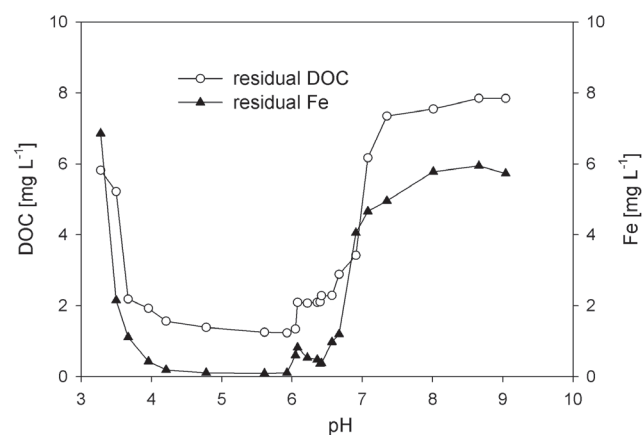
Fig. 3 Jar tests with peptides/proteins - dependence of residual DOC and Fe on pH value (D_{Fe} = 7 mg l^{-1}).

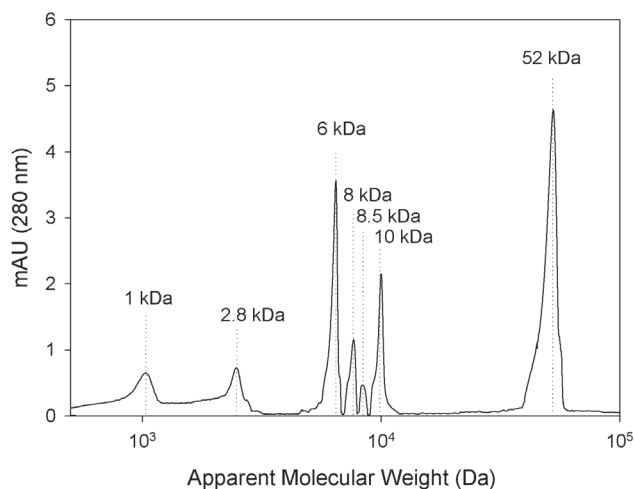**Fig. 4** HPSEC profile of complex forming peptides/proteins.

Fig. 5 Jar tests with kaolinite + peptides/proteins-dependence of residual DOC, Fe and turbidity on pH value ($D_{Fe} = 7$ mg l^{-1}).

al metallothioneins, cysteine-rich peptides/proteins that bind, sequester and buffer the excess intracellular metal cations through the thiol group of its cysteine residues (Turner and Robinson 1995). The isolated iron-binding protein of MW 52 kDa probably is the cyanobacterial metalloenzyme bidirectional hydrogenase, which has an affinity for iron and is present in *M. aeruginosa* (Tamagnini et al. 2007). Fe-binding protein of a similar molecular weight was also isolated in several other studies (Pivokonsky et al. 2006, 2012; Takaara et al. 2007).

Coagulation of Kaolinite Together with COM Peptides and Proteins

Coagulation tests with kaolinite (25 mg l^{-1}), peptides/proteins (DOC 8 mg l^{-1}) and ferric sulphate (7 mg l^{-1} = 0.125 mmol l^{-1} of Fe) revealed that the optimum pH conditions were within almost the same range as the above described coagulation tests with peptides and proteins. Kaolinite particles, peptides/proteins and iron were efficiently removed at pHs between 4 and 5.5 (Fig. 5). As the pH value rose, the DOC removal efficiency decreased and the peptide/protein coagulation ceased at pH about 7. Further, Fig. 5 also shows that the removability of kaolinite particles is closely connected with the coagulation of COM peptides/proteins. In the presence of these organic substances, kaolinite was removed even at pHs < 5.5. However, as demonstrated before, kaolinite particles were not removed within this pH range in the absence of peptides/proteins. The probable mechanisms involved in the coagulation of peptides/proteins and kaolinite are again charge neutralization and adsorption. At pHs < 5.5, not only electrostatic interactions between positively charged iron hydroxocomplexes and negatively charged ionized functional groups of peptides/proteins occur (as described for coagulation of peptides/proteins), but there are also electrostatic interactions between positively charged peptide/protein functional groups (e.g. –NH$_3^+$) and negatively charged kaolinite particl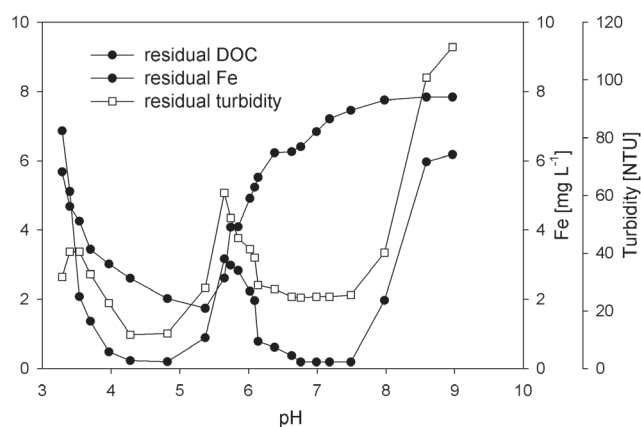es. These interactions lead to the gradual neutralization of the surface charge of both kaolinite particles and peptides/proteins and subsequently enable the formation of uncharged micro-aggregates (Fig. 6). Furthermore, kaolinite was also removed within the pH range 6.5–8 resulting in low residual turbidity and iron concentrations, but peptides/proteins obviously did not participate in the coagulation process and their residual content remained high. This pH optimum for removal of kaolinite corresponds to the optimum for coagulation in the test performed only with kaolinite and ferric sulphate (Fig. 2). Moreover, as in the case of coagulation tests with peptides/proteins (Fig. 3), there is a peak of residual iron at a pH of about 6 in Fig. 5. This peak is likely to be caused by two distinct features. Firstly, it can be attributed to the formation of soluble Fe-peptide/protein complexes, similar to the coagulation of peptides/proteins in the absence of kaolinite. Secondly, it may represent the transition between two different processes, i.e. the coagulation of peptides/proteins and kaolinite together at pH 4–5.5 and coagulation of kaolinite itself at pH 6.5–8. Finally, at pH > 8, no coagulation occurred due to the excess of the negative charge of all particles in the system – kaolinite, peptides/proteins and also iron constituents.

HPSEC analysis performed after coagulation tests with kaolinite, peptides/proteins and ferric sulphate demonstrated that high-MW proteins are removed under optimal reaction conditions (HPSEC profile at pH 5), whereas low-MW peptides/proteins remain in the solution (Fig. 7). These peptides/proteins were found to have MW 10, 8.4, 7.7, 6.5, 2.8 and 1 kDa. Interestingly, these peptides/proteins were shown by affinity chromatography to form soluble complexes with iron, which is consistent with findings of other studies (Pivokonsky et al. 2009a, 2015; Ma et al. 2012), in which high-MW COM compounds were removed with higher efficiency than low-MW compounds. In addition, only negligible amounts of peptides/proteins were removed during coagulation at pH 8.
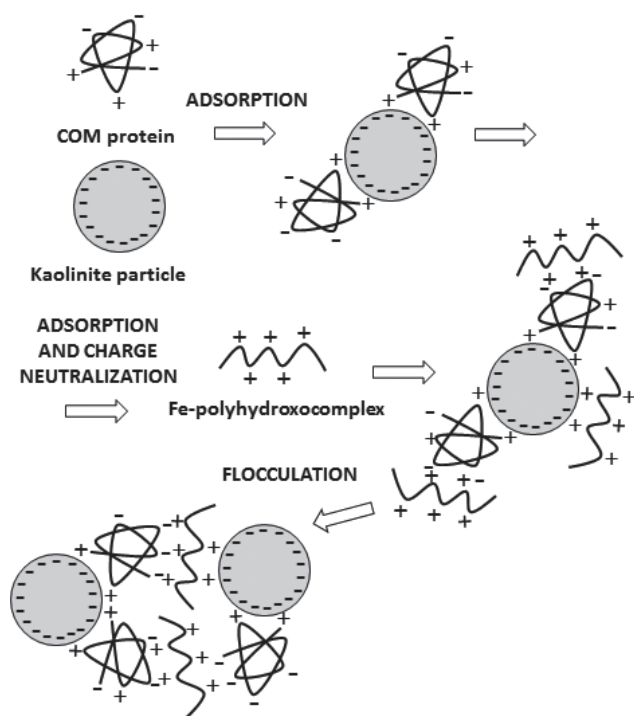
Fig. 6 Mechanism of coagulation of peptides/proteins and kaolinite.

Fig. 7 HPSEC profile of peptides/proteins after coagulation tests at pH values 8 and 5.

Acknowledgements

Conclusions

This research demonstrates that the removal of COM peptides/proteins during water treatment is strongly pH-dependent and that COM peptides/proteins affect the removal of kaolinite particles. The coagulation process is commonly performed at neutral pH during water treatment. This pH value is suitable for treatment of highly turbid waters, which is supported by our finding that kaolinite particles are efficiently removed within a pH range of 6.5 to 8. Nevertheless, the results of coagulation tests showed that the optimum pH for COM peptides/proteins (DOC) removal by ferric sulphate is in the range of 4–6, when electrostatic interactions between positively charged iron constituents and negatively charged sites on peptide/protein molecules enable coagulation through charge neutralization and adsorption. Interestingly, at relatively low pHs (4–5.5), COM peptides/proteins contribute to the removal of kaolinite. The present findings suggest that during the seasonal growth of cyanobacteria, decrease in reaction pH is a prerequisite for the efficient removal of COM proteins and is also convenient for clearing turbid water. Regarding peptide/protein characteristics related to coagulation, HPSEC analysis showed that high-MW proteins are effectively removed at optimal reaction pHs (4–5.5), whereas low-MW proteins are poorly removed. Moreover, it was found that several peptides/proteins are able to form soluble complexes with iron used as a coagulant at a pH of about 6. This feature deteriorates the coagulation of COM peptides/proteins and of kaolinite particles.
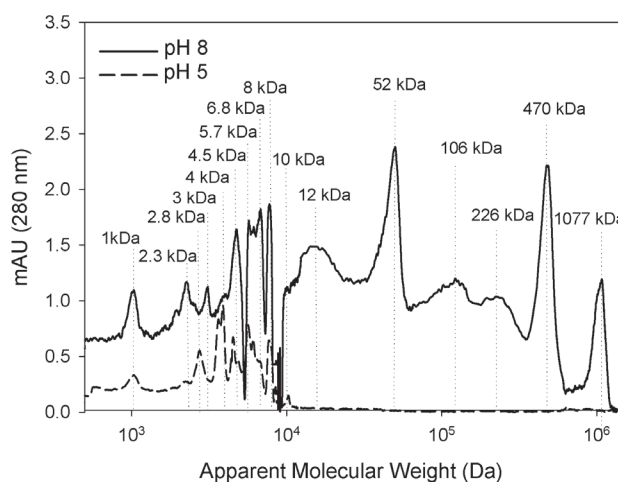
REFERENCES

Albrecht-Gary AM, Crumbliss AL (1998) Coordination chemistry of siderophores: thermodynamics and kinetics of iron chelation and release. In: Sigel A, Sigel H (eds) Metal Ions in Biological Systems - Iron Transport and Storage in Microorganisms, Plants and Animals. Marcel Dekker, New York, pp. 239–327.

Bache DH, Gregory R (2007) Flocks in Water Treatment. IWA Publishing, London.

Bernhardt H, Hoyer O, Shell H, Lüsse B (1985) Reaction mechanisms involved in the influence of algogenic organic matter on flocculation. Z Wasser-Abwasser-Forsch 18: 18–30.

Bratby J (2006) Coagulation and Flocculation in Water and Wastewater Treatment. 2nd ed. IWA Publishing, London.

Campinas M, Rosa MJ (2010) Assessing PAC contribution to the NOM fouling control in PAC/UF systems. Water Res 44: 1636–1644.

Coles CA, Yong RN (2002) Aspects of kaolinite characterization and retention of Pb and Cd. Appl Clay Sci 22: 39–45.

Dawson RMC, Elliott DC, Elliott WH, Jones KM (1986) Data for Biochemical Research. 3rd ed. Oxford University Press, New York.

Fang J, Yang X, Ma J, Shang C, Zhao Q (2010) Characterization of algal organic matter and formation of DBPs from chlor(am)ination. Water Res 44: 5897–5960.

Harada K-I (2004) Production of secondary metabolites by freshwater cyanobacteria. Chem Pharm Bull 52: 889–899.

Henderson RK, Baker A, Parsons SA, Jefferson B (2008) Characterisation of algogenic organic matter extracted from cyanobacteria, green algae and diatoms. Water Res 42: 3435–3445.

Hnatukova P, Kopecka I, Pivokonsky M (2011) Adsorption of cellular peptides of *Microcystis aeruginosa* and two herbicides onto activated carbon: effect of surface charge and interactions. Water Res 45: 3359–3368.

Huang J, Graham N, Templeton MR, Zhang Y, Collins C, Nieuwenhuijsen M (2009) A comparison of the role of two blue-green algae in THM and HAA formation. Water Res 43: 3009–3018.

Kim JS, Kang LS (1998) Investigation of coagulation mechanisms with Fe(III) salt using jar tests and flocculation dynamics. Environ Eng Res 3: 11–19.

Li L, Gao N, Deng Y, Yao J, Zhang K (2012) Characterization of intracellular & extracellular algae organic matters (AOM) of *Microcystis aeruginosa* and formation of AOM-associated disinfection byproducts and odor & taste compounds. Water Res 46: 1233–1240.

Lüsse B, Hoyer O, Soeder CJ (1985) Mass cultivation of planktonic freshwater algae for the production of extracellular organic-matter (EOM). Z Wasser-Abwasser-Forsch 18: 67–75.

Ma M, Liu R, Liu H, Qu J, Jefferson W (2012) Effects and mechanisms of pre-chlorination on *Microcystis aeruginosa* removal by alum coagulation: Significance of the released intracellular organic matter. Sep Pur Technol 86: 19–25.

Maksimova IV, Bratkovskaya LB, Plekhanov SE (2004) Extracellular carbohydrates and polysaccharides of the alga *Chlorella pyrenoidosa* Chick S-39. Biol Bull 31: 175–181.

Pivokonska L, Pivokonsky M, Tomaskova H (2008) Optimization of NOM removal during water treatment. Separ Sci Technol 43: 1687–1700.

Pivokonsky M, Kloucek O, Pivokonska L (2006) Evaluation of the production, composition and aluminum and iron complexation of algogenic organic matter. Water Res 40: 3045–3052.

Pivokonsky M, Polasek P, Pivokonska L, Tomaskova H (2009a) Optimized Reaction Conditions for Removal of Cellular Organic Matter of *Microcystis aeruginosa* During the Destabilization and Aggregation Process Using Ferric Sulphate in Water Purification. Water Environ Res 81: 514–522.

Pivokonsky M, Pivokonska L, Bäumeltova J, Bubakova P (2009b) The effect of cellular organic matter produced by cyanobacteria *Microcystis aeruginosa* on water purification. J Hydrol Hydromech 57: 121–129.

Pivokonsky M, Safarikova J, Bubakova P, Pivokonska L (2012) Coagulation of peptides and proteins produced by *Microcystis aeruginosa*: Interaction mechanisms and the effect of Fe-peptide/protein complexes formation. Water Res 46: 5583–5590.

Pivokonsky M, Naceradska J, Brabenec T, Novotna K, Baresova M, Janda V (2015) The impact of interactions between algal organic matter and humic substances on coagulation. Water Res 84: 278–285.

Pivokonsky M, Naceradska J, Kopecka I, Baresova M, Jefferson B, Li X, Henderson K (2016) The impact of algogenic organic matter on water treatment plant operation and water quality: A review. Crit Rev Env Sci Technol 46: 291–335.

Pivokonsky M, Safarikova J, Baresova M, Pivokonska L, Kopecka I (2014) A comparison of the character of algal extracellular versus cellular organic matter produced by cyanobacterium, diatom and green alga. Water Res 51: 37–46.

Stumm W, Morgan JJ (1996) Aquatic Chemistry. 3rd ed. John Wiley and Sons, New York.

Takaara T, Sano D, Konno H, Omura T (2007) Cellular proteins of *Microcystis aeruginosa* inhibiting coagulation with polyaluminum chloride. Water Res 41: 1653–1658.

Takaara T, Sano D, Masago Y, Omura T (2010) Surface-retained organic matter of *Microcystis aeruginosa* inhibiting coagulation with polyaluminium chloride in drinking water treatment. Water Res 44: 3781–3786.

Tamagnini P, Leitão E, Oliveira P, Ferreira D, Pinto F, Harris D J, Heidorn T, Lindblad P (2007) Cyanobacterial hydrogenases: diversity, regulation and applications. FEMS Microbiol Rev 31: 692–720.

Turner JS, Robinson NJ (1995) Cyanobacterial metallothioneins: biochemistry and molecular genetics. J Ind Microbiol 14: 119–125.

Van Raij BV, Peech M (1972) Electrochemical properties of some oxisols and alfisols of the tropics. Soil Sci Soc Am Pro 36: 587–593.

Xie P, Ma J, Fang J, Guan Y, Yue S, Li X, Chen L (2013) Comparison of Permanganate and Preozonation on Algae Containing Water: Cell Integrity, Characteristics, and Chlorinated Disinfection Byproduct Formation. Environ Sci Technol 47: 14051–14061.

FACTORS AFFECTING METAL AND RADIONUCLIDE POLLUTION IN THE BALTIC SEA

MARTIN LODENIUS*

Department of Environmental Sciences, University of Helsinki, Finland
* Corresponding author: martin.lodenius@helsinki.fi

ABSTRACT

External pollution load in the Baltic Sea originates from urban, agricultural and industrial sources. Emissions of heavy metals have decreased substantially in the catchment area but the temporal trends are not always significant and differ with sample, area and pollutant. The most significant source of anthropogenic radioactivity in the Baltic Sea is fallout from the Chernobyl accident in 1986. Many factors affect the future development of pollutant concentrations including anthropogenic emissions, political decisions and changes in salinity, temperature and water currents, in eutrophication and oxygen status, in fisheries and in atmospheric deposition of pollutants. Large scale changes like eutrophication and climate change affect ecosystems in many ways, directly and indirectly, causing biological and abiotic effects. These factors are interrelated and difficult to predict. Measures aiming to enhance the ecological status of the Baltic Sea will certainly give positive results but this will take at least several decades.

Keywords: Baltic Sea, cadmium, lead, mercury, radionuclides, pollution, pressure

Introduction

The Baltic Sea is one of the most polluted seas in the world and its ecological status is affected by it being relatively shallow, slow water renewal and a salinity gradient increasing from zero to 2.5%. Salinity and temperature stratification limit water exchange and oxygen depletion is common at the bottom in deep areas. In addition to the thermocline there is a halocline at a depth of about 40–70 m. The salinity increases from 2–4 PSU in the Bothnian Bay to 6–8 PSU in the Baltic proper, while the water below the permanent halocline is up to 13–20 PSU (Elmgren 2001). The area of the Baltic Sea is approximately 350,000 km^2 with a drainage area covering 1.74 million km^2 in fourteen countries. The catchment area of the Baltic Sea consists of forests (54%), agricultural land (26%), wetlands or drained wetlands (20%) and built-up areas 4%." (HELCOM 2007a). Urbanization and industrialization started early and forests and wetlands are far from their natural state. The catchment of the Baltic Sea is under heavy anthropogenic influence with many industrial areas and a population of 85 million people. None of the sub-basins of the Baltic Sea is considered to have an acceptable environmental status and the whole sea is contaminated with hazardous substances with a status of mainly moderate (HELCOM 2010b).

The volume of the Baltic Sea is approximately 20,000 km^3 (HELCOM 2007a) and the theoretical time for complete exchange of water with the North Sea is approximately 25–35 years (Skowrońska et al. 2009). Baltic Sea consists of nine sub-basins that differ in size, physiographic and biological properties and pollution load. Biodiversity is limited due to these special conditions. Pollutants in the Baltic Sea has been monitored intensively for decades by HELCOM (Helsinki Convention on the Protection of the Marine Environment of the Baltic Sea Area) and its member states. This has revealed the distribution, trends in and ecological importance of pollutants. In relation to HELCOM target levels PCB is top of the listed pollutants followed by Pb, Hg and ^{137}Cs (HELCOM 2010a). Eutrophication, hazardous substances in biota and oxygen depletion in bottom waters and sediments are the most important issues in the Baltic Sea environment. In this review the focus is directed towards concentrations and trends in pollutant levels of three metals (Cd, Pb and Hg) and radionuclides and the factors influencing these trends.

Many factors affect the concentrations of pollutants, including anthropogenic emissions, political decisions and legislation, climate change, eutrophication and fisheries. These factors are interrelated and the outcome difficult to predict. These complex ecological-social systems require holistic approaches like EBM (Ecosystem Based Management) or DPSIR (Drivers, Pressures, State changes, Impacts and Responses) (e.g. Skowrońska et al. 2009, Elmgren et al. 2015). Increasing environmental awareness, technological development and the collapse of communism in Eastern Europe have resulted in the
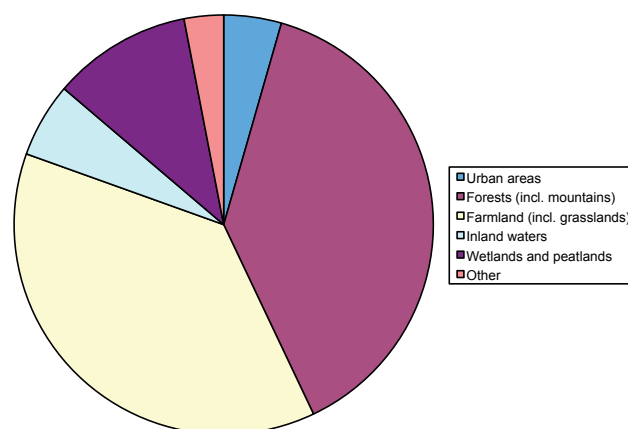

Fig. 1 Land use around the Baltic Sea (data from HELCOM 2002).

closure of many polluting industries (Vallius 2014). Although emissions of heavy metals and other persistent pollutants have decreased substantially in the catchment area over the last few decades there are still worryingly high concentrations in parts of the Baltic ecosystem.

Loads of Heavy Metals

External pollution comes via rivers and coastal sources, from the North Sea and the atmosphere. Emissions originate from urban, agricultural and industrial sources. The waterborne emissions of Cd, Pb and Hg from rivers are considerably bigger than the atmospheric deposition (Table 1). The waterborne inputs include runoff from terrestrial areas (diffuse, urban and industrial sources including hotspot areas). The great rivers contribute significantly to the load of Cd, Pb and Hg (Table 2). A list of hotspot areas was established by HELCOM in 1992 and over two thirds of these sites have now been removed from the list. The remaining 45 sites include industrial, agricultural and municipal sources.

Table 1 Annual waterborne emissions and atmospheric deposition (tonnes) of three metals in the Baltic Sea (inputs of Hg from Polish rivers not included).

	Cd	Pb	Hg
Waterborne inputs (HELCOM 2011)	47.7	282	0.8
Atmospheric deposition (HELCOM 2007b)	5.7	235	2.9
Total input	53.4	517	3.7

Table 2 The most important inputs (t; average annual inputs for 2005–2007) of Cd, Pb and Hg via rivers into the Baltic Sea (HELCOM 2010b).

	Cd	Pb	Hg
Kemijoki	–	–	0.06
Lule älv	–	4	–
Vistula	9	27	–
Swedish Bothnian Sea coast	4	–	–
Kyrönjoki	0.24	–	–
Dalälven	0.24	–	0.05
Karvianjoki	0.18	–	–
Götaälven	0.19	9	–
Kokemäenjoki	1.3	10	–
Polish open sea coast	–	–	0.6
Neva	29	125	–
Narva	–	8	0.14
Slupia	–	–	0.19
Daugava	2.5	14	–
Lupawa	–	–	0.12
Nemunas	0.12	9	0.8
Leba	–	–	0.29
Pasleka	–	–	0.06
Total	38	206	2.3

The atmospheric deposition of lead remained rather high even after European Union banned the use of leaded gasoline in vehicles in 2000. According to EMEP (2013) the annual atmospheric deposition of cadmium had increased in 2011 to 7.2 tonnes while that of lead and mercury had decreased to 194 and 2.8 tonnes respectively (Table 3). The greatest emissions came from Poland. The deposition of Cd is approximately 5–10 g/km^2 in the northern parts (Bothnian Bay, Bothnian Sea, Archipelago Sea, Gulf of Finland) and approximately 20 g/km^2 in the southern parts (Gulf of Riga, Baltic Proper, Western Baltic, The Sound, Kattegat). For lead the deposition is approximately 0.5 kg km^{-2} and approximately 0.7 kg km^{-2} in the south. For mercury the figures are approximately 6 g km^{-2} and 10 g km^{-2}, respectively (Gusev 2015).

The annual amounts of heavy metals deposited from the atmosphere into the Baltic Sea decreased in the period from 1990 to 2012 by 53% for cadmium, 23% for mercury and 79% for lead (Gusev 2014). The annual anthropogenic emission from HELCOM countries made up approximately 37% of the cadmium, 20% of the lead and approximately 14% of the mercury, respectively, deposited into the Baltic Sea in 2011 (Gusev 2009).

Table 3 Atmospheric deposition (t a^{-1}) of three metals in 1990, 2000 and 2013 into the Baltic Sea (Gusev 2015).

	Cd	Pb	Hg
1990	16.0	913	4.5
2000	12.0	429	4.0
2013	5.6	177	3.2

Heavy Metals in Sediments

Concentrations of heavy metals in sea water are generally very low and old results are not necessarily reliable. Dippner and Pohl (2004) report mean concentrations of total (dissolved and particulate) metals in the Western Baltic Sea of 15.5, 84 and 7 ng l^{-1} for Cd, Pb and Hg, respectively. The concentrations are similar above and below the halocline. The concentrations show a decreasing trend over the period 1990–1995: 62%, 66% and 74% for Cd, Pb and Hg, respectively. A small but essential part of the heavy metals in the water is exported into the North Sea (14%, 4.1% and 26% for Cd, Pb and Hg, respectively). According to Zalewska et al. (2015) reference values (for a period of little anthropogenic pressure) for Cd, Pb and Hg are 0.3 mg kg^{-1}, 30 mg kg^{-1} and 0.05 mg kg^{-1}, respectively, in the southern parts of Baltic Sea.
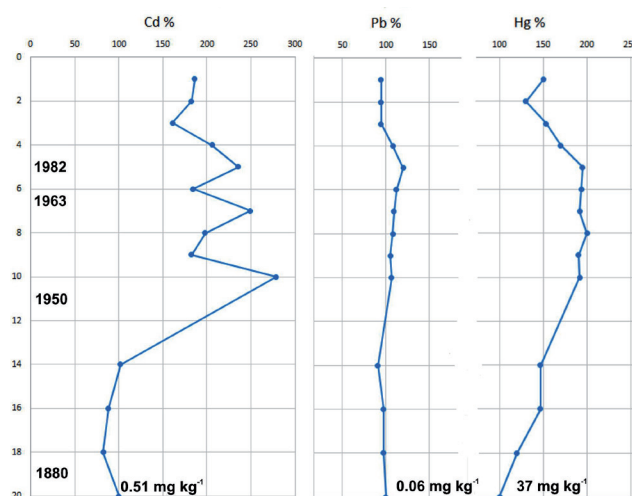
In aquatic environments metals and radionuclides are to a great extent bound to inorganic or organic particles and sedimented. There are estimates of surface sediment concentrations and metal accumulation for the northern parts of the Baltic Sea (Table 4). Metals are removed from the water phase mainly by sedimentation and fishing. Sediments act as a sink for heavy metals as new organic

and inorganic material cover older sediments. The concentrations in sediment cores indicate decreasing loads (Vallius and Leivuori 1999; Leivuori 2000; Vallius 2014). Heavy metals may be strongly but not totally irreversibly bound to sulphides or in other forms under anoxic conditions (e.g. Calmano et al. 1993). The binding to more or less insoluble sulphides is very strong for Cd and Pb, whereas Hg is enriched to a lesser extent at anoxic sites. The bioavailability of metals depends on chemical binding and solubility. In shallow water, especially, biological activity and currents may mix the sediments and bring metals back into circulation. As the physical and biological conditions of bottoms vary within a wide range it is difficult to quantify the amounts of metals that are recirculated. The estimated annual sedimentation of Cd, Pb and Hg is 113, 3084 and 6.8 tonnes, respectively, for the entire Baltic Sea in the 1980's (Borg and Jonsson 1996). These figures are much higher than the estimated input in 2004 (Table 1).

Sediment cores from deep water may reveal temporal trends in metal sedimentation but dating and interpretation of the results are not always straightforward. The vertical distribution of metals in sediments varies widely between different areas. In many cases background values can be found in sediments from the 19th century, while anthropogenic influence increases during the 20th century. Over the last few decades sediment concentrations have decreased as a result of decreased emissions. In the Gulf of Riga this development is clear for Cd and Hg, while surprisingly there is only a small decrease in Pb (Fig. 2; Leivuori et al. 2000). In the Gulf of Gdansk the highest Pb concentrations (63–147 µg g^{-1}) were measured in sediments deposited between 1960s and 1970s and the fraction of anthropogenic Pb was estimated to be 93% (Zaborska 2014). Also in the Gulf of Finland most trends in heavy metal concentrations (including Cd, Pb and Hg) are decreasing (Vallius 2012), whereas earlier

Fig. 2 Vertical sediment profiles for Cd, Pb and Hg in the Gulf of Riga as percentages of background concentrations (mg kg^{-1} d.w.). Age of dated sediment layers indicated to the left (data from Leivuori et al. 2000).

Vallius and Leivuori (1999) noted increasing Cd concentrations in the Gulf of Finland.

Heavy metals, especially cadmium, may be toxic to benthic organisms. This toxicity may be strongly dependent on temperature, salinity and oxygen concentration. In general, decreasing salinity and increasing temperature increases the toxicity of cadmium and other heavy metals. For lead toxicity stressful salinity enhance the toxic effects, while temperature has no significant effect. Suboptimal salinity and temperature may increase the sensitivity of benthic animals to mercury (McLusky et al. 1986; Strode and Balode 2013).

Heavy Metals in Biota

In the marine environment heavy metals and radionuclides are partly sedimented and partly taken up by the biota, including fish. The concentrations in fish vary widely but in most cases the trend is decreasing (Polak-Juszczak 2009, 2013; Voigt 1999, 2007).

A great part of the heavy metals and radionuclides in the Baltic Sea is bound to living and dead organisms and biota may significantly affect the fluxes of pollutants. Knowledge of the different food chains and their dynamics is essential for understanding the circulation of pollutants. Concentrations and trends of heavy metals in fish, mussels and sediments have been reported for some decades. During the 1980's and 1990's there was an increase and then a decrease after that. The temporal trends are not always significant and they are different for different samples, areas and pollutants (HELCOM 2010a).

Fish samples, e.g. sprat, herring, cod and flatfish, analyzed from different parts of the Baltic Sea revealed significant downward trends for Cd, Hg and Pb (Polak-Juszczak (2010, 2013; Table 5). When analyzing temporal trends in heavy metals in fish (liver for Cd and

Table 4 Average concentrations (mg kg^{-1} d.w.) of Cd, Pb and Hg in surface sediments and total annual accumulation (t a^{-1}) in four sea areas (data from Leivuori et al. 2000). Estimates for the whole Baltic Sea for the 1980s from Borg and Jonsson 1996 (1) and Leivuori et al. 2000 (2; based on accumulation in the four northern sea areas).

		Cd	Pb	Hg
Gulf of Finland	concentration	1.06	50	0.13
	accumulation	10.70	452	1.60
Bothnian Bay	concentration	0.94	79	0.27
	accumulation	4.20	356	1.20
Bothnian Sea	concentration	0.37	42	0.09
	accumulation	1.60	185	0.40
Gulf of Riga	concentration	0.73	39	0.10
	accumulation	3.30	175	0.50
Baltic Sea	accumulation (1)	113	3084	6.80
	accumulation (2)	55	3244	10.30

Pb, muscle for Hg) from different parts of the Baltic Sea (Jensen 2012) found both increasing (two areas) and decreasing (one area) trends in the period 1980–2010 for cadmium but only decreasing trends for lead (five areas) and mercury (five areas) in herring. Metal concentrations are usually measured in muscle or liver samples but whole fish concentrations might reflect the environmental status better (Boalt et al. 2014).

A removal of biomass e.g. through fishing may significantly reduce the total amounts of pollutants in the aquatic environment (e.g. Mackenzie et al. 2004; Szefer 2013). However, the rough estimates of the amounts of metals removed from the Baltic Sea through fishing (Table 6) seem to be much smaller compared to the above mentioned (Table 4; Borg and Jonsson 1996) amounts sedimented in the 1980's.

Table 5 Concentrations (means ± S.D. wet weight) of Cd, Pb and Hg in the muscle of fish from the Southern Baltic Sea in the period 1994–2003 (Polak-Juszczak 2009, 2010).

Flounder	Year	n	Cd µg/kg	Pb µg/kg	Hg µg/kg
	1996	21	2.4 ± 2.3	22.0 ± 9.0	66 ± 26
	2003	26	1.0 ± 1.0	4.4 ± 3.6	50 ± 21
Herring	1994	40	16.0 ± 6.0	39.0 ± 25.0	84 ± 12
	2003	54	6.1 ± 3.0	8.0 ± 9.0	22 ± 13
Sprat	1994	36	29.0 ± 15.0	44.0 ± 31.0	68 ± 25
	2003	41	14.0 ± 2.4	11.0 ± 10.0	14 ± 5.0
Cod	1994	9	4.0 ± 1.0	17.0 ± 5.0	118 ± 11
	2003	30	0.1 ± 0.4	5.0 ± 7.0	31 ± 22

Table 6 Annual removal of Cd, Pb and Hg (kg) by fishing estimated using catch statistics for 2010 (ICES) and fish muscle concentrations for 2003 (Polak-Juszczak 2009, 2010; concentration for "others" means those for the above mentioned species). The figures are adjusted upwards by 35% in order to take into account discards and recreational fishing (Zeller et al. 2011).

	Cd	Pb	Hg
Herring	0.32	1.4	16.0
Sprat	2.90	3.8	10.0
Cod	1.1	0.86	1.1
Flounder	0.002	0.10	0.63
Others	0.13	0.17	0.72
Total	**4.4**	**6.3**	**29.0**

Radionuclides in the Baltic Sea

The most significant sources of anthropogenic radioactivity in the Baltic Sea is fallout from nuclear weapons tests carried out in the 1950s and 1960s and from the Chernobyl accident in 1986 (Table 7). The majority of the radionuclide emissions from Chernobyl were

short-lived and ^{137}Cs was the most important long-lived isotope. The estimated amount of ^{137}Cs entering the Baltic Sea from this accident was estimated to be 4.7 PBq (HELCOM 2009). For radionuclides the general trend in the Baltic Sea environment (water, surface sediments and fish) is steadily decreasing (HELCOM 2009; Zalewska and Suplińska 2013).

In the sediments anthropogenic radioactive isotopes are unevenly distributed with the highest concentrations in the Gulf of Riga (max. 385 Bq ^{137}Cs kg^{-1} in the uppermost layer) and lower concentrations in the north and west. In the southern Baltic Sea the mean deposition varied from 1900 in the Bornholm Deep to 5500 Bq m^{-2} in the Gulf of Gdansk. In benthic plants ^{137}Cs concentration from 3 to 40 Bq kg^{-1} d.w. were recorded. In bivalves and crustaceans the ^{137}Cs concentrations varied from 1 to 5 Bq kg^{-1} d.w. and the ^{90}Sr concentrations varied from 0.6 to 1.2 Bq kg^{-1} d.w. In herring the ^{137}Cs concentrations have decreased steadily from approximately 15 in 1989 to under 5 in 2010 Bq kg^{-1} d.w. (Zalewska and Suplińska 2013).

Table 7 Sources of inputs (%) of two radionuclides into the Baltic Sea (HELCOM 2009).

	^{137}Cs	^{90}Sr
Sources beyond the Baltic Sea	4	6
Nuclear weapons testing	14	81
Chernobyl accident	82	13

The greatest part (64–65%) of ^{90}Sr and ^{137}Cs in sediments is in the Bothnian Sea, while ^{241}Am is more evenly distributed between the sea basins. The total sediment loads of ^{90}Sr, ^{241}Am and ^{137}Cs is estimated to be 21, 8.4 and 2050 TBq respectively (Hutri et al. 2013). The sediment concentrations of these nuclides is very variable (Table 8). In the Baltic Sea the effective half-life of ^{137}Cs is estimated to be approximately 10 years and that of ^{90}Sr 16 years (Ikäheimonen et al. 2009).

Table 8 Mean concentrations (Bq m2) of ^{90}Sr, ^{241}Am and ^{137}Cs in sediments in the Baltic Sea (Hutri et al. 2013).

	N	Mean	S.D.
^{90}Sr	22	225	433
^{241}Am	19	65	66
^{137}Cs	22	20,350	26,680

Large-scale Environmental Changes and Interacting Multiple Stressors

Anthropogenic pollution, eutrophication and climate change are large-scale (global or regional) drivers affecting the Baltic Sea environment. A great number of factors affect the future development of metal concentrations

and these factors are often interrelated and the outcome difficult to predict:
– anthropogenic emissions that are related to technological and economic development,
– changes in atmospheric deposition of pollutants,
– political decisions and legislation in countries around the Baltic sea,
– climate change and changes in temperature, salinity and water currents,
– changes in eutrophication and oxygen status, and related changes in biota and
– changes in fisheries and fish stocks.

The factors governing pollutant levels in the Baltic Sea are to a great extent interrelated (Table 9). Many papers deal with the predicted effects of an ongoing and future global climate change (e.g. Philippart et al. 2011; Störmer 2011; Blenckner et al. 2015). Scenarios for future development of the Baltic Sea environment are complicated and uncertain.

Temperature and Ice Cover

The mean temperature in the Baltic Sea area has been predicted to increase by approximately 2–5 °C by the end of this century (HELCOM 2007a; Neumann 2010; Störmer 2011; Meier et al. 2012; Andersson et al. 2015). Increasing temperatures will lead to spatially and temporally decreasing ice cover: up to 50–85% decrease in ice extent by 2100 (Andersson et al. 2015). Decreasing ice cover affects photosynthesis and other biological processes. Warming could lead to a lengthening of the growing season by as much as 20 to 50 days for northern areas and 30–90 days for southern areas by the late 21st century (HELCOM 2007a). These changes in temperature will most probably also affect the species composition in the Baltic marine ecosystem with more freshwater species and fewer marine species (e.g. Schiedek et al. 2007). A possible global rise in sea level will also affect the Baltic Sea and e.g. the exchange of water with the North Sea.

Increasing temperature may affect both exposure to heavy metals and other hazardous substances and their toxic effects (Heugens et al. 2001; Cherkasov et al. 2006; Lanning et al. 2006). Species of marine origin and cold water species have limited possibilities to adapt to decreasing salinity and increasing temperature (Schiedek et al. 2007). Higher temperatures may be more favourable for warm water species including bloom-forming toxic cyanobacteria (HELCOM 2007a). Elevated temperatures may enhance bioavailability and toxicity of some hazardous substances (Heugens et al. 2001). Reduced salinity may enhance uptake of heavy metals by aquatic organisms (McLusky et al. 1986). Exposure to heavy metals in combination with elevated temperature may increase the oxygen demand of aquatic organisms (Cherkasov et al. 2006; Lanning et al. 2006).

Input and Concentrations of Heavy Metals and Radionuclides

The emissions of heavy metals have steadily decreased during the last decades due to technological improvements. This development will probably continue but perhaps more slowly than in the past. Heavy metals will still be strongly bound by anoxic sediments and mostly separated from the marine ecosystem. Although the trends for heavy metals in fish are not unambiguously decreasing it is reasonable to predict lower concentrations in the long run.

Normally the emissions of radionuclides are very low and the amounts are decreasing as a result of decay. Accidents at nuclear facilities may unpredictably cause emissions and deposition of ^{137}Cs or other radionuclides.

Precipitation, Water Inflow, Evaporation, Salinity and Acidification

Several estimates (e.g. Graham et al. 2008; Blenckner et al. 2015) indicate increasing precipitation and increasing inflow of freshwater from rivers. Precipitation may increase up to 30% in the north, causing both a decrease in salinity and increase in the input of organic matter. An increased river runoff will increase the inputs of harmful substances including nutrients and heavy metals bound to organic matter (Andersson et al. 2015).

Increase in precipitation in the Baltic Sea area will cause a decrease in salinity, which may affect water stratification and the oxygen concentration in deep water (e.g. Störmer 2011; Carstensen et al. 2014; Blenckner et al. 2015). Warmer water and decreased salinity may have significant consequences for aquatic organisms. The concentrations of CO_2 in the atmosphere is continuously increasing, which may lead to increased risk of marine acidification (Meier et al. 2012). Increasing CO_2 may also enhance photosynthesis. Salinity greatly affects the bioavailability of substances, e.g. metals, the usual trend being an increase in uptake at lower salinities. For the Baltic Sea it is important to remember that most organisms are living in suboptimal conditions which make them more vulnerable to changes in environmental conditions (Heugens et al. 2001).

Predicted future changes in climate for different parts of the Baltic Sea vary with the largest changes in sea surface water expected in summer in the north (Bothnian Sea and Bothnian Bay) and in spring in the Gulf of Finland (Andersson et al. 2015; Blenckner et al. 2015). However, the predicted decrease in salinity at the surface of the sea will be largest in the southern regions (Danish sea areas).

Eutrophication – Oxygen Depletion

In future the direct emissions of nutrients will probably decrease due to changes in agricultural practices and

more effective treatment of waste waters, but the total runoff will increase and have uncertain effects on nutrient runoff, primary production and the oxygen status of the Baltic Sea. In the long run eutrophication and algal blooms will decrease but no rapid enhancement can be expected (e.g. Elmgren et al. 2015). The Baltic Sea is the largest anthropogenically induced hypoxic sea area in the world (Carstensen et al. 2014) and a significant improvement in its oxygen status is unlikely (Störmer 2011; Meier et al. 2012). It is likely there will also be large areas with hypoxic/anoxic bottom waters and sediments in the future but the trend is uncertain.

Fish, Other Biota and Biodiversity

Decreasing salinity will cause a change towards more brackish and freshwater species (e.g. Niiranen et al. 2013). Fishing affects the amounts of pollutants and nutrients removed from the ecosystem but also through changes in populations of fish and other aquatic organisms (e.g. zooplankton). Older fish usually contain higher concentrations of hazardous substances, which means that fishing policy could also be used to direct the flows of heavy metals (Elmgren et al. 2015). Climate change will most probably affect both the exposure to (bioavailability) and toxic effects (including regulation processes) of harmful substances (Heugens et al. 2001; Schiedek et al. 2007).

Table 9 Interrelated factors and pressures governing pollutant levels in the Baltic Sea.

Direct anthropogenic influence: – Emissions to water and air – Atmospheric deposition – Fishing
Natural processes: – Riverine inflow, exchange with North Sea – Evaporation – Sedimentation
Changes related to climate change: – Temperature, ice cover – Precipitation, water inflow, salinity
Changes related to eutrophication: – Emissions and concentrations of nutrients – Eutrophication, photosynthesis, biomass – Anoxia or hypoxia in sediments – Fish and other biota, biodiversity

Legal Framework, Political Strategies and Economic Consequences

In order to reduce pollution and enhance coordinated measures for the protection of the marine environment the Helsinki Commission, HELCOM, was established as a result of a convention that was accepted in 1992 and entered into force in January 2000. The convention lists harmful substances, including heavy metals and radioactive substances. HELCOM adopted the Baltic Sea Action Plan (BSAP) in 2007 and this plan was revised in 2013. The plan aims to limit or reduce eutrophication and concentrations of hazardous substances and promote scientific cooperation and monitoring. A good ecological status of the Baltic marine environment should be achieved by 2021. The action areas include agriculture, industry, urban areas, hazardous substances, wastes and marine littering as well as planning, monitoring and establishment of protection areas. The goals for hazardous substances are:
– Concentrations of hazardous substances close to natural levels.
– All fish are safe to eat.
– Healthy wildlife.
– Radioactivity at the pre-Chernobyl level.

The HELCOM strategy in relation to climate change is to mitigate adverse effects and enhance the resilience of the Baltic marine environment to future changes in climate. This will include measures:
– to mitigate eutrophication by intensifying the reduction of waterborne and airborne nutrient inputs,
– to continue and intensify measures to reduce inputs of heavy metals and persistent or hazardous organic pollutants,
– to reduce emissions from maritime transport and stop vessels from releasing ballast water,
– to enhance the protection of marine and coastal landscapes and habitats and, in particular, the conservation of native Baltic species (HELCOM 2007a).

Heavy metal emissions are also regulated by the Convention on Long-Range Transboundary Air Pollution by heavy metals (CLRTAP-HM). It was adopted in Aarhus (Denmark) in 1998 and entered into force in 2003. It targets, especially, mercury, cadmium and lead. According to the convention participating countries are committed to reduce their emissions of these three metals below their levels in 1990 by using the best available techniques.

The ultimate target level of the BSAP is to reach near-background concentrations of cadmium and mercury in fish. The maximum levels for fish muscle is 50 and 500 µg kg^{-1} cadmium and mercury, respectively (higher levels permitted in pike and eel). Especially for mercury, the background levels in fish are usually clearly lower than the maximum levels (e.g. Voigt 1999, 2007; Polak-Juszczak 2009, 2010). For ^{137}Cs the target is pre-Chernobyl levels, which is 2.5 Bq kg^{-1} (w.w.) for herring muscle and 2.9 Bq kg^{-1} (w.w.) for plaice and flounder muscle. During the period immediately after the establishment of HELCOM and BSAP the inputs of heavy metals into the Baltic Sea were significantly reduced. The legal base for BSAP is two EU directives directly relevant to the Baltic Sea environment: the Water Framework Directive (WFD) and the Marine Strategy Framework (MSFD). The strategical base is an ecosystem-based management (EBM) with humans as integral parts of the managed system (e.g. Blenckner et al. 2015).

A healthy sea has several benefits for the general public: recreation, fishing, boating etc. Eutrophication and pollution are a considerable nuisance as they result in unhealthy fish and a decrease in recreational value. Different combinations of eutrophication, climate change and fishing policies may affect the stocks of cod, sprat and herring very differently (e.g. Niiranen et al. 2013). These changes may also have considerable economic effects. Climate change is estimated to cause cost the Baltic Sea area: 15 billion euros if the climatic change is moderate and 36 billion euros if it is extreme (Ahlvik and Hyytiäinen 2015).

Concluding Remarks

Eutrophication and climate change are major problems for the marine environment of the Baltic Sea. The amounts of heavy metals circulating in biota are small but it is still important to monitor their concentrations and effects, even though the emissions have been significantly reduced. Metal concentrations in water, sediments and biota are still too high in many areas. This is true e.g. for cadmium and mercury in sediments (Vallius 2014). The amounts of radionuclides are small and their activity decreasing. Large scale changes, like eutrophication and climate change affect ecosystems in many ways, directly and indirectly, causing biological and abiotic effects. The factors influencing metal concentrations are interacting in a complex manner that is difficult to predict. The HELCOM cooperation has been successful but there are many serious problems that remain to be resolved including many of the predicted effects related to climate change. Measures aiming to enhance the ecological status of the Baltic Sea will certainly give positive results but this will take at least several decades (Noyes et al. 2009; HELCOM 2010b; Sobek et al. 2015). The time scale is very short in a geological sense but long in a political context.

REFERENCES

Ahlvik L, Hyytiäinen K (2015) Value of adaptation in water protection - Economic impacts of uncertain climate change in the Baltic Sea. Ecol Econ 116: 231–240.

Andersson A, Meier M, Ripszam M, Rowe O, Wikner J, Haglund P, Eilola K, Legrand C, Figueroa D, Paczkowska J, Lindehoff E, Tysklind T, Elmgren R (2015) Projected future climate change and Baltic Sea ecosystem management. Ambio 44: S345–S356.

Blenckner T, Österblom H, Larsson P, Andersson A, Elmgren R (2015) Baltic Sea ecosystem-based management under climate change: Synthesis and future challenges. Ambio 44: S507–S515.

Boalt E, Miller A, Dahlgren H (2014) Distribution of cadmium, mercury, and lead in different body parts of Baltic herring (*Clupea harengus*) and perch (*Perca fluviatilis*): Implications for environmental status assessments. Mar Pollut Bull 78: 130–136.

Borg H, Jonsson P (1996) Large-Scale Metal Distribution in Baltic Sea Sediments. Mar Pollut Bull 32: 8–21.

Calmano W, Hon J, Förstner U (1993) Binding and Mobilization of Heavy-Metals in Contaminated Sediments Affected by pH and Redox Potential. Water Sci Technol 28: 223–235.

Carstensen J, Andersen J, Gustafsson B, Conley D (2014) Deoxygenation of the Baltic Sea during the last century. PNAS 111: 5628–5633.

Cherkasov A, Biswas PK, Ridings DM, Amy H, Ringwood AH, Sokolova IM (2006) Effects of acclimation temperature and cadmium exposure on cellular energy budgets in the marine mollusk *Crassostrea virginica*: linking cellular and mitochondrial responses. J Exp Biol 209: 1274–1284.

Dippner JW, Pohl C (2004) Trends in heavy metal concentrations in the Western and Central Baltic Sea waters detected by using empirical orthogonal functions analysis. J Mar Syst 46: 69–83.

Elmgren R (2001) Understanding Human Impact on the Baltic Ecosystem: Changing Views in Recent Decades. Ambio 30: 222–231.

Elmgren R, Blenckner T, Andersson A (2015) Baltic Sea management: Successes and failures. Ambio 44: S335–S344.

EMEP (2013) Atmospheric Supply of Nitrogen, Lead, Cadmium, Mercury and Dioxins/Furans to the Baltic Sea in 2013. In: Bartnicki J, Gusev A, Aas W, Valiyaveetil S, Nyíri A (eds) EMEP/MSC-W TECHNICAL REPORT 2/2013.

Graham LP, Deliang C, Christensen OB, Kjellström E, Krysanova V, Meier HEM, Radziejewski M, Räisänen J, Rockel B, Ruosteenoja K (2008) Projections of future anthropogenic climate change. In: BACC Author Team (eds) Assessment of climate change for the Baltic Sea basin. Springer, Berlin and Heidelberg.

Gusev A (2009) Atmospheric deposition of heavy metals to the Baltic Sea. HELCOM Indicator Fact Sheets 2009. Available at http://www.helcom.fi/environment2/ifs/ifs2009/en_GB/hmdeposition/.

Gusev A (2014) Atmospheric deposition of heavy metals. Atmospheric deposition of heavy metals on the Baltic Sea. Baltic Sea Environment Fact Sheet 2014, Published 22.10.2014.

Gusev A (2015) Atmospheric deposition of heavy metals on the Baltic Sea. HELCOM Baltic Sea Environment Fact Sheets [Published: 27 October 2015, Viewed 27.4.2016], http://www.helcom.fi/baltic-sea-trends/environment-fact-sheets/.

HELCOM (2002) Environment of the Baltic Sea area 1994–1998 (2002) HELCOM, Baltic Sea Environ Proc No. 82B.

HELCOM (2007a) Climate Change in the Baltic Sea Area – HELCOM Thematic Assessment in 2007. Baltic Sea Environ Proc 111.

HELCOM (2007b) Heavy Metal Pollution to the Baltic Sea in 2004. Baltic Sea Environ Proc 108.

HELCOM (2009). Radioactivity in the Baltic Sea, 1999-2006. HELCOM thematic assessment. Baltic Sea Environ Proc No. 117.

HELCOM (2010a) Hazardous substances in the Baltic Sea An integrated thematic assessment of hazardous substances in the Baltic Sea. Baltic Sea Environ Proc No. 120B.

HELCOM (2010b) Ecosystem Health of the Baltic Sea 2003–2007: HELCOM Initial Holistic Assessment. Baltic Sea Environ. Proc. No. 122.

HELCOM (2011) The Fifth Baltic Sea Pollution Load Compilation (PLC-5). Baltic Sea Environ Proc No. 128.

Heugens EHW, Hendriks AJ, Dekker T, vanStraalen N, Admiraal W (2001) A review of the effects of multiple stressors on aquatic organisms and analysis of uncertainty factors for use in risk assessment. Crit Rev Toxicol 31: 247–284.

Hutri K-L, Mattila J, Ikäheimonen T, Vartti V-P (2013) Artificial radionuclides ^{90}Sr and ^{241}Am in the sediments of the Baltic Sea: Total and spatial inventories and some temporal trends. Mar Pollut Bull 70: 210–218.

Ikäheimonen TK, Outola I, Vartti V, Kotilainen P (2009) Radioactivity in the Baltic Sea: inventories and temporal trends of ^{137}Cs and ^{90}Sr in water and sediments. J Radioanal Nucl Chem 282: 419–425.

Jensen JN (2012) Contaminants in Herring. Temporal trends in contaminants in Herring in the Baltic Sea in the period 1980-2010. Baltic Sea Environment Fact Sheet 2012.

Lanning G, Cherkasiv AS, Sokolova IM (2006) Temperature dependent effects of cadmium on mitochondrial and whole-organism bioenergetics in oysters. Mar Environ Res 62: S79–S82.

Leivuori M (2000) Distribution and Accumulation of Metals in Sediments of the Northern Baltic Sea. Finnish Inst Marine Res – Contributions 2.

Leivuori M, Jokòas K, Seisuma Z, Kulikova I, Petersell V, Larsen B, Pedersen B, Floderus S (2000) Distribution of heavy metals in sediments of the Gulf of Riga, Baltic Sea. Boreal Env Res 5: 165–185.

Mackenzie BR, Almesjö L, Hansson S (2004) Fish, fishing, and pollutant reduction in the Baltic Sea. Environ Sci Technol 38: 1970–1976.

McLusky D, Bryant V, Campbell R (1986) The Effects of Temperature and Salinity on the Toxicity of Heavy Metals to Marine and Estuarine Invertebrates. Oceanogr Mar Biol Ann Rev 24: 481–520.

Meier M, Andersson H, Arheimer B, Blenckner T, Chubarenko B, Donnelly C, Eilola K, Gustafsson B, Hansson A, Havenhand J, Höglund A, Kuznetsov I, MacKenzie B, Müller-Karulis B, Neumann T, Niiranen S, Piwowarczyk J, Raudsepp U, Reckermann M, Ruoho-Airola T, Savchuk O, Schenk F, Schimanke S, Väli G, Weslawski J-M, Zorita E (2012) Comparing reconstructed past variations and future projections of the Baltic Sea ecosystem – first results from multi-model ensemble simulations. Environ Res Lett 7: 034005 doi:10.1088/1748-9326/7/3/034005.

Neumann T (2010) Climate-change effects on the Baltic Sea ecosystem: a model study. J Mar Syst 81: 213–224.

Niiranen S, Yletyinen J, Tomczak MT, Blenckner T, Hjerne O, MacKenzie BR, Müller-Karulis B, Neumann MT, Meier M (2013) Combined effects of global climate change and regional ecosystem drivers on an exploited marine food web. Global Change Biol 19: 3327–3342.

Noyes P, McElwee M, Miller H, Clark B, Van Tiem L, Walcott K, Erwin K, Levin E (2009) The toxicology of climate change: Environmental contaminants in a warming world. Environ Internat 35: 971–986.

Philippart CJM, Anadón R, Danovaro R, Dippner JW, Drinkwater KF, Hawkins SJ, Oguz T, O'Sullivan G, Reid PC (2011) Impacts of climate change on European marine ecosystems: Observations, expectations and indicators. J Exper Mar Biol Ecol 400: 52–69.

Polak-Juszczak L (2009) Temporal trends in the bioaccumulation of trace metals in herring, sprat, and cod from the southern Baltic Sea in the 1994–2003 period. Chemosphere 76: 1334–1339.

Polak-Juszczak L (2010) Bioaccumulation and temporal trends of trace elements in flounder from the southern Baltic Sea for the 1996–2003 period. J Toxicol Environ Health A73: 1186–1193.

Polak-Juszczak L (2013) Trace elements in the livers of cod (*Gadus morhua* L.) from the Baltic Sea: levels and temporal trends. Environ Monit Assess 185: 687–694.

Schiedek D, Sundelin B, Readman J, Macdonald R (2007) Interactions between climate change and contaminants. Mar Pollut Bull 54: 1845–1856.

Skowrónska K, Chrzanowski W, Namiesnik J (2009) Identification of Chemical Pollution Problems and Causes in the Baltic Sea in Relation to Socio-Economic Drivers. Polish J Environ Studies 18: 701–709.

Sobek A, Sundqvist K, Assefa A, Wiberg K (2015) Baltic Sea sediment records: Unlikely near-future declines in PCBs and HCB. Sci Total Environ 518–519: 8–15.

Strode E, Balode M (2013) Toxico-resistance of Baltic amphipod species to heavy metal. Crustaceana 86: 1007–1024.

Störmer O (2011) Climate Change Impacts on Coastal Waters of the Baltic Sea. In: Schernewski G et al. (eds) Global Change and Baltic Coastal Zones, Chapter 4. Coastal Research Library 1, pp: 51–69 DOI 10.1007/978-94-007-0400-8_4.

Szefer P (2013) Safety assessment of seafood with respect to chemical pollutants in European Seas. Oceanol Hydrobiol Studies 42: 110–118.

Vallius H (2012) Arsenic and heavy metal distribution in the bottom sediments of the Gulf of Finland through the last decades. Baltica 25: 23–32.

Vallius H (2014) Heavy metal concentrations in sediment cores from the northern Baltic Sea: declines over the last two decades. Mar Pollut Bull 79: 359–364.

Vallius H, Leivuori M (1999) The distribution of heavy metals and arsenic in recent sediments of the Gulf of Finland. Boreal Environ Res 4: 19–29.

Vallius H (2014) Heavy metal concentrations in sediment cores from the northern Baltic Sea: Declines over the last two decades. Mar Pollut Bull 79: 359–364.

Voigt H-R (1999) Concentrations of heavy metals in fish from coastal waters around the Baltic Sea. ICES J Mar Sci 56 (Suppl.): 140–141.

Voigt H-R (2007) Heavy Metal (Hg, Cd, Zn) Concentrations and Condition of Eelpout (*Zoarces viviparus* L.), around Baltic Sea. Polish J Environ Stud 16: 909–917.

Zaborska A (2014) Anthropogenic lead concentrations and sources in Baltic Sea sediments based on lead isotopic composition. Mar Pollut Bull 85: 99–113.

Zalewska T, Suplińska M (2013) Anthropogenic radionuclides ^{137}Cs and ^{90}Sr in the southern Baltic Sea ecosystem. Oceanol 55: 485–517.

Zalewska T, Woroń J, Danowska B, Suplińska M (2015) Temporal changes in Hg, Pb, Cd and Zn environmental concentrations in the southern Baltic Sea sediments dated with ^{210}Pb method. Oceanol 57: 32-43.

Zeller D, Rossing P, Harper S, Persson L, Booth S, Pauly D (2011) The Baltic Sea: Estimates of total fisheries removals 1950–2007. Fish Res 108: 356–363.

EFFLUX OF CO_2 FROM SOIL IN NORWAY SPRUCE STANDS OF DIFFERENT AGES: A CASE STUDY

EVA DAŘENOVÁ*, TOMÁŠ FABIÁNEK, and MARIAN PAVELKA

Global Change Research Institute, Czech Academy of Sciences, Bělidla 4a, 603 00 Brno, Czech Republic
* Corresponding author: darenova.e@czechglobe.cz

ABSTRACT

Efflux of CO_2 from soil is a major component of the terrestrial ecosystem and plays an important role in the global carbon cycle. In this study the efflux of CO_2 from soil was measured in three stands of Norway spruce. We investigated differences in the efflux of CO_2 from soil in different age classes of the forest: two young (Y_R and Y_{BK}) and one old (O_R) stand, during the growing season in 2010. The lowest amount of soil CO_2 released was recorded in O_R (14.9 t ha^{-1}), which was just over half that recorded in the young stands. There were no significant differences in total soil CO_2 released recorded in Y_R and Y_{BK} (29.3 and 27.2 t ha^{-1}). Efflux of CO_2 recorded in O_R and Y_R during July was low because of lack of rain. When the efflux of CO_2 from soil in O_R and Y_R, respectively, was estimated on the basis of the soil moisture measured at Y_{BK}, the modelled cumulative amount of soil CO_2 released increased by 10.9 and 11.4%. Our results indicate that the age of a stand can be an important and easily obtained factor for predicting the amount of soil CO_2 released at the regional level.

Keywords: spruce forest, *Picea abies*, soil temperature, moisture, respiration

Introduction

Soil respiration is the second-largest flux of carbon in terrestrial ecosystems and plays an important role in the global carbon cycle. It is estimated that 45–90% of forest ecosystem respiration is from soil cycling (Goulden et al. 1996; Boldstad et al. 2004; Guan et al. 2006). Therefore, soil respiration has a great effect on the atmospheric concentration of CO_2, and consequently, as CO_2 is one of the greenhouse gases, on global warming.

In the temporal dynamics of the efflux of CO_2 from soil, temperature and soil moisture are the most important factors. There is a mostly positive relationship between soil respiration and temperature and this relationship is often described as exponential (Davidson et al. 2006). Low and high soil moisture may limit the efflux of CO_2 from soil (Jassal et al. 2008).

As forests develop from young to mature stages, there can be changes in sources of organic carbon used in soil respiration, which includes assimilates (in roots), plant residues, rhizo-deposits or soil organic matter (Kuzyakov 2006). Age-related variation is recorded in, for example, soil organic matter (Saiz et al. 2006a), litter input (Klopatek 2002) and root biomass (Fang et al. 1998). To estimate the efflux of CO_2 from soil on a large spatial scale would demand many different analyses and measurements of the various factors. Some of these can be similar for a given forest age class. Therefore, assessing and understanding the efflux of CO_2 from soil in forests of different ages is important for accurately estimating the global carbon balance.

In this study, we measured the efflux of CO_2 from soil in three Norway spruce (*Picea abies* (L.) Karst.) stands of different ages, including a 32- and a 110-year-old stand in an upland region and a 29-year-old stand at a mountain-ous location. The aim was to estimate the efflux of CO_2 from soil in the three tree stands of different ages and describe the seasonal course of the efflux of CO_2 from soil in these stands during the experimental season.

Material and Methods

Measurements were carried out in three Norway spruce forests in the Czech Republic at Bily Kriz and Rajec-Nemcice.

Bily Kriz is situated in the Moravian–Silesian Beskydy Mts. The stand (Y_{BK}) was planted after clear-cut of a first-rotation forest that had grown on former pasture. Characteristics of the site and the stand are summarized in Table 1.

The efflux of CO_2 from soil was measured at eight positions using an automatic closed gasometrical system SAMTOC (Pavelka et al. 2004) from 1 May to 25 October 2010. Soil temperature was measured at a depth of 1.5 cm within each chamber (Pavelka et al. 2007). Precipitation in the area was measured using a MetOne 386 rain gauge (Met One Instruments, Inc., USA). Soil moisture was measured using a TRIME-FM 2/3 device (Mesa Systems Co., USA) in a 0–32 cm profile.

Rajec-Nemcice is situated in Drahanska Upland. We studied two stands at this site – one 32 years old (Y_R) and the other 110 years old (O_R). The stands were established by reforesting clear-cut areas. Characteristics of the site and the stands are summarized in Table 1.

Measurements of the efflux of CO_2 from soil at O_R were made at three positions using SAMTOC-II from 26 April to 8 November 2010. Soil temperature was measured at a depth of 4.5 cm inside each chamber (according to Rayment and Jarvis 1997). Measurements of the efflux

Table 1 Characteristics of the sites and the stands.

	Bily Kriz Y_{BK}	Rajec-Nemcice Y_R	Rajec-Nemcice O_R
Altitude (m a.s.l.)	890	625	625
Mean air temperature (°C)	5.5	6.5	6.5
Precipitation (mm)	1318	717	717
Age (years)	29	32	110
Tree height (m)	14.9	13.6	31.6
Tree density (trees ha^{-1})	1420	1888	609
Soil type (FAO classification)	Haplic Podzol	Cambisol	Cambisol
Carbon in organic layer (t ha^{-1})	19.8	21.1	28.8
Carbon in mineral layers (t ha^{-1})	100.0	92.6	169.3
Thickness of organic layer (cm)	8	5	8
Thickness of mineral layers (cm)	42	55	42

of CO$_2$ from soil at Y$_R$ were made manually at 16 positions using a portable Li-8100 (Li-Cor, Inc., USA) from 23 April to 17 October 2010. Soil temperature was measured 1 cm alongside the positions at a depth of 4.5 cm during each CO$_2$ measurement. In addition, soil temperature at 4.5 cm was measured continuously for the entire season using a PT 1000 sensor (HIT Ldt., CZ).

Soil moisture was measured at three positions in each stand using a CS616 Reflectometer (Campbell Scientific, USA) at 1 h intervals and over a profile of 0–30 cm. Precipitation was measured in an open area using a MetOne 370/375 rain gauge (Met One Instruments).

Data Analyses

Efflux of CO$_2$ from soil (R_S) was plotted against soil temperature (T_S) and this was fitted by an exponential regression curve using the regression equation

$$R_S = \beta e^{\alpha T_S}, \tag{1}$$

where a and β are the regression coefficients.

Q_{10} (the proportional change in CO$_2$ efflux for a 10 °C increase in temperature) was calculated using the equation:

$$Q_{10} = e^{10\alpha}, \tag{2}$$

where a is the regression coefficient obtained from equation (1). For continuous automatic measurement data, Q_{10} was calculated for each chamber for several short periods when the efflux of CO$_2$ from soil was not disturbed by rainfall. For manual measurement data, one value of Q_{10} was calculated from all the measurements of the efflux of CO$_2$ from soil at different temperatures.

Then, efflux of CO$_2$ from soil was normalized for the temperature of 10 °C (R_{10}):

$$R_{10} = \frac{R_S}{Q_{10}^{\frac{T_S - 10}{10}}}, \tag{3}$$

where R_S is the measured rate of efflux of CO$_2$ from soil at soil temperature (T_S). R_{10} was determined for each measurement.

Missing data for the efflux of CO$_2$ from soil in the continuous measurements were replaced using the equation

$$R_M = \frac{R_{10}}{Q_{10}^{\frac{10 - T_S}{10}}}, \tag{4}$$

where values of Q_{10} and R_{10} were estimated from measurements for the periods of 3 to 5 d before and after the gap in the data.

Gaps in R_{10} in the manual measurements from Y$_R$ were filled by interpolating the measured data. Then, mean efflux of CO$_2$ from soil was calculated for each day according to equation (4), where T_S was replaced by values of mean daily soil temperature.

To exclude the effect of differences in rainfall at the two sites, we determined the effect of soil moisture on the efflux of CO$_2$ from soil and recalculated the efflux using soil moisture data collected at Y$_{BK}$. We plotted the efflux of CO$_2$ from soil recorded at O$_R$ against soil temperature. Then, the data were fitted with an exponential regression curve and residuals from the regression were estimated. These were plotted against soil moisture and logarithmic relationships of the residuals and soil moisture were estimated for four periods: 26 April–18 June, 19 June–17 July (with low precipitation), 18 July–4 October and 5 October–8 November. The equations for estimating the efflux of CO$_2$ according to soil temperature and moisture were defined on the basis of equation (1) and the logarithmic relationship of the residuals and the efflux of CO$_2$ from soil. Similarly, the data for Y$_R$ were recalculated (with one regression of the residuals on moisture).

Statistical calculations were done using analytical software SigmaPlot 11.0 and SPSS 17.0. For data comparison one-way ANOVA and Games–Howell test (when a test of equal variance failed) were used. Statistical significance was tested with α = 0.05.

Results

Environmental conditions (soil temperature, air temperature, soil moisture and precipitation) recorded at the different sites are presented in Fig. 1 and Table 2.
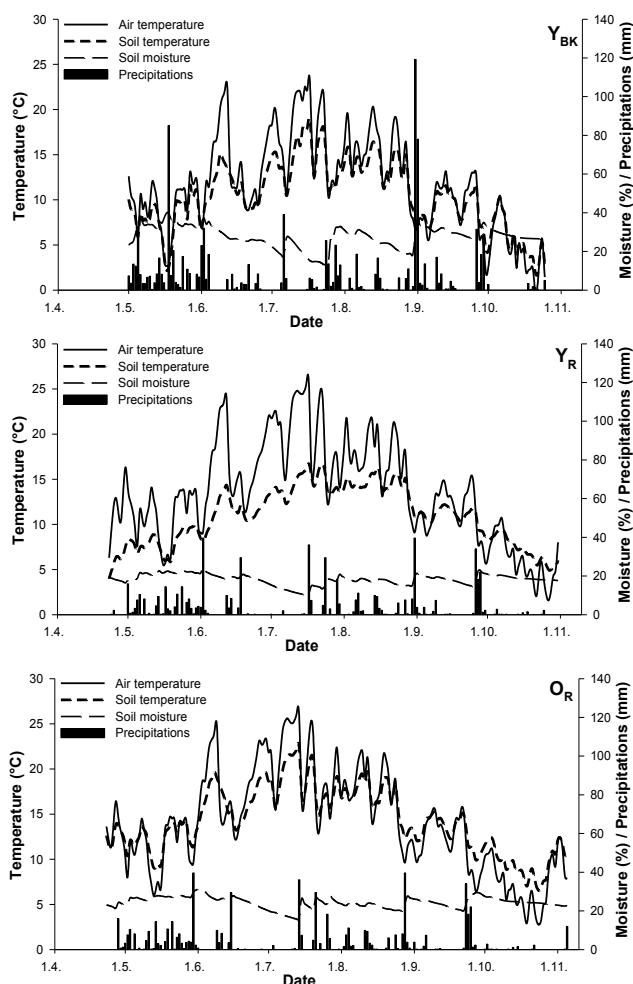
Fig. 1 Soil temperature, air temperature, soil moisture and precipitation in the young stand at Bily Kriz (Y_{BK}) and old (Y_R) and young (O_R) stands at Rajec-Nemcice.

Table 2 Mean seasonal (1 May-25 October 2010) values of chosen characteristics and parameters.

|	Y_{BK}	Y_R	O_R
Soil temperature (°C)	10.5	11.3	14.6
Air temperature (°C)	11.7	13.7	14.7
Soil moisture (%)	28.6	18.4	24.5
Total precipitation (mm)	1034	568	568

Efflux of CO_2 from soil was positively related to soil temperature at all sites. When analysing the continuous measurements recorded at Y_{BK} and O_R, this relationship was stronger for Y_{BK}, with its coefficient of determination (R^2) equal to 0.58, than for O_R, with R^2 of 0.38.

Values of Q_{10} were 1.60, 2.25 and 1.82 for Y_{BK}, Y_R, and O_R, respectively. Mean daily R_{10} at Y_{BK} ranged between 2.0 and 6.0 µmol m^{-2} s^{-1} and increased at the beginning of the growing season. The maximum values were reached at the end of July and during August. At Y_R and O_R, we recorded no increase in R_{10} during June and July. This was possibly due to a lack of precipitation during this period. R_{10} values were between 2.0 and 4.5 µmol m^{-2} s^{-1} at Y_R and 1.0 and 2.5 µmol m^{-2} s^{-1} at O_R (Fig. 2).

The amount of CO_2 released from soil at Y_{BK} was 27.2 t ha^{-1} during the period 1 May–25 October 2010. The amount of CO_2 released from soil at Y_R was 29.9 t ha^{-1} during the season 23 April–25 October 2010 (29.3 t ha^{-1} for the same period as that for Y_{BK}). The amount of CO_2 released from soil at O_R was 15.6 t ha^{-1} during the whole period (26 April–8 September 2010). This amount was 14.9 t ha^{-1} for the same period as that for Y_{BK} and was
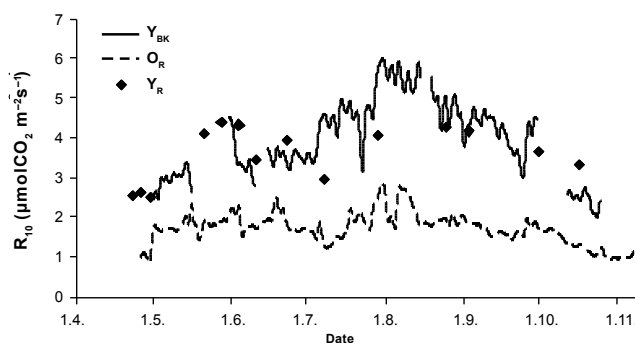
Fig. 2 Efflux of CO_2 from soil adjusted to a temperature of 10 °C (R_{10}) for the young stand at Bily Kriz (Y_{BK}) and the old (O_R) and young (Y_R) stands at Rajec-Nemcice.
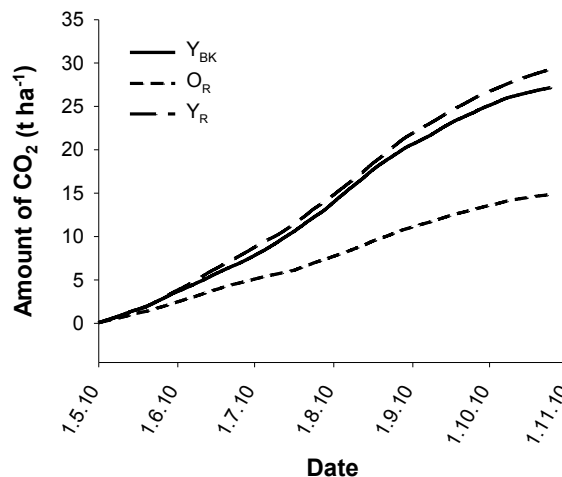
Fig. 3 Cumulative amount of CO_2 released from soil in the young stand at Bily Kriz (Y_{BK}) and the old (O_R) and young (Y_R) stands at Rajec-Nemcice from 1 May-25 October 2010.
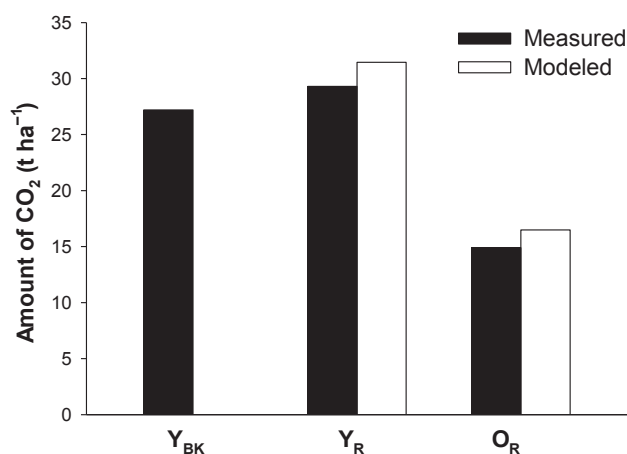
Fig. 4 Seasonal amount of CO$_2$ released from soil in the young stand at Bily Kriz (Y$_{BK}$) and the old (O$_R$) and young (Y$_R$) stands at Rajec-Nemcice during 1 May–25 October 2010. Black columns are measured data and white columns modelled amounts of CO$_2$ recalculated based on soil moisture recorded at Bily Kriz.

significantly less than at Y$_{BK}$ and Y$_R$ (amounting to 54.7 and 50.7% of the CO$_2$ production at Y$_{BK}$ and Y$_R$, respectively). There was no significant difference between Y$_{BK}$ and Y$_R$ (p = 0.058) (Fig. 3).

To exclude the effect of the differences in rainfall at the two sites, we determined the effect of soil moisture on the efflux of CO$_2$ from soil at O$_R$ and recalculated this to the soil moisture measured at Y$_{BK}$. The residuals of the efflux of CO$_2$ from soil from the regression of the relationship between the efflux of CO$_2$ from soil and temperature were statistically significant in their correlation with soil moisture in all four periods. The modelled data for the efflux of CO$_2$ from soil were in a good agreement with the measured data (R^2 = 0.86) and there was no statistically significant difference between measured and modelled efflux of CO$_2$ from soil (paired t-test, p > 0.05). When the efflux of CO$_2$ from soil was recalculated based upon soil moisture measured at Y$_{BK}$, the modelled seasonal (1 May–25 October 2010) amount of CO$_2$ released was increased by 10.9% to 16.5 t ha^{-1}.

The data from Y$_R$ were recalculated in the same way but we used the regression of the residuals on moisture that was statistically significant. The modelled seasonal (1 May–25 October 2010) amount of soil CO$_2$ increased by 11.4% to 31.5 t ha^{-1} after recalculation based upon soil moisture recorded at Y$_{BK}$ (Fig. 4).

Discussion

In this study, we measured the efflux of CO$_2$ from soil in three Norway spruce stands. Two stands (Y$_{BK}$ and Y$_R$) were young and one was old (O$_R$). Efflux of CO$_2$ from soil standardized to 10 °C for Y$_{BK}$ showed a seasonal trend. A similar trend with a maximum occurring in summer is reported for a pine stand in a study by Law et al.

(1999), and these authors attributed the trend to fine root growth. Similarly, Yan et al. (2011) report that changes in fine root biomass is one factor influencing seasonal variation in the efflux of CO$_2$ from soil in young poplar stands. Epron et al. (2001) report a seasonal trend in temperature-normalized rhizospheric respiration in young beech forest with a maximum in July, at which time fine root growth was greatest. We did not record such a trend in R$_{10}$ at Y$_R$, and O$_R$. This is most likely due mainly to the dry period in June and July, which reduced the efflux of CO$_2$ from soil due to the limited availability of water.

We recorded a significantly lower efflux of CO$_2$ from soil at O$_R$ than at Y$_{BK}$ and Y$_R$ during the experimental season. Age-dependent efflux of CO$_2$ from soil is described in other studies, which involved stands of different ages. For example, increasing efflux of CO$_2$ from soil with age in pine or poplar stands is recorded (Wiseman et al. 2004; Zhang et al. 2011), but with a maximum stand age of 25 years. Kolari et al. (2004) describe a steep increase in the efflux of CO$_2$ from soil in 12 year old pine stands, after which it decreased until the age of 75 years. Luan et al. (2011) report an increase in cumulative growing season efflux of CO$_2$ from soil with age in oak stands (40–143 years). They explained the trend in terms of substrate availability and organic matter quality. Yan et al. (2011) report a decrease in the efflux of CO$_2$ from soil and R$_{10}$ in poplar stands from the age of 2 years to 12 years. This was explained as an effect of soil temperature, moisture and fine root biomass decreasing with age. Similarly, Saiz et al. (2006b) report a decreasing trend in the efflux of CO$_2$ from soil with age in spruce stands between 10 and 47 years old. They also report a decreasing trend in the fine root biomass with stand age and that the changes in the efflux of CO$_2$ from soil associated with variations in temperature and moisture were more obvious for the youngest stands. Klopatek (2002), too, points to the amount of fine root biomass as an important factor in age-related variations in the efflux of CO$_2$ from soil. He studied 20-year-old, 40-year-old and old-growth Douglas fir stands. The 40-year-old stand had both the lowest annual amount of carbon release through soil efflux and lowest fine root biomass. In old stands, there is usually a lower tree density than in young stands. Therefore, it can be difficult to separate the effects of age and tree density on the amount of fine root biomass (Borja et al. 2008). Fine root biomass was not assessed in our study, but we assume that this could have had an effect on the differences in the efflux of CO$_2$ from soil at the stands studied, as discussed above.

Concerning the effect of the differences in rainfall at our sites, we recalculated the CO$_2$ efflux at Y$_R$ and O$_R$ using the soil moisture recorded at Y$_{BK}$. A very important period was the drought in June and July when the regression of the residuals and moisture was steep. Under conditions of low water availability, soil moisture becomes the driving factor in the efflux of CO$_2$ from soil (Jassal et al. 2008). We measured soil moisture in a profile

of 0–32 cm at Y_{BK} and 0–30 cm at Y_R and O_R. Moisture measurements at these depths can miss the changes in moisture in the shallow soil layers. The top layer of soil is very active in respiration and also sensitive to low rainfall, which may not affect soil moisture in deeper layers. This top-soil can also easily dry out.

Conclusions

In this study, the difference in the cumulative amount of soil CO_2 released in two young stands was much lower than the differences between that released in the young and old stands. The amount of CO_2 released by soil in the old stand was just over half that released in the young stands. From the comparison of the two stands located at the same site we assume an effect of stand age on the physical properties of the soil, such as soil temperature or moisture, due to changes in the structure of the aboveground biomass. Stand age can also generally influence other soil properties, such as the amount of soil carbon or root biomass. Although fine root biomass was not assessed in this study, we consider that stand age in combination with measurements of temperature and moisture can help to predict the amount of soil CO_2 released at the regional level.

Acknowledgements

REFERENCES

Bolstad PV, Davis KJ, Martin J, Cook BD, Wang W (2004) Component and whole-system respiration fluxes in northern deciduous forests. Tree Physiol 24: 493–504.

Borja I, de Wit ha, Steffenrem A, Majdi H (2008) Stand age and fine root biomass, distribution and morphology in a Norway spruce chronosequence in southeast Norway. Tree Physiol 28: 773–784.

Davidson EA, Janssens IA, Luo YQ (2006) On the variability of respiration in terrestrial ecosystems: moving beyond Q_{10}. Global Change Biol 12: 154–164.

Epron D, le Dantec V, Dufrene E, Granier A (2001) Seasonal dynamics of soil carbon dioxide efflux and simulated rhizosphere respiration in a beech forest. Tree Physiol 21: 145–152.

Fang C, Moncrieff JB, Gholz HL, Clark KL (1998) Soil CO_2 efflux and its spatial variation in a Florida slash pine plantation. Plant Soil 205: 135–146.

Goulden ML, Munger JW, Fan SM, Daube BC, Wofsy SC (1996) Measurements of carbon sequestration by long-term eddy covariance: Methods and a critical evaluation of accuracy. Global Change Biol 2: 169–182.

Guan DX, Wu JB, Zhao XS, Han SJ, Yu GR, Sun XM, Jin CJ (2006) CO_2 fluxes over an old, temperate mixed forest in northeastern china. Agr Forest Meteorol 137: 138–149.

Jassal RS, Black TA, Novak MD, Gaumont-Guay D, Nesic Z (2008) Effect of soil water stress on soil respiration and its temperature sensitivity in an 18-year-old temperate Douglas-fir stand. Global Change Biol 14: 1305–1318.

Klopatek MJ (2002) Belowground carbon pools and processes in different age stands of Douglas-fir. Tree Physiol 22: 197–204.

Kolari P, Pumpanen J, Rannik Ü, Ilvesniemi H, Hari P, Berninger F (2004) Carbon balance of different aged Scots pine forests. Global Change Biol 10: 1106–1119.

Kuzyakov Y (2006) Sources of CO_2 efflux from soil and review of partitioning methods. Soil Biol Biochemi 38: 425–448.

Law BE, Ryan MG, Anthoni PM (1999) Seasonal and annual respiration of a ponderosa pine ecosystem. Global Change Biol 5: 169–182.

Luan J, Liu S, Wang J, Zhu X, Shi Z (2011) Rhizospheric and heterotrophic respiration of warm-temperate oak chronosequence in China. Soil Biol Biochem 43: 503–512.

Pavelka M, Acosta M, Janous D (2004) A new device for continuous CO_2 flux measurement in forest stand. Ekologia-Bratislava 23: 88–100.

Pavelka M, Acosta M, Marek MV, Kutsch W, Janous D (2007) Dependence of the Q_{10} values on the depth of the soil temperature measuring point. Plant Soil 292: 171–179.

Rayment MB, Jarvis PG (1997) An improved open chamber system for measuring soil CO_2 effluxes in the field. J Geophys Res-Atmos 102: 28779–28784.

Saiz G, Byrne KA, Butterbach-Bahl K, Kiese R, Blujdea V, Farrell EP (2006a). Stand age related effects on soil respiration in a first rotation Sitka spruce chronosequence in central Ireland. Global Change Biol 12: 1007–1020.

Saiz G, Green C, Butterbach-Bahl K, Kiese R, Avitabile V, Farrell EP (2006b) Seasonal and spatial variability of soil respiration in four Sitka spruce stands. Plant Soil 287: 161–176.

Wiseman PE, Seiler JR (2004) Soil CO_2 efflux across four age classes of plantation loblolly pine (*Pinus taeda* L.): on the Virginia Piedmont. Forest Ecol Manag 192: 297–311.

Yan M, Zhang X, Zhou G, Gong J, You X (2011) Temporal and spatial variation in soil respiration of poplar plantations at different developmental stages in Xinjiang, China. J Arid Environ 75: 51–57.

Zhang J, Shangguan T, Meng Z (2011) Changes in soil carbon flux and carbon stock over a rotation of poplar plantations in northwest China. Ecol Res 26: 153–161.

DISTRIBUTION, PARASITOIDS AND CYCLIC APPEARANCE OF RUSSIAN WHEAT APHID *DIURAPHIS NOXIA* (MORDVILKO, 1913) (HEMIPTERA, APHIDIDAE) IN ALGERIA

MALIK LAAMARI*, SOUMIA BOUGHIDA, and HALIMA MEROUANI

LATPPAM Laboratory, Institute of Veterinary and Agronomic Sciences, Department of Agronomy, University of Batna, 05000, Algeria
* Corresponding author: laamarimalik@yahoo.fr

ABSTRACT

This information on the Russian wheat aphid *Diuraphis noxia* (Hemiptera, Sternorrhyncha, Aphididae) in those regions of Algeria where cereals are grown is based on a nineteen year study. This revealed that this aphid is widely distributed in the high plateaus and interior plains with semi-arid climates. The mummies of this aphid found among its colonies were collected and 4 parasitoids (Hymenoptera, Braconidae, Aphidiinae) where identified. These were *Diaeretiella rapae* (M'Intosh), *Aphidius matricariae* (Haliday), *Aphidius rhopalosiphi* (Destefani) and *Lysiphlebus testaceipes* (Cresson), with *D. rapae* the most abundant. Moreover, this study also indicates that the cyclical appearance of this aphid is determined by the intensity of precipitation during winter and spring.

Keywords: *Diuraphis noxia*, distribution area, parasitoids, periodic infestation, Algeria

Introduction

The Russian wheat aphid *Diuraphis noxia* (Mordvilko 1913) is one of the most damaging aphid species infesting wheat and barley (Rechmany et al. 1993; Al Ayedh 2000). Its very toxic saliva causes leaves to develop longitudinal chloroses, stunts growth, impairs the quality of the grain and even causes plants to desiccate (Calhoun et al. 1991). This aphid was originally described from the Caucasus region in 1900 and probably spread to Africa from western Asia (Walters et al. 1980). *D. noxia* was first encountered in Ethiopia in 1973, at a time when a drought started in the northern part of the country (Haile and Megenasa 1987). This aphid was first reported in South Africa in 1978 (Miller et al. 1993). In this country, Robinson (1994) mentions that losses may amount to up to 92% of the production. In North Africa (Algeria, Morocco, Tunisia, Libya and Egypt), *D. noxia* was reported for the first time in 1987 (Miller et al. 1993).

In Algeria, Tahir cited by Miller et al. (1993) estimate the area of wheat infested with this aphid was about 200 ha in Sétif (eastern Algeria) in 1989. During the same year, it was reported in Sidi Bel Abbès by Maatougui in Tiaret (western Algeria) and by Mekni (Miller et al. 1993). More recently, it was reported in Constantine in 1991 on *Hordeum vulgare* L. and *Triticum aestivum* L. and in Batna in 1992 on *Phalaris brachystachys* Link. (Laamari 2004). Oufroukh et al. (2011) report that *D. noxia* is one of the aphids implicated in the transmission of Barley yellow dwarf virus (BYDV) in some regions of Algeria. Despite its importance, this aphid has been poorly studied in Algeria. Many aspects, including its biology, distribution, economic effect and the action of abiotic and biotic factors on this aphid are unstudied. This study was conducted in order to delimit the area of distribution of this aphid in Algeria. In addition, climate data for five years is used to determine the effect of climate on infestations of this aphid in the Batna region. Finally, the Hymenopteran parasitoids associated with this aphid in the regions of Batna, Khenchela and Oum El Bouaghi, are identified.

Material and Methods

Distribution Area

This study was carried out in the major cereal producing areas in Algeria. From thirty seven localities (Table 1), samples were collected from February till June from 1992–2009, depending on the growing season at each locality. Considering the importance of the area surveyed, the localities selected were not visited in the same year. At each locality, samples were taken from different cereal crops. The infested tillers were placed in plastic boxes already labelled and brought back to the laboratory where the numbers of aphids were counted. The GPS coordinates and altitude of each field were recorded and the distribution plotted on a map (Fig. 1).

Parasitoids

This part of the study was done in fields of cereals located in the departments of Oum El Bouaghi (locality El Harmelia), Khenchela (locality Kais) and Batna (locality Hemla). On each sampling date and from each field, twenty tillers were carefully collected at random and transported to the laboratory. Each tiller bearing colonies of living and mummified aphids was kept in a separate vial. Each vial was numbered and labelled with the date, the field and locality. The vials were inspected daily for the presence of mummies. Once they were detected, they were carefully removed from the leaves and kept individ-

ually in small plastic boxes. A circular opening was cut into the lid of each box and covered with muslin for ventilation. Each plastic box was labelled with the number of the vial the mummy was removed from. The samples were reared in the laboratory at room temperature for 2–3 weeks, until all adult parasitoids emerged.

Cyclic Appearance

In order to determine the effect of temperature and rain fall on population fluctuations of the Russian wheat aphid, the data recorded in the Batna region (Locality Hemla) for the years 1992, 1999, 2008, 2009 and 2010 were used. According to Miller et al. (1993) climatic conditions in winter and spring determine the levels of infestation of cereals by this aphid. For this reason, the data on temperature and rain fall for five months (January–May) of each year were taken into consideration. To follow the level of infestation by *D. noxia* in the Batna region, each year samples were collected from March to May in barley fields, which is the principal crop in this region. Within each field, 20 tillers were collected at random at 5 different places (total of 100 tillers per field).

Table 1 Coordinates and years of the surveys of the different localities studied.

Departments	Locality	Altitude (m)	Lat. (N) Long. (E or O)	Years sampled
Oum El Bouaghi	Ain Mlila	781	36.02°N 6.33°E	2000, 2008
	Ain Kercha	807	35.55°N 6.40°E	2008
	El Hermelia	794	35.92°N 6.62°E	2008
Batna	Ain Djasser	864	35.51°N 6.00°E	2008
	Tzouket	1547	35.23°N 6.25°E	2008
	Bouhmar	1382	35.26°N 6.21°E	2008
	Hemla	1128	35.32°N 6.04°E	1992, 1999, 2008, 2009, 2008, 2010
	Batna	1058	35.32°N 6.08°E	1992, 1993,2008
	Arris	1205	35.17°N 6.24°E	1995, 2001, 2008
	El Madher	881	35.63°N 6.38°E	1994, 2006, 2008
Biskra	El Kantara	466	35.12°N 5.41°E	2006, 2007
	El Outaya	221	34.97°N 5.58°E	2004, 2007
	Ain Benoui	110	34.81°N 5.66°E	2002, 2004
Tebessa	Cheria	1085	35.15°N 7.44°E	1999
Tiaret	Mehdia	910	35.26°N 1.46°E	1999, 2002
Djelfa	Ain Oussara	675	35.28°N 2.54°E	2006
Saida	Youb	636	34.55°N 0.10°E	2004
Sétif	Sétif	1040	36.11°N 5.23°E	2008
	Guellal	902	36.03°N 5.33°E	1995, 2000, 2004, 2005
	Oum Ladjoul	905	35.55°N 5.54°E	1995, 1996, 1997, 1998
	Hammam Sokhna	905	35.58°N 5.50°E	1996, 1997, 1998, 2008, 2009
	El Eulma	963	36.16°N 5.69°E	2009
Sidi Bel Abbès	Telagh	888	34.59°N 0.29°E	2006
Annaba	El Hadjar	13	36.76°N 7.66°E	2008, 2009
Guelma	Guelma	423	36.44°N 7.41°E	2009
Constantine	El khroub	619	36.16°N 6.40°E	2007, 2008, 2009
	Ain Abid	876	36.13°N 6.57°E	1995
M'sila	Megra	565	35.36°N 5.5° E	1999
Bourdj Bou-Arreridj	Ras El Oued	1086	35.54°N 4.58°E	1992, 1999
	Bordj Ghedir	1271	35.53°N 4.56°E	1992, 1998
El Oued	Hassi Khelifa	51	33.56°N 6.99°E	2006
Taref	El Kous	5	36.79°N 7.85°E	2005, 2009
Khenchela	Kais	1193	35.25°N 7.07°E	1994, 2001,2008
	Bouhmama	1157	35.19°N 6.45°E	1996, 2004
Mila	Chelghoum El Aid	766	36.11°N 6.13°E	1997, 2008
	Teleghma	782	36.4°N 6.20°E	2008

Results

Distribution Area

Colonies of the Russian wheat aphid were found in several fields of durum wheat, common wheat, barley and oats at 34 localities in 15 Departments (Fig. 1). It is completely absent in the departments Taref, Annaba and Guelma.

Parasitoids

In total, 56 specimens of Hymenopteran parasitoids were collected and identified. Four parasitoids emerged from the mummies of Russian wheat aphid collected from the localities at El Hermelia (Oum El Bouaghi), Kais (Khenchela) and Hemla (Batna) in 2008 (Table 2).

Cyclic Appearance

At the different localities surveyed in 2009 and 2010, *D. noxia* was not present in cereal fields that are usually moderately or heavily infested. The same phenomenon is reported in some European countries, particularly Albania by Stary in 2008 (personal communication, 2011). Compared to previous years, 2009 was exceptional, especially the spring. Based on the data in table 3, it appears that the precipitation recorded during the first 5 months of 2009 (245.6 mm) and during the months of January (67.9 mm) and April (75.1 mm) was higher than in other years (Table 3). Average maximum (16.6 °C) and minimum (3.4 °C) temperatures and the average temperature (9.9 °C) in 2009 are very similar to other years. It is noteworthy that the average temperatures in April (11 °C) and May (17.5 °C) in 2009 were slightly lower than in 1999 and 2008.

Discussion

The Russian wheat aphid, *D. noxia,* was recorded infesting cereals on the high plateaus and plains in the interior of Algeria. All these regions have a semi-arid climate (cold in winter and hot and dry in summer). The temperature variation is important and rain very irregular. All these regions are located at altitudes between 565 m (M'sila) and 1547 m (Batna). According to Stary and Lukasova (2002) dense colonies of *D. noxia* are usually recorded on cereals grown in the highest regions. It should be noted that over several years alatae were trapped in barley fields at El Oued and Biskra (Algerian Sahara). These regions are in an arid bioclimatic area and at a mean altitude of 51 m. In addition, surveys carried out in coastal areas, characterized by a humid and sub-humid climate revealed the complete absence of this aphid. Indeed Basky (2003) mentions that the high relative humidity is not favourable for the development of the Russian aphid.
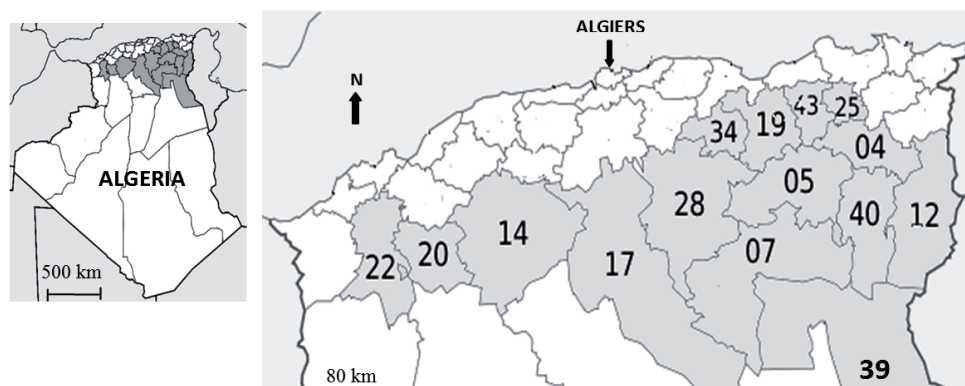
Fig. 1 Distribution area of *Diuraphis noxia* in Algeria. Numbers correspond to administrative codes of departments where Russian wheat aphid is present**,** 04, Oum El Bouaghi, 05, Batna, 07, Biskra, 12, Tebessa, 14, Tiaret, 17, Djelfa, 19, Sétif, 20, Saida, 22, Sidi Bel Abbès, 25, Constantine, 28, M'sila, 34, Bordj Bou Arreridj, 39, El Oued, 40, Khenchela, 43, Mila.

Table 2 Numbers of parasitoids reared from mummies that developed in colonies of *Diuraphis noxia* collected at different localities in 2008.

Localities	Host plants	*Diaeretiella rapae*	*Aphidius matricariae*	*Aphidius Rhopalosiphi*	*Lysiphlebus testaceipes*	Total
Hemla (Batna)	*Hordeum vulgare*	7	0	0	0	**7**
El Hermelia (Oum El Bouaghi)	*H. vulgare*	14	0	4	10	**28**
	Avena sativa	4	0	0	0	**4**
	Triticum aestivum	6	0	6	0	**12**
Kais (Khenchela)	*H. vulgare*	0	5	0	0	**5**
	Total	**31**	**5**	**10**	**10**	**56**

From mummies found in colonies of this aphid, four primary parasitoids emerged (Table 1). Among the parasitoids found, *Aphidius matricariae* was introduced into South Africa from Turkey to control populations of *D. noxia* (Berner 2006). Compared to previous species, *Diaeretiella rapae* is more common. It was found at several localities in all cereal crops. It is considered to be the most important parasitoid of the Russian aphid in central Asia, east and western Europe, the Mediterranean region and Northern and Southern Africa (Kovalev et al. 1991; Bernal and Gonzalez 1997). Even in Iran, Rakhshani et al. (2008) indicates that the parasitoid *D. rapae* is mostly associated with *D. noxia*. These authors also mention that this parasitoid is used as a biological control agent against this pest in Iran. *Lysiphlebus testaceipes* emerged from the mummies collected from barley at Oum El Bouaghi. It was less abundant than the three previously mentioned parasitoids. Despite the absence of chemical treatments, the number of parasitoids is very low. Compared to other cereal aphids, the Russian wheat aphid prefers to live inside rolled up leaves. Indeed, Berner (2006) report that this aphid prefers to feed at the base of rolled leaves

Table 3 The temperatures (°C), precipitation (mm) and level of infestation (aphid/tiller) by *Diuraphis noxia* recorded in five years in barley fields in Batna (locality Hemla).

Years	Months	Temperatures			Precipitation	Level of infestation
		T. Max.	T. min.	T. Mean		
1992	January	10.2	−2.8	3.7	28.2	3
	February	12.9	4.5	8.9	22.7	
	March	13.7	2.9	8.3	42.7	
	April	17.5	4.7	11.1	21.3	
	May	23.0	8.8	15.9	81.7	
	Mean	**15.5**	**3.6**	**9.6**	**39.3**	
	Total				**196.6**	
1999	January	12.0	0.4	6.2	41.9	18
	February	10.5	−0.7	4.9	8.1	
	March	16.7	1.9	9.3	28.9	
	April	22.3	5.5	13.9	17.7	
	May	30.7	12.9	21.8	6.2	
	Mean	**18.4**	**4.0**	**11.2**	**20.6**	
	Total				**102.8**	
2008	January	13.7	0.0	6.7	9.6	12
	February	15.3	0.1	7.7	2.3	
	March	16.8	2.7	9.7	39.3	
	April	22.7	5.4	14.1	3.3	
	May	26.4	11.8	19.1	107.0	
	Mean	**18.9**	**4.0**	**11.5**	**32.3**	
	Total				**161.5**	
2009	January	11.2	1.6	6.2	67.9	0
	February	12.2	0.4	6.0	21.4	
	March	16.7	1.7	9.1	27.9	
	April	17.0	4.6	11.0	75.1	
	May	25.8	8.5	17.5	53.3	
	Mean	**16.6**	**3.4**	**9.9**	**49.1**	
	Total				**245.6**	
2009	January	13.3	2.1	7.7	36.2	0
	February	15.7	3.5	9.6	15.7	
	March	18.2	5.1	11.7	28.4	
	April	21.5	7.9	14.7	56.1	
	May	23.2	8.6	15.9	37.7	
	Mean	**18.6**	**5.4**	**11.92**	**34.8**	
	Total				**174.0**	

(Data from the meteorological station at Batna, 821.29 m.)

where it is protected from natural enemies. In addition, to mortality due to hyper-parasitism, many mummies are trapped inside tightly rolled leaves. Crushed or deformed mummies were frequently recorded in colonies of this aphid.

Monitoring the level of infestation of barley in the Batna region for five years has shown that this aphid is very sensitive to climatic factors. In 2009, heavy rainfall recorded in winter and spring was followed by a major reduction in the abundance of this aphid. Miller et al. (1993) report that the losses of yield caused by *D. noxia* are very high during periods of prolonged drought. In terms of temperature, there were no important differences between the five years of the study. It seems that, Russian wheat aphid can tolerate low winter temperatures. According to Kiplagat (2005), this aphid tolerates temperatures down to −27 °C. Moreover, Basky (1993) reports that in summer time, this aphid can survive a temperature of 30 °C. According to Ashfaq et al. (2007) the optimum development of this aphid occurs between 13.7 and 30.3 °C. Despite this, 2010 was less rainy than 2009, but no aphids were recorded on barley. It is possible that it needs several favourable years to achieve high levels of infestation in cereal crops.

Conclusions

Surveys carried out over 19 years (1992-2010) revealed the presence of *Diuraphis noxia* on durum wheat, common wheat, barley and oats at 34 localities in 15 Algerian departments. This aphid occurs mainly in semi-arid areas with cold winters. In addition, the mummies found in colonies of this aphid were produced by four Hymenopteran parasitoids (*Aphidius matricariae*, *Aphidius rhopalosiphi*, *Diaeretiella rapae* and *Lysiphlebus testaceipes*). *Diaeretiella rapae* was the most common parasitoid. It was found in all the departments monitored for parasitoids. The study of the infestation level of barley in the Batna region over a five year period revealed that the appearance of this aphid is cyclical. Apparently, the amount of rainfall recorded in the spring of 2009, particularly during the months of February and April resulted a significant reduction in the abundance of this aphid.

REFERENCES

Al-Ayedh HY (2000) Field biology of Russian wheat aphid, *Diuraphis noxia* (Mordvilko) (Homoptera: Aphididae) on wheat's differing in categories of resistance. Doctorate Thesis, University of Bio-agricultural Sciences and Pest Management, Colorado, USA.

Ashfaq M, Iqbal J, Ali A, Farooq U (2007) Role of abiotic factors in population fluctuation of aphids on wheat. Pakistan Entomol 29: 117–122.

Basky Z (1993) Incidence and population fluctuation of *Diuraphis noxia* in Hungary. Crop Prot 12: 205–209.

Basky Z (2003) Biotypic and pest status differences between Hungarian and South African populations of Russian wheat aphid, *Diuraphis noxia* (Kurdjumov) (Homoptera: Aphididae). Pest Manag Sc 59: 1152–1158.

Bernal J, Gonzalez D (1997) Reproduction of *Diaeretiella rapae* on Russian Wheat Aphid hosts at different temperatures. Entomol Exp Appl 82: 159–166.

Berner J (2006) Biochemistry of Russian Wheat Aphid resistance in Wheat: Involvement of Lipid-like products. Doctorate Thesis, University of the Free State, Bloemfontein, South Africa.

Calhoun DS, Burnett PA, Robinson J, Vivar HE, Gilchrist L (1991) Field resistance to the Russian Wheat aphid in Barley: II. Yield Assessment. Crop Sci 31: 1468–1472.

Haile A, Megenasa T (1987) Survey of aphids on barley in parts of Shewa, Welo and Tigrai, Ethiopia. Ethiopian J Agr Sci 3: 39–53.

Kiplagat OK (2005) The Russian Wheat Aphid (*Diuraphis noxia* Mord.) damage on Kenyan wheat (*Triticum aestivum* L.) Varieties and possible control through resistance breeding. Doctorate Thesis, University Aula of Wageningen, Kenya.

Kovalev OV, Poprawski TJ, Stekolshchikov AV, Vereshchagina AB, Grandrabur SA (1991) *Diuraphis aizenberg* (Homoptera: Aphididae): key to apterous viviparous females, and a review of Russian language literature on the natural history of *Diuraphis noxia* (Kurdjumov 1913). J Appl Entom 112: 425–436.

Laamari M (2004) Etude éco-biologique des pucerons des cultures dans quelques localités de l'Est Algérien. Thèse Doctorat, Institut National d'Agronomie, Alger, Algérie.

Miller RH, Tanigohi LK, Buschman LL, Kornosor S (1993) Distribution and ecology of Russian wheat aphid, *Diuraphis noxia* Mordvilko (Homoptera: Aphididae) in western Asia and northern Africa. Arab J Plant Prot 11: 45–52.

Oufroukh A, Khelifi D, Dehimat L (2011) Contribution à l'étude des maladies foliaires des céréales "approche à l'étude épidémiologique et identification de la jaunisse nanisante de l'orge dans les céréales d'hiver dans les régions de l'Est algérien". Sci Tech C 33: 53–61.

Rakhshani E, Tomanovic Z, Starý P, Talebi AA, Kavallieratos NG, Zamani AA, Stamenkovic S (2008) Distribution and diversity of wheat aphid parasitoids (Hymenoptera: Braconidae: Aphidiinae) in Iran. Eur J Entomol 105: 863–870.

Rechmany N, Miller RH, Traboulsi AF, Kfoury L (1993) The Russian Wheat Aphid *Diuraphis noxia* (Kurdjmov) (Homoptera: Aphididae) and its Natural Enemies in Northern Syria. Arab J Plant Protect 11: 92–99.

Robinson J (1994) Identification and characterization of resistance to the Russian wheat aphid in small-grain cereals: investigation at CIMMYT, 1991–92. CIMMYT, Mexico.

Stary P, Lukasova H (2002) Increase of Russian wheat aphid, *Diuraphis noxia* (Kurdj.) in hot and dry weather (2000) (Hom., Aphididae). J Pest Sci 75: 6–10.

Walters MC, Penn F, Du Toit F, Botha TC, Aalbersberg K, Hewitt PH, Boodryk KW (1980) The Russian wheat aphid. Farm South Africa 3: 1–6.

ARE BARK BEETLES RESPONSIBLE FOR DROUGHTS IN THE ŠUMAVA MTS.? A MINI-REVIEW

KAROLÍNA BÍLÁ*

Department of Biodiversity Research, Global Change Research Institute CAS, Bělidla 986/4a, 603 00 Brno, Czech Republic
* Corresponding author: kcerna@volny.cz

ABSTRACT

We attempt here to review recent studies focusing on droughts and hydrology in the Šumava Mts. The main question is can bark beetles affect water regimes in forest and what kind of measures might be taken – if any – to prevent bark beetle attacks. We compared results for natural forest, clear-cuts in managed forest and dead forest killed by a bark beetle attack. As expected, there was more water and a lower air temperature above the soil surface in natural forest. Dead trees shade undergrowth and so moderate temperature fluctuations. The conditions in clear-cuts are the worst for natural forest regeneration. There are no significant changes in the water cycle in catchment areas affected by bark beetle infections. However, it is predicted there is likely to be a slow decline in the amount of water due to a local change in climate, i.e. air temperature increase and precipitation decrease. It is concluded that droughts might occur more often and independently of bark beetle outbreaks in the future.

Keywords: bark beetle, climate change, forest management, hydrological cycle

Introduction

Bark beetles are an inseparable part of the forest ecosystems in the Šumava National Park (NP). These tiny beetles recently became a hot topic in scientific discussions and a tool of political decisions on forest management in the national park. However, scientific and political views are often contradictory (Kindlmann and Křenová 2016).

In 2015, there were extensive droughts in Western and Central Europe including the Czech Republic (CZ). The annual precipitation was only 500 mm, measured from November 2014 to October 2015. It was the lowest rainfall for the last 55 years (similarly there was a low rainfall in 1973). This dry weather was preceded by a below-average hydrological year (2014) in Bohemia. The deficiency in rainfall continued for two years and as a consequence there was a negative moisture balance, soil drought and a ground water deficit (Bečka and Beudert 2016). The levels of most streams were lower than normal and some ran dry. The Šumava NP also experienced one of the driest years in the last half-century (Bečka and Beudert 2016).

This study focuses on current problems with bark beetles and especially their effect on the hydrological situation (Fig. 1) in the Šumava NP. We attempt to compare natural forest, managed forest and dead forest (after bark beetle attack) in relation to different aspects of the water and temperature regimes in the area studied.

Photographs of the three forest types compared are shown in Figs. 2–4. Fig. 2 shows a green forest without signs of damage in the unmanaged zone, Fig. 3 is a "grey" forest about 10 years after a bark beetle attack, in which natural regeneration of the forest is occurring, and Fig. 4 is of a clearing aimed to stop bark beetles spreading.

WATER REGIME

Precipitation and Water Vapour Circulation in the Atmosphere

Does the amount of precipitation affect the cover or type of vegetation?

A deforested landscape is much warmer and receives less rainfall than a forested landscape. But is it likely that a bark beetle outbreak and resultant dead forest affects the climate? Pokorný and Hesslerová (2011) and Makarieva and Gorshkov (2007) describe a biotic pump in which water vapour condenses above cold tree crowns producing fog, which falls as rain and so retains moisture in the ecosystem. At the same time, air pressure decreases and air with water from surrounding areas is drawn into the area above the forest. If such a pump works in this way, the amount of rain falling on dead and dry forests would decrease significantly. The question is, is this type of forest dryer? When we compare dead and green undamaged forests the dead forest may be dryer, at least
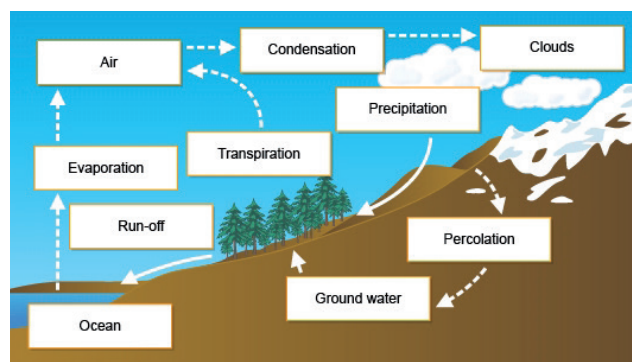

Fig. 1 The hydrological cycle (source: www.bbc.co.uk).

Fig. 2 Green forest without signs of damage in the unmanaged zone (photo: P. Kindlmann).

in the initial phases after the attack, before the massive re-growth of new trees occurs. But what about forest that has been clear cut to stop a bark beetle attack?

It is already known that less rain water drains away in rivers in forested ecosystems than in grassland or drained fields (Gutierrez 2016). The question is how much of the rainfall drains away from dead forest with rich green undergrowth, however.

Surface Water

Does surface run-off increase in a catchment area where the forest is damaged by bark beetles?

One of the largest areas with dead trees due to bark beetle attack is located in the Modravský potok catch-ment area in the surroundings of Březník, which is in an unmanaged forest zone. In this area it is possible to determine whether floods and droughts are more likely where the forest is dead. The catchment area of Modravský potok includes three areas: one covered with green forest, one with dead forest and one with clearings and other land. The run-off from these areas was measured using a limnigraph above Modrava village and the amount of precipitation was obtained from a nearby meteorological station (Filipova Huť). The data for this study was collected from 1971–2015. Changes in the precipitation/run-off ratio would indicate that forest clearings have an effect. However, the annual run-off of the Modravský potok did not change (Hruška et al. 2016). The increase in run-off in March and April could have been caused by several factors (Hais et al. 2006). This could be partly due

Fig. 3 "Grey" forest about 10 years after the bark beetle attack, in which natural regeneration of the forest is occurring (photo: K. Bílá).

Fig. 4 Clear felling aimed at stopping the bark beetle from spreading (photo: P. Kindlmann).

to a change in the vegetation cover as snow in treeless landscapes or in forest without mature trees is not shaded and melts earlier. Furthermore, an evident air temperature increase causes an earlier snow melt in the Czech Republic and that's why the spring maximum run-offs shift from April/May to March/April in mountainous areas (Hruška et al. 2016).

Leaving dead trees at a site and its effect on water balance was studied by Bečka and Beudert (2016) in the natural unmanaged zone Roklan-Luzný from 1992–2013. During this period, precipitation did not change significantly. However, annual run-offs increased by about 15% with 146 l/m² recorded in Forellenbach and 127 l/m² in Große Ohe after 30% of the spruce died in this forest in 1999. Bečka and Beudert (2016) also compare these streams in these relatively small catchment areas with larger streams in the Bavarian Forest NP over the period 1978–2013. Although the annual precipitation remained the same over this period, they detected a decrease in annual run-offs in catchment areas that were disturbed to a lesser extent (< 36%). This is a consequence of an increased evaporation of water from the area studied and an increase in the summer temperature (see below). As indicated by previous research, the annual run-off from the most disturbed catchments in their long-term study, Vydra upper stream and Große Ohe (57% and 58%, respectively, of dead trees), remained unchanged.

One of the most serious negative effects that resulted from anthropogenic modifications of the river bed (artificial adjustments to the geometry of the river bed and stabilization of the banks or bottoms with non-indigenous material of different roughness) occurred in the lower parts of the stream in arable land with dense settlements. These might influence the flow rates in the upper streams where the forests subject to bark beetle attack are located. Thus, this data could be misinterpreted as indicating a negative effect of bark beetles on the run-off of surface water. The most modified catchment areas in the Šumava NP are: lower Blanice, middle and lower Otava and middle Ostružná, Spůlka and Volyňka.

Groundwater

Can bark beetles affect groundwater?

It is sometimes claimed that water quality in dead forests deteriorates, with pH increasing about 11% and decomposition of dead wood increasing nitrogen oxide (NO_x) concentrations, which also negatively affect the drinking quality of groundwater (Vicena 2004). But scientific results based on field research show the opposite. Groundwater was enriched with nitrogen oxides during the bark beetle outbreak, but only temporarily. The increased NO_x concentration was detected when 20% of

the forest was dead and during the second bark beetle attack (60% of the trees in the forest were dead) there was no additional water enrichment with NO_x as a slow decrease occurred. In the 10 years after the bark beetle outbreak, NO_x concentrations decreased below the original value and groundwater quality even improved (Beudert et al. 2015).

Another factor associated with bark beetle outbreaks is a higher groundwater level. This is due to a temporary decrease in evapotranspiration from dead forest, which can result in muddy soil surface, unstable tree roots and uprooting of trees. This is why the use of heavy machinery when dealing with a bark beetle outbreak will mechanically disturb the soil surface and accelerate soil erosion (Kindlmann et al. 2012).

Evapotranspiration

Transpiration in dead forest is lower than in mature green forest but does it differ in amount when we consider the fast spontaneous regeneration in such forests?

Evapotranspiration rates depend on vegetation structure. Plants take up water from rain and ground water via their roots, which is transported from the roots to the leaves where it is transpired through stomata. Energy absorbed in water vapour is released when it condenses back into water, which happens in a cool environment after reaching the dew point. Therefore, evapotranspiration and condensation have a double effect on climate: a) plants cool down by transpiring, b) vapour condenses into water and this process releases heat, which warm the environment. Evapotranspiration can equalize local and day /night differences in temperature (Pokorný et al. 2011).

Bečka and Beudert (2016) record that in extensively disturbed spruce forest at Forellenbach and Große Ohe evapotranspiration decreased to about 120 l/m² and 90 l/m², respectively. Evapotranspiration in spruce forest in the Šumava NP is around 600 l/m². It consists of evaporation, the physical vaporization of precipitation on the surfaces of trees (cca 200–400 l/m²) and transpiration, the release of water vapour from the needles via their stomata (cca 250–350 l/m²). Evapotranspiration decreases in infested woods, because a greater amount of the rain falls directly onto the soil because dead trees have a smaller surface area than live and green ones and dead trees do not respire water. More water soaks into the soil, groundwater supplies improve, stream flow increase and the annual run-off increases. Despite rainfall remaining constant over a long period, annual run-off decreased in the catchment areas where the extent of disturbance was low (< 36%). This clearly accounts for the increased evapotranspiration caused by a significant climate warming (see below). The higher evapotranspiration obviously accounts for the decrease in run-off in summer; however, summer precipitation increased in comparison to the past. As in the first study, the annual

run-offs over a long period of time from the most disturbed catchment areas, upper Vydra and Große Ohe (57% and 58% dead trees, respectively), did not decline. It is also clear that evapotranspiration declined in areas that were extensively disturbed. A lower transpiration compensates for the increased evaporation due to climate change, but only temporarily. The fast regenerating vegetation quickly comes to use the same amount of water as untouched forests. However, water slowly disappears from these catchment areas because of local climate change.

To ensure the ecological functions of the forest, it is necessary to achieve the original evapotranspiration rate. In the case of the spontaneous regeneration in the unmanaged zone of the Šumava NP, almost 15% of young trees had reached a height of 2 m 15 years after the disturbance. In clear-cut areas fewer spruces regenerated spontaneously and trees were planted (often repeatedly) in order to reach the required number of trees. There are also differences in the herbaceous and moss floor regeneration and in the survival of indigenous forest species (for example *Vaccinium myrtillus*, *Athyrium distentifolium*, *Dryopteris dilatata*, *Lycopodium annotinum*, *Soldanella montana*). No change in numbers of these species were detected in dead forest but they often disappeared from clearings. Mosses responded to cutting even more dramatically as they were absent during the first year after the clear-cut. The artificially forest planted in the clearings will be more prone to disturbance in the future and is likely to have a shorter lifetime than spontaneously regenerated forest (Hubený and Čížková 2016).

TEMPERATURE REGIME

Sunshine and Vegetation Cover

What is more favourable for forest regeneration, dead forest or clearings? Is there a difference in their vegetation cover and exposure to sun? And what is the role of dead standing trees?

As mentioned above, vegetation structure is very important for evapotranspiration, which equalizes temperature fluctuations and disperses energy from the sun via its cooling effect. In dead forest herbaceous plants and mosses survive undamaged and it is assumed their evapotranspiration and dispersal of energy from the sun is greater than occurs in clearings. However, no field measures exist to prove this.

Next assumption is the positive effect of the shading by dead trees on the undergrowth even though these trees no longer transpire. Temperatures of the atmosphere and soil measured in green mature forest, dead forest and clearings are similar (Hais and Pokorný 2004; Tesař et al. 2004; Hais and Kučera 2008; Pokorný et al. 2011; Kindlmann et al. 2012).

Undergrowth and Air Temperature

Are the temperature fluctuations in dead forest and clearings similar, comparable but different from those recorded in contrary to the green forest?

Tesař et al. (2004) measured temperature in the undergrowth 5 cm above the surface of the soil when midday temperature reached values above 30 °C. The midday temperature in the clearing fluctuated between 23–25 °C. In the green mature forest, it reached only 22 °C as a consequence of the distance of the soil surface from the tree crown surface that cools by absorbing sunshine. These authors claim that dead forest is significantly less stable thermally than a clearing. Pokorný (2011) mentions an increase in the maximum temperature in dead forest by almost 20 °C, same as in the clearing. He predicts a water shortage because of the higher sunshine input and consequent drying out of the soil. Similar results are presented by Kindlmann et al. (2012), namely maximum air temperatures at a height of 2 m in green forest of 21.6 °C, dead forest of 34.6 °C and clearings of 39.7 °C. These results confirm those of Hais and Kučera (2008) that the daily fluctuations in temperature recorded in dead spruce forests are higher in summer than in green forest however, temperatures in clearings are even higher than in dead spruce forests.

Lower temperatures recorded in the undergrowth in dead spruce forests (compared to clearings) are due to the shading effect of standing or lying dead tree trunks. Zielonka and Piatek (2004) also note that lying dead trunks accumulate water during their decomposition and so increase undergrowth moisture and evaporation, and as a consequence decrease undergrowth temperature. Temperature and air moisture can differ depending on climate, sensor location and stage of succession, nevertheless the assumption that clearings are more stable than dead forest, is wrong.

Bečka and Beudert (2016) also mention a statistically significant increase in summer temperatures since 1978 of about 2 °C. Such a warming, especially from May till August, will result in higher evapotranspiration in the Šumava Mountains.

Soil Temperature

As for air temperature it is interesting to ask if the fluctuations in soil temperature in dead forest and clearings are similar to those in green forest? Or, if not, does the shade from the dead trees together with that of the undergrowth moderate the fluctuations in temperature?

The daily fluctuations in temperatures recorded at the surface of the soil in clearings are noticeably greater than those recorded in green and dead forest. Hais and Kučera (2008) consider clearings to be unfavourable localities for forest regeneration just because of the extreme temperatures and dry conditions, soil impoverishment and ero-

sion that limit the chance of tree seedlings overgrowing the herbaceous plants. Similar soil temperatures are cited by Kindlmann et al. (2012): green forest 21.5 °C, dead forest 27.4 °C and clearings 38.3 °C (maximum temperatures). High soil temperatures in clearings could negatively affect soil revitalization and regeneration. That's why clear-cuts in mountainous spruce forests are considered to be the least suitable method of management aimed at reducing the incidence of bark beetle outbreaks in the Šumava NP.

Conclusions

The main aim of the Šumava NP is to have the highest possible proportion of the area covered by natural forests and to preserve the current hydrological situation. But forest age structure changes and diversifies over time and the current stage of decay (overlapping with the stage of regeneration) is prone to natural disturbances such as windstorms and attack by pests (Fig. 5). Old trees are extensively damaged over large areas instead of dying one by one. However, young seedlings quickly develop and a new generation of trees replace the dead trees. Such regeneration can occur within decades unlike in the zones that are managed by clear-cutting.

Unfortunately, droughts currently occur more frequently and independently of bark beetle outbreaks (Bečka and Beudert 2016). Water regime in the Šumava NP does not remain constant. However, this is not due to unmanaged zones with spontaneous forest regeneration but due to climate warming and changes in the distribu-
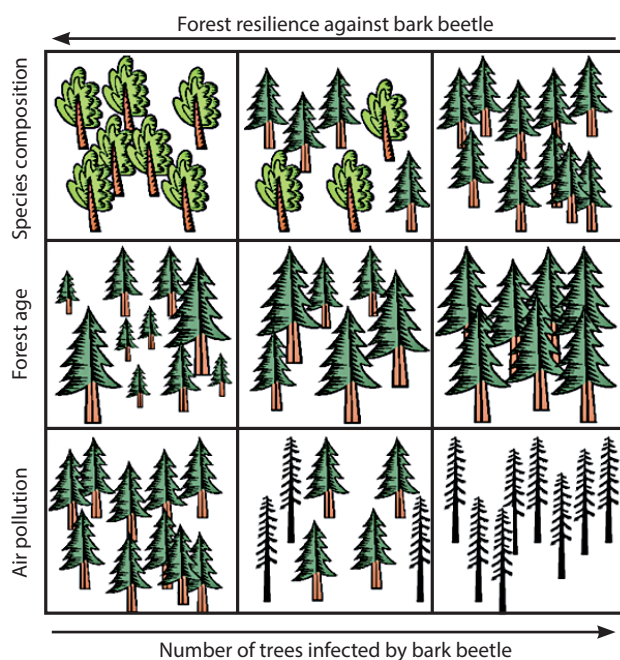
Fig. 5 Forest resilience against attacks by bark beetles associated with different types of weakening: species structure, age structure and air pollution.

tion of the annual precipitation. These changes are most obvious in winter, the period when rainfall is lowest. The highest temperature increase occurred in April (3–4 °C) and this strongly affects snow melt. Snow cover melts about 3–5 weeks earlier now than 40 years previously, which also affects the water regime in summer.

The fact that the spontaneous forest regeneration cannot be allowed to occur in the whole NP, especially in the boundary between the core, unmanaged zones and economic forests. A convenient solution to this problem is in a proper zonation of the unmanaged forests (core zones) and economic forests. This would require replacing the current 135 small and isolated zones by fewer and larger core zones that in total have a shorter peripheral border, i.e. a decrease in the area where it will be neccessary to fell trees attacked by bark beetles. It is important to realize that the current problem we face is not a choice between green or dead forest but do we want clearcuts or dead regenerating forest. Pokorný et al. (2016) mention that there are a number of negative effects associated with dead forest but the negative effects associated with clear-cut areas are much more serious. Both the cooling effect of green forest and the decrease in evapotranspiration when green forest dies occur, but this is also true for clear-cut areas to an even greater extent. However, vegetation loss does not necessarilly mean an increase in water run-off, which is supported by the long-term measurments recorded for Modravský potok (Hruška et al. 2016) and upper Vydra and Große Ohe (Bernstein et al. 2015).

Moreover, bark beetles could be used as a natural means of restoring more natural mountainous forests (Jonášová and Prach 2004; Hais et al. 2009). Hais et al. (2009) studied several plots in the Šumava NP that were managed in two different ways after bark beetle attack: 1. Forest left uncut and 2. forest completely felled. They recorded a significant difference in the spectral reflection from the vegetation in aerial photographs taken from 1985 to 2007. The reflection from plots that were not clear cut was the most similar to that of normal healthy forest and that from the clear cut plots deviated significantly from the normal state.

In the case of national parks, natural processes should be promoted rather than clear cutting followed by the planting of trees, particularly in the core zones of the NP. Economics should not endanger the protection of nature and the water regime.

Acknowledgements

REFERENCES

Bečka P, Beudert B (2016) Kůrovec a voda. Jak bezzásahovost ovlivňuje vodní režim na Šumavě. Šumava, jaro: 16–17.

Bernstein J, Bässler C, Zimmermann L, Langhammer J, Beudert B (2015) Changes in runoff in two neighbouring catchments in the Bohemian Forest related to climate and land cover changes. J Hydrol Hydromech 63: 342–352.

Beudert B, Bässler C, Thorn S, Noss R, Schröder B, Dieffenbach-Fries H, Foullois N, Müller J (2015) Bark beetles increase biodiversity while maintaining drinking water quality. Conserv Lett 8: 272–281.

Gutierrez V (2016) Management lesů a jeho význam pro vodu a klimatizaci krajiny. Vodní hospodářství 2: 24–25.

Hais M, Brom J, Procházka J, Pokorný J (2006) Effect of water drainage on the forest microclimate; case study of two small catchments in the Šumava mountains. Ekológia Bratislava 25: 18–26.

Hais M, Jonášová M, Langhammer J, Kučera T (2009) Comparison of two types of forest disturbance using multitemporal Landsat TM/ETM+ imagery and field vegetation data. Remote Sens Environ 113: 835–845.

Hais M, Kučera T (2008) Surface temperature change of spruce forest as a result of bark beetle attack: remote sensing and GIS approach. Eur J Forest Res 127: 327–336.

Hais M, Pokorný J (2004): Změny teplotně-vlhkostních parametrů krajinného krytu jako důsledek rozpadu horských smrčin. Aktuality šumavského výzkumu 2: 49–55.

Hruška J, Lamačová A, Chuman T (2016) Bezzásahový režim nemá zásadní vliv na hydrologii šumavských povodí. Ochrana přírody: 35–38.

Hubený P, Čížková P (2016) Šumavské lesy pod lupou. Správa Národního parku Šumava, Vimperk.

Jonášová M, Prach K (2004) Central-Europen mountain spruce forests: regeneration of tree species after a bark beetle outbreak. Ecol Eng 23: 15–27.

Kindlmann P, Křenová Z (2016) Biodiversity: Protect Czech park from development. Nature 531: 448.

Kindlmann P, Matějka K, Doležal P (2012) Lesy Šumavy, lýkožrout a ochrana přírody. Karolinum, Praha.

Makarieva A, Gorshkov V (2007) Biotic pump of atmospheric moisture as driver of the hydrological cycle on land. Hydrol Earth Syst Sci 11: 1013–1033.

Pokorný J (2011) Co dokáže strom. In: Kleczek J (ed) Voda ve vesmíru, na zemi, v životě a v kultuře. Radioservis Praha, pp. 429–431.

Pokorný J, Hesslerová P (2011) Odlesňování a klima. Klimatické změny v Mau Forest v západní Keni. Vesmír 9010): 573–578.

Pokorný J, Hesslerová P, Jirka V (2011) Změny povrchové teploty les jako následek ztráty vody a poklesu evapotranspirace. Lesnická práce 12: 26/819–29/822.

Tesař M, Šír M, Zelenková E (2004) Vliv vegetace na vodní a teplotní režim tří povodí ve vrcholovém pásmu Šumavy. Aktuality šumavského výzkumu 2: 84–88.

Vicena I (2004) Příroda je více než kůrovec. Lesnická práce 9.

Zielonka T, Piątek G (2004) The herb and dwarf shrubs colonization of decaying logs in subalpine forest in the Polish Tatra Mountains. Plant Ecol 172: 63–72.

COMPARATIVE LANDSCAPE TYPOLOGY OF THE BOHEMIAN AND BAVARIAN FOREST NATIONAL PARKS

TOMÁŠ JANÍK* and DUŠAN ROMPORTL

Department of Physical Geography and Geoecology, Faculty of Science, Charles University, Prague, Albertov 6, 128 43 Prague 2, Czech Republic
* Corresponding author: janikt@natur.cuni.cz

ABSTRACT

Landscape typologies provide their users with a spatial framework, which could be used for management, assessment of landscape changes and monitoring of biodiversity or natural processes. The aim of this article is to distinguish and compare landscape types across the largest natural area within Central Europe. Cluster analysis based on physical-geographical data was used to differentiate particular types of environmental conditions. The results are suitable for comparing both national parks and their management.

Keywords: landscape typology, Bohemian Forest NP, Bavarian Forest NP, cluster analysis

Introduction

The Bohemian and Bavarian Forests make up the largest wilderness area in Central Europe (Křenová and Hruška 2012) and is extensively protected by two transboundary national parks of the same name. Dynamic changes in landscape caused by bark beetle outbreaks across the whole area call for appropriate management of the forest ecosystems. However, the management differs greatly in the two national parks. This inconsistency in the management is often justified by different natural conditions on the German and Czech side (Křenová and Hruška 2012; Bláha et al. 2013). Therefore, a comparative study such as a landscape classification is urgently needed if we want to describe similarities or differences within this region.

Methods

Study Area

Focal area of the landscape classification is defined by the boundaries of both national parks, which together cover about 1,000 km^2. The physical-geography of the Bohemian and Bavarian Forests are similar, but there are several important differences (Fig. 1). The Bohemian and Bavarian Forests, belong to the same geomorphologic unit and together form the largest and oldest mountain system in Central Europe (Czech Geological Survey 2012). There is a typical relict high mountain plateau in the central part of the area, where there is a mosaic of long flat forested ridges and a high number of peat bogs, especially on the Czech side (Spitzer and Bufková 2008). On the edges of this high mountain plateau are deep brook and river valleys with rocky slopes. The mean altitude of the whole mountain range is about 922 m, the highest peak is 1457 m (Křenová and Kiener 2012). Ver-

tical heterogeneity is much greater on the Bavarian side due to the steep gradients of the slopes. The topography was shaped by glaciers and there are eight glacial lakes and several other glacial features in the area. The mean temperature depends on altitude and varies from 6.0 °C at 750 m to 3.0 °C at 1300 m (Tolasz et al. 2007). The mean annual precipitation varies from 800 to 900 mm in the foothills to 1600 mm in the central area (Dohnal et al. 2011). Soils are mainly cryptopodzols and cambisols, and are generally acidic (Jonášová and Prach 2004; Babůrek 2006).

The forest cover in the whole area is ca. 60%, but reaches 90% in the central parts of the national parks. Vast areas of original mixed forests have been changed into Norway spruce plantations. The remains of the native forest ecosystems have survived as a network of islands of natural climax spruce forests (*Picea abies*), mixed beech-fir-spruce forests (*Fagus silvatica*, *Abies alba*) and relict pine forests (*Pinus silvestris*) (Dohnal et al. 2011). The wetlands, namely raised mires and bottom-valley peat bogs, are valuable natural stands in this area. Big parts of the forests and some secondary forestless areas (especially on the Czech side of the mountains) are currently left to develop spontaneously without human intervention (Dohnal et al. 2011).

The whole region has been influenced by human activities since the Iron Age and later period of Celtic settlements. Slavic tribes came in the 7th and 8th century (Řezníčková in Anděra 2003). The most important period of colonization started in the 16th century when timber extraction needed for mines and glass manufacture led to extensive deforestation and changes in forest structure. In the 19th century, at the time of the highest population density, the mountain plateau was afforested with spruce and several large-scale bark beetle outbreaks occurred in the region (Jonášová and Prach 2004). The most significant event that resulted in a separate land-
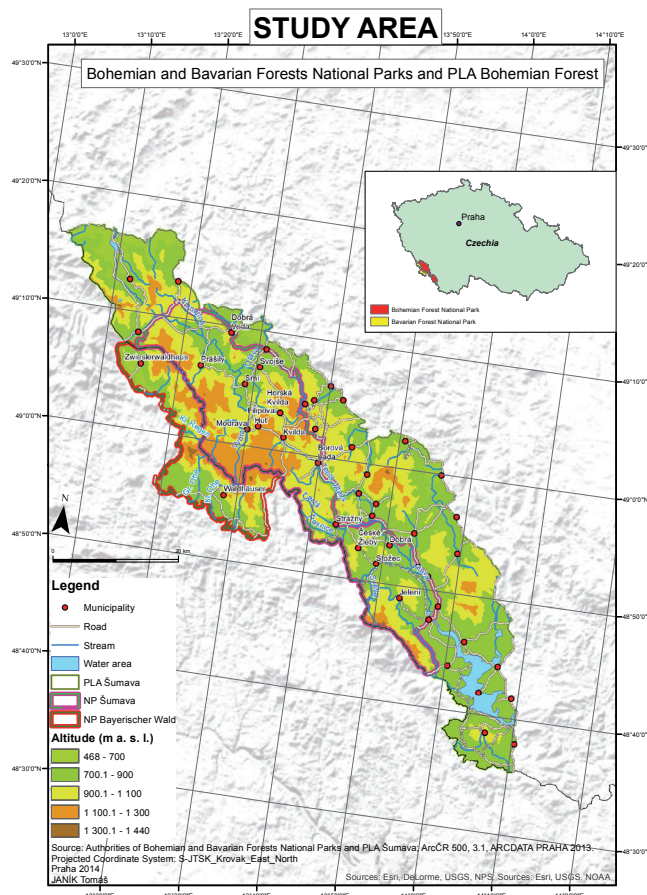
Fig. 1 Map of study area.

scape development was World War II, after which the German residents were expelled and an inaccessible border zone established on the Czech side. The population in the region was reduced to less than a third of what it had been previously, therefore, almost all human activities decreased. Since the 1970s in Bavaria and 1990s in Bohemia, nature protection and tourism have dominated regional development (Perlín and Bičík 2010).

Landscape Typology

Landscape classification provides defined classes, which are described by variables. We can organize environmental gradients into systematically recognized objects (Jongman et al. 2006). Landscape typology and classification are widely used in landscape assessments, evaluation and protection. Typology can characterize a region based on its values and differences (Kolejka and Lipský 2008). Diversity of European cultural landscapes can be expressed by a complex classification using data on both physical (climate, relief, soil, geology) and cultural (land use) features of the environment (Chuman and Romportl 2010).

We used the typological approach (Metzger 2005; Wascher 2005; Chuman and Romportl 2010) based on quantitative statistical methods to identify particular spatial units. Our goal was to carry out classifications, which would provide its users with a spatial framework

for assessing differences between both national parks, evaluation of nature conservation, forest management and human activities in general. We used the typological approach (Metzger 2005; Wascher 2005; Chuman and Romportl 2010) to identify particular spatial units. All relevant input data describing the landscape (climate, geology, topography, soils, land cover and land use) were processed within a regular grid covering the area studied.

Physical Landscape Typology

Development of GIS software offered new, easier and better ways of achieving an objective analysis (Chuman and Romportl 2010). We carried out an analysis in STATISTICA 12 and then integrated the data in the software ArcGIS 10.2. We worked with data provided by the authorities of the National Parks (2006–2012) and GEODIS Company (2006).

The area studied, both national parks, was overlaid with a regular grid of 100×100 m cells.

Physical conditions in each cell in the regular grid were described by twelve variables: mean altitude, mean slope, heat load index, incidence of south facing slopes, annual mean temperature, seasonality (the difference between annual min and max temperature), the difference between average temperature in the coldest and warmest month, mean temperature of the warmest quarter of the year, mean temperature of the coldest quarter of the year, annual precipitation, mean precipitation in the coldest quarter of the year and mean precipitation in the warmest quarter of the year. Topography data were provided by the authorities of the Bohemian and Bavarian Forest National Parks; the climatic data were obtained from the WorldClim database (Hijmans et al. 2005). The next necessary step was standardization of the data because we need each variable to be in the same format for the analyses. Classes were identified using k-means cluster analysis in STATISTICA 12. We obtained a class num-

Table 1 Land cover types.

Land cover	LC Code
Without forest	1
Coniferous forest	2
Broad-leaved forest	3
Meadows	4
Peatbogs	5
Rocks	6
Mixed forest	7
Dead-prostrate forest	8
Dead-standing forest	9
Succession	10
Built up areas	11
Water	12

ber for each cell based on a Cluster analysis of the data describing the landscape mentioned above. Classes were visualised in ArcGIS 10.2.

Functional Landscape Typology

We distinguished twelve types of land cover (Table 1) based on the land cover data provided by GEODIS (2008). Land cover typology was used to reduce the input dimensions of land cover data and determine the typical combination of land cover classes within cells in the regular grid. Therefore, k-means cluster analysis was used to identify so called functional types of landscape. Five clusters were identified, for which shares of particular land cover classes were calculated (Fig. 2). This description helps us to understand the distribution of the land cover in both national parks, and provides us with another framework for assessing the landscape in the area studied.
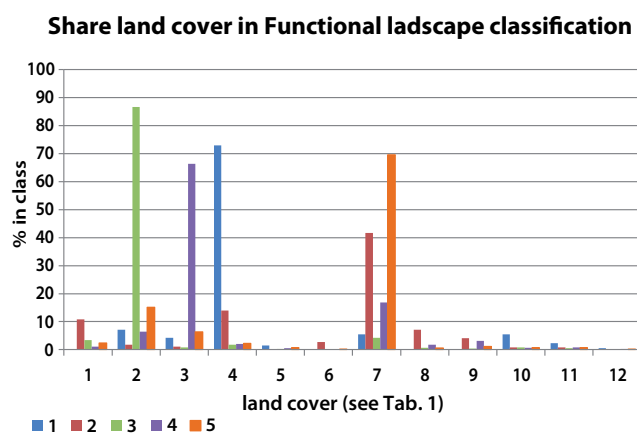
Share land cover in Functional ladscape classification

Fig. 2 Share of land cover in Functional landscape classification.

Results

Physical Landscape Typology

First step of the complex landscape classification based on physical-geographical attributes only produced five types of landscape (Fig. 3). Their spatial distribution and calculated characteristics (Table 2) show logical correlations and a continuous gradient in the factors altitude and precipitation. Slope is an important differential var-

iable, helpful for further describing our results. We can distinguish three large scale flat types of landscape and two small scale transitional types of landscape with steep slopes. Names of particular types of physical-landscape are therefore derived from their topographical characteristics.

The largest type of landscape *"high plateaus"* covers the highest parts of the region studied including some mountain peaks. Mean slope is just 6.65°, therefore there are a lot of peat bogs here. High annual precipitation and low temperatures are recorded here. This type of landscape occurs almost only in the Czech part of the area studied, because in the German part of the mountains the slopes are much steeper. This high plateau is usually surrounded by *"edge of plateau"* which is a transitional type of landscape covering the smallest part of the region studied. It includes an enormous number of deep and steep valleys and canyons. Distribution is quite similar in both national parks. Similar types of landforms can be found in another type of landscape named *"mid-slopes"*. The main difference is generally a lower altitude and precipitation and also its spatial distribution as this this type of landscape is widespread in the Czech part of the area studied, especially in regions not connected with the central plateau. *"Higher foothills"* are scattered spatially within the whole area studied and is another transitional type of landscape between other neighbouring levels. Steep slopes and differences in precipitation are typical characteristics of this type. The last type of landscape *"Lower foothills"* occurs in most of the Bavarian national park. In the Czech Republic this type of landscape occurs along rivers, for example, the Vltava River. Despite its name, this type of landscape also includes some flat valleys.
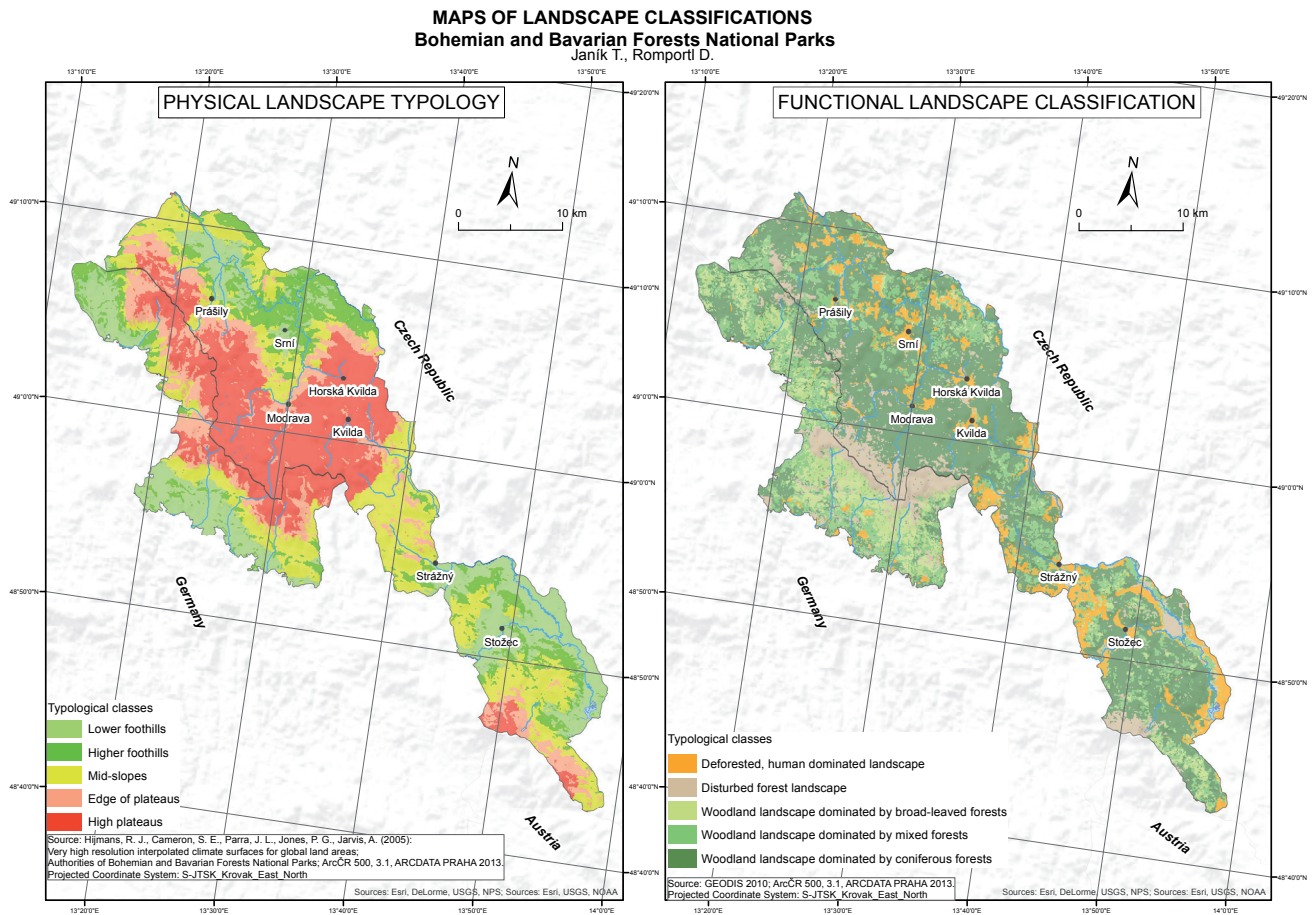
Based on our results, topography is the most important factor, when describing differences within both national parks. These differences are nicely shown in the form of an irregular and patchy distribution of all the physical types of landscape mentioned above.

Functional Landscape Classification

The second step in the complex classification was run only using land cover characteristics. Based on the distribution of land cover classes, five functional types of landscape were identified. A *"Disturbed forest landscape"* is typical of the region studied and consists of large ar-

Table 2 Average values for Physical landscape typology.

Type	Mean altitude (m a. s. l.)	Slope (°)	Precipitation (mm/year)	Area (km^2)
Mid-slopes	932.22	7.67	1090.1	229.3
Edge of plateaus	1048.90	14.32	1139.5	126.1
Higher foothills	845.76	12.27	1025.4	127.4
Lower foothills	778.94	4.21	1016.5	190.5
High plateaus	1141.30	6.65	1187.1	255.9

MAPS OF LANDSCAPE CLASSIFICATIONS
Bohemian and Bavarian Forests National Parks
Janík T., Romportl D.

Fig. 3 Maps of landscape classifications.

eas of dead-standing spruce trees resulting from wind storms and bark beetle attacks. This type of landscape occurs widespread along the borders of both national parks, however larger areas occur on the Czech side. The main difference between the national parks is in the distribution of forest types of landscape. The Czech side is dominated by *"woodland landscape dominated by coniferous forests",* whereas in Germany *"woodland landscape dominated by broad-leaved forests"* and *"woodland landscape dominated by mixed forests"* are much more wide spread. In addition, in particular on the Czech side, the *"deforested, human dominated landscape"* includes meadows, settlements and other deforested areas subject to human activity (Fig. 3). For a correct interpretation it is necessary to know the percentage of land cover in each class (Fig. 2).

Discussion

We can distinguish two types of conditions based on our typologies. Physical abiotic conditions determined by natural long-term processes, connected to climate and geomorphological conditions have resulted in the physical landscape typology. It is a convenient framework for

evaluating the processes occurring in the area studied (Kolejka and Lipský 2008; Chuman and Romportl 2010) and for determining the differences among the classes, which can be useful for obtaining a more accurate picture of the landscape.

Secondly the classification goes further in revealing the functional types of landscape. Land cover is the variable most affected by humans. There are differences between the German and Czech parts caused by different forest management, in particular that which occurs during and after the most common disturbances in mountain forests in Central Europe, wind throws and subsequent bark beetle outbreaks (Jonášová and Prach 2004; Nováková and Edward-Jonášová 2015). Many studies in both national parks conclude that the forest is able to regenerate after disturbances (Fischer et al. 2002; Jonášová and Prach 2004; Jonášová at al. 2010; Nováková and Edward-Jonášová 2015). On the German side the forests regenerated without human help after the wind throw in 1983. The Czech side was affected by a wind throw in 2007 and its management is very unclear (Křenová and Kiener 2012). Our typology reveals larger areas of dead forest in the central area of the national park on the Czech side.

Conclusion

These classifications provide users with an objective spatial framework for further investigation. It is easy to determine similarities and differences in physical conditions and reveal uniqueness, rareness or threats to particular types of landscape within both national parks. Moreover, it is possible to evaluate the effect of human activity, level of nature protection and efficiency of landscape management in both national parks. Such transboundary classifications help us to better understand the geographical conditions and provide valuable information about the spatial distribution of the different types of landscape.

On the other hand, processes are very dynamic and therefore it important to have more than a spatial perspective. We need to analyse temporal changes, which are associated with human activity, because on the Czech side, in particular, the interested parties have discussed its future management for a long time. It depends on the representatives of the national park, municipality, industry and region, and politicians at the national level, agreeing.

Software and Map Design

Software STATISTICA 12 was used for the statistical analyses and ESRI ArcGIS 10.2 for all spatial analyses and visualisation.

Main output of our study are two maps that visualize the spatial distribution of both clusters analyzed. For particular types of landscape we chose colour to express gradual change in an understandable way by representing instinctive similarities between colours and classes.

REFERENCES

Anděra M, Zavřel P (2003) Šumava: příroda, historie, život [Sumava: Nature, history and life]. Issued. 1. Praha, 2003.

Babůrek J (2006) Průvodce geologií Šumavy [Sumava geology guide]. Správa Národního parku Šumava a Chráněné krajinné oblasti Šumava. Vimperk.

Bláha J, Křenová Z, Romportl D (2013) Can NATURA 2000 mapping be used to zone the Šumava National park? Eur J Environ Sci 3: 57–64.

Chuman T, Romportl D (2010) Multivariate classification analysis of cultural landscapes: An example from the Czech Republic. Landscape Urban Plan 98: 200–209.

Czech Geological Survey (2012) Ministry of the Environment of the Czech Republic. http://maps.geology.cz/geocr_25/.

Dohnal T, Hubený P, Jablonská L, Löw J, Novák J, Zimová E (2011) Krajina Národního parku Šumava [Landscape of the Sumava National park]. Správa Národního parku a Chráněné krajinné oblasti Šumava, Vimperk.

Fischer A, Lindner M, Abs C, Lasch P (2002) Vegetation Dynamics in Central Europe Forest Ecosystem (Near-natural as well as managed after storm events). Folia Geobot 37: 17–32.

Hijmans RJ, Cameron SE, Parra JL, Jones PG, Jarvis A (2005) Very high resolution interpolated climate surfaces for global land areas. Int J Climatol 25: 1965–1978. Database WorldClim.

Jonášová M, Prach K (2004) Central-European mountain spruce (*Picea abies* (L.) Karst.) forests: regeneration of tree species after a bark beetle outbreak. Ecol Eng 23: 15–27.

Jongman RHG, Bunce RGH, Metzger MJ, Mucher CA, Howard DC, Mateus VL (2006) Objectives and applications of a statistical environmental stratification of Europe. Landscape Ecol 21: 409–419.

Kolejka J, Lipský Z (2008) Landscape mapping and typology in the Czech Republic. Klasyfikacja krajobrazu. Teoria i praktyka. Problemy Ekologii Krajobrazu 20: 67–78.

Kolejka J (1999) Krajinné mapy a jejich klasifikace [Landscape maps and their classifications]. Geodetický a kartografický obzor, Praha: ČKS, Vol. 45/87: 273–278.

Křenová Z, Hruška J (2012) Proper zonation – an essential tool for the future conservation of the Šumava National Park. Eur J Environ Sci 2: 62–72.

Křenová Z, Kiener H (2012) Europe's Wild Heart – still beating? Experiences from a new transboundary wilderness area in the middle of the Old Continent. Eur J Environ Sci 2: 115–123.

Lipský Z, Romportl D (2007) Typologie kulturní krajiny – výzva pro geografii [Typology of cultural landscape – challenge for geography]. In: Herber V (ed) Fyzickogeografický sborník 4. Fyzická geografie – teorie a praxe. Masarykova univerzita, Brno, pp. 148–154.

Metzger MJ (2005) A climatic stratification of the environment of Europe. Global Ecol Biogeogr 14: 549–563.

Nováková MH, Edwards-Jonášová M (2015) Restoration of Central-European mountain Norway spruce forest 15 years after natural and anthropogenic disturbance. Forest Ecol Manag 344: 120–130.

Perlín R, Bičík I (2010) Lokální rozvoj na Šumavě [Local development in the Sumava]. 2010. vyd. Správa NP a CHKO Šumava.

Romportl D, Chuman T, Lipský Z (2013) Typologie současné krajiny Česka [Landscape typology of Czechia]. Geografie 118: 16–39.

Spitzer K, Bufková I (2008): Šumavská rašeliniště [Peat bogs of Sumava]. Správa Národního parku a Chráněné krajinné oblasti Šumava, Vimperk.

Tolasz R et al. (2007) Atlas podnebí Česka [Climate Atlas of Czechia]. Český hydrometeorologický ústav, Praha, Universita Palackého, Olomouc.

Wascher DM (2005) European Landscape Character Areas – Typologies, Cartography and Indicators for the Assesment of Sustainable Landscapes.